Optical Frequency Comb Source for Next Generation Access Networks

Rui Zhou

B.Eng., M.Eng.

A Dissertation submitted in fulfilment of

the requirements for the award of

Doctor of Philosophy (Ph.D.)

to the

Dublin City University

Faculty of Engineering and Computing

School of Electronic Engineering

Supervisors:

Prof. Liam P. Barry

Dr. Prince M. Anandarajah

September 2014

Declaration

I hereby certify that this material, which I now submit for assessment on the programme of study leading to the award of Doctor of Philosophy is entirely my own work, and that I have exercised reasonable care to ensure that the work is original, and does not to the best of my knowledge breach any law of copyright, and has not been taken from the work of others save and to the extent that such work has been cited and acknowledged within the text of my work.

Signed: _____

ID No.: _____

Date: _____

Contents

Abstract

Within the recent decades, the exponential growth of converged telecommunication services around the global range and the increasing demands for video rich multimedia applications have triggered the vast development and adaptation of fibre communication technology to resolve the capacity “bottleneck” at metropolitan-access aggregations. To further enhance overall performance, next generation optical access networks will most likely require highly efficient wavelength division multiplexing (WDM) technology beyond the capability of current standard time division multiplexed (TDM) systems. The successful implementation of future-proof WDM access networks depends on advancements in high performance novel transmission schemes as well as economical and practical electronic/photonic devices. Under these circumstances, this thesis focuses on an investigation of the use of optical frequency comb sources, and spectrally efficient modulation formats, in high throughput WDM based optical access systems. A novel injected gain switched comb generation technique, which delivers simplicity, reliability, and cost efficiency has been proposed and verified through experimental work. In addition, a detailed characterisation of the optical comb source has been undertaken with special attention on the phase noise property of the comb lines. The potential of the injected gain switched comb source is demonstrated in a digital coherent receiver based long reach WDM access scenario, which intends to facilitate 10 - 40 Gb/s per channel high speed data delivery. Furthermore, an optical scalar transmission scheme enabling the direct detection of higher order modulation format signals has been proposed and experimentally investigated.

Acknowledgements

First I would like to express my deepest gratitude to Prof. Liam P. Barry, my supervisor, for accepting me as part of his research group, and for his constant trust and support throughout my PhD. The same gratitude goes to my co-supervisor Dr. Prince M. Anandarajah, who has enlightened me with his extensive knowledge and great personality both in research and in life. Without the patient guidance and enthusiastic encouragement from Liam and Prince, this work would not have been possible. I also owe special thanks to Liam and Prince for their critical reviews of the entire thesis and the many constructive suggestions for improving it.

I wish to acknowledge Dr. Sylwester Latkowski, who is now with Eindhoven University of Technology, The Netherlands, for his kind guidance during the early stage of my PhD study. The outstanding research skills and experiences he has shown to me will always be beneficial for my future career and continued research.

I am truly grateful to Tam N. Huynh, for his helpful comments and strong support in part of this thesis. My grateful thanks are also extended to some of the other colleagues in Radio and Optical Communications Lab: Vidak Vujicic and M. Deseada Gutierrez Pascual, for their timely assistance in experiments; Fernando A. Gutiérrez, Dr. Sean P. O' Duill and Dr. Tong Shao, for their valuable advice and inspiring discussions.

I want to express my sincere appreciation for the great help and support provided by the Optical Networks Group, University College London, which has directly resulted in the experimental work in Chapter 4, Section 4.3. I am deeply indebted to the group members involved: Dr. Robert Maher, Dr. Domaniç Lavery, Milen Paskov, Dr. Benn C. Thomsen, Dr. Seb J. Savory, and Prof. Polina Bayvel.

Regarding funding, my thanks go to the China Scholarship Council for generous grants throughout my 4-year PhD.

Finally, this work is dedicated to my mother, Zhaohua Wu, my father, Dejian Zhou, and my fiancée, Wenjing Huang.

To mum, dad,

and my lovely fiancée,

Wenjing.

List of Acronyms

ADC Analogue-to-Digital Converter

AMZI Asymmetric Mach-Zehnder Interferometer

AON Active Optical Network

APD Avalanche Photodiode

ASE Amplified Spontaneous Emission

ATM Asynchronous Transfer Mode

AWG Arrayed Waveguide Grating

B2B Back-to-Back

BER Bit Error Rate

BLS Broadband Light Source

BPF Band-Pass Filter

BPON Broadband Passive Optical Network

CapEx Capital Expenditures

CLS Centralised Light Source

CMA Constant Modulus Algorithm

CO Central Office

CW Continuous-Wave

DBA Dynamic Bandwidth Allocation

DBR Distributed Bragg Reflector

DD Dual-Drive

DFB Distributed Feedback

DL Delay Line

DLI Delay Line Interferometer

DM Discrete Mode

DP Dual-Parallel

DPSK Differential Phase Shift Keying

DQPSK Differential Quadrature Phase Shift Keying

DSH Delayed Self-Heterodyne

DSL Digital Subscriber Lines

DSP Digital Signal Processing

DWA Dynamic Wavelength Allocation

ECL External Cavity Laser

ED Error Detector

EDFA Erbium Doped Fibre Amplifier

EFMA Ethernet in the First Mile Alliance

EML Electroabsorption Modulated Laser

ENOB Effective Number of Bits

EO Electro-Optic

EOM Electro-Optic Modulator

EPON Ethernet Passive Optical Network

ESA Electrical Spectrum Analyser

FBG Fibre Bragg Grating

FEC Forward Error Correction

FIR Finite Impulse Response

FM Frequency Modulation

FP Fabry-Pérot

FSAN Full Service Access Network

FSR Free Spectral Range

FTTB Fibre-To-The-Building

FTTH Fibre-To-The-Home

FWM Four-Wave Mixing

GPON Gigabit Passive Optical Network

HDTV High Definition Television

HFC Hybrid Fibre-Coaxial

HPF High-Pass Filter

IEEE Institute of Electrical and Electronics Engineers

IF Intermediate Frequency

IL Injection Locking

IP Internet Protocol

I/Q In-phase/Quadrature

ITLA Integrable Tunable Laser Assembly

ITU International Telecommunication Union

ITU-T ITU Telecommunication Standardization Sector

LED Light-Emitting Diode

LMS Least Mean Square

LO Local Oscillator

LPF Low-Pass Filter

LR Long Reach

MBW Modulation Bandwidth

MLL Mode Locked Laser

MPN Mode Partition Noise

MZM Mach-Zehnder Modulator

NGA Next Generation Access

NG-PON Next Generation Passive Optical Network

NRZ Non-Return-to-Zero

OBPF Optical Band-Pass Filter

OC Optical Carrier

OCDM Optical Code Division Multiplexing

OCDMA Optical Code Division Multiple Access

ODL Optical Delay Line

ODN Optical Distribution Network

O-E-O Optical-Electrical-Optical

OFCG Optical Frequency Comb Generator

OFDM Orthogonal Frequency Division Multiplexing

OFDMA Orthogonal Frequency Division Multiple Access

OLT Optical Line Terminal

ONT Optical Network Terminal

ONU Optical Network Unit

OOK On Off Keying

OpEx Operational Expenditures

OSA Optical Spectrum Analyser

OTDM Optical Time Division Multiplexed

PC Polarisation Controller

PD Photo detector

PDM Polarisation Division Multiplexed

PEV Phase-Error Variance

PFL Passive Feedback Laser

PM Phase Modulator

PON Passive Optical Network

PPG Pulse Pattern Generator

PRBS Pseudorandom Binary Sequence

PSD Power Spectral Density

QAM Quadrature Amplitude Modulation

QD Quantum Dot/Dash

QoS Quality of Service

QPSK Quadrature Phase Shift Keying

RDE Radially Directed Equaliser

REAM Reflective Electroabsorption Modulator

RF Radio Frequency

RIN Relative Intensity Noise

RN Remote Node

ROSA Receiver Optical Subassembly

RPN Resonance Phase Noise

RSOA Reflective Semiconductor Optical Amplifier

SCM Subcarrier Multiplexed

SG Signal Generator

SLD Super-Luminescent Diode

SMSR Side Mode Suppression Ratio

SNR Signal-to-Noise-Ratio

SOA Semiconductor Optical Amplifier

SSB Single Side-Band

SSMF Standard Single Mode Fibre

TDM Time Division Multiplexing

TDMA Time Division Multiple Access

TL Tunable Laser

TOF Tunable Optical Filter

TWDM Hybrid Time and Wavelength Division Multiplexing

UD Ultra-Dense

VCSEL Vertical Cavity Surface Emitting Laser

VOA Variable Optical Attenuator

VoD Video on Demand

VoIP Voice over IP

WDM Wavelength Division Multiplexing

Wi-Fi Wireless Fidelity

WiMAX Worldwide Interoperability for Microwave Access

XG-PON 10-Gigabit-capable Passive Optical Network

XLG-PON 40-Gigabit Time Division Multiplexed Passive Optical Network

Preface

The unprecedented growth of Internet data traffic in the recent decades has brought about a series of changes for the global telecommunication infrastructure. In the metropolitan/ access regions, high speed fibre optic communication technology has now started to penetrate into the "last mile" of the communication network and deliver uncontended bandwidth directly to the final users. Within such a context, the time division multiplexed passive optical networking (TDM-PON) has been achieving considerable success and become the main technology of choice for the previous and current generation of optical access networks. Various TDM-PON standards have been formulated and adopted worldwide to serve the increasing number of optical access users.

Nevertheless, the current TDM-PON specifications are only exploiting a small part of the potential of fibre communication technology. To cope with further increase in the capacity demand, wavelength division multiplexed (WDM)-PON has been proposed for enhanced bandwidth and improved quality of service. The WDM-PON technology is in general considered to be a more efficient way of utilising the available spectrum and has been recognised as one of the most suitable candidates for next generation optical access networks. A major obstacle preventing the large scale implementation of WDM-PON in reality is attributed to the cost sensitive nature of the access market; that is, the mature WDM technology appropriate for the backbone network has turned out to be too expensive for the access segment. As a result, a lot of research and discussions have been dedicated on finding cost efficient solutions for the realisation of these systems. Part of the efforts is notably from the uplink perspective which focuses on a "colourless" approach for the network users.

This thesis intends to create some discussions from another perspective of the WDM-PON system, by concentrating on the downlink portion of the network where bandwidth intense access services are delivered from the centre of the network to the end customers. To provide cost efficiency, optical frequency comb sources have been proposed to support the WDM-PON downlink transmission. An optical comb source offers simultaneous multi-wavelength-channel emission with simplicity, reliability, and some other benefits as will be detailed in the thesis. Within the framework of this thesis, the investigations on a specific kind of gain switched

comb source will be demonstrated with experimental studies, which reveal the fundamental characteristics and some implementation potentials of the device. From the author's point of view, the major contributions resulting from this research work can be outlined as follows:

- The generation and characterisation of a type of optical frequency comb source based on optical injection and gain switching techniques. The notable advantages of this comb source compared to other existing comb generation schemes include its simplicity, inherent stability, low intensity and phase noise, and flexibility in wavelength and free spectral range.
- The application of the proposed injected gain switched comb source in a coherent access downlink scenario. This entails the use of a digital coherent receiver and spectrally efficient optical modulation formats. The demonstrated WDM-PON downlink system offers high data rate, large loss budget, and long transmission distance.
- The proposal and demonstration of a novel pilot tone aided optical scalar detection architecture for the downlink receiver of WDM-PON. Applications of injected gain switched optical comb sources in the proposed network are investigated, and the simple direct detection based system shows large laser phase noise tolerance for the reception of high order modulation formats.

Based on these novel contributions, the remainder of this thesis is organised as follows:

Chapter 1 provides a general introduction on optical access networks, in terms of the motivation of introducing fibre communication technology into the access areas, different types of PON systems, and the benefits of employing comb sources in WDM-PONs. Existing PON standards are reviewed, and the future-proof long reach PON systems are discussed.

Chapter 2 introduces the concept of optical frequency combs, and discusses a few types of comb sources. The selected comb generation schemes include mode locked laser based comb generators, electro-optic modulation based comb generators, and gain switched laser based comb generators. The working principle, basic characteristics, and previous demonstration for access applications of these comb sources are reviewed.

Chapter 3 demonstrates the initial experimental outcomes of this thesis by showing the

generation and basic characterisation of injected gain switched comb sources. Three types of injected gain switched comb sources, together with their salient properties such as spectral bandwidth, noise properties, linearity, and flexibilities are examined.

Chapter 4 presents a detailed phase noise analysis on the injected gain switched comb source, and discusses the potential influence of comb line phase noise on coherent communications. The implementation of the comb source in a long reach coherent access network scenario is also demonstrated and evaluated in terms of receiver sensitivity and system loss budget.

Chapter 5 proposes a novel receiver architecture to allow the reception of high order modulation formats with simple direct detection. The proposed technique is verified through three schemes with the use of three different gain switched comb sources. These schemes are evaluated in terms of transmission distance and receiver sensitivity; their advantages and drawbacks are examined and compared.

Chapter 6 summarises the research outcomes and concludes the thesis. A few possible schemes for future research are also proposed and discussed.

Chapter 1

Optical Access Networks

The aim of this chapter is to provide a general overview on optical access networks. The chapter starts off with a brief review on fibre communication technology and the typical communication network architecture. Major limiting factors in the access network segment are highlighted and fibre access technology is proposed as the optimum solution to provide high bandwidth intensive multi-media services. Hence in this context, Fibre-to-the-x (FTTx) technology is discussed in detail, with the focus placed on the passive optical network (PON) and two of its enabling forms: time division multiplexed (TDM) PON and wavelength division multiplexed (WDM) PON. Key features of these PON architectures are discussed and the evolutionary process of the optical access network is presented. The long reach optical access technology is then introduced as an efficient and economical method for future metro/access consolidation. Finally, the chapter is concluded with a summary.

1.1 General Introduction

1.1.1 Broadband fibre communications

Fibre optic communication has revolutionised the modern society. It has brought in dramatic changes to the global communication infrastructure and largely influenced our daily life. Nowadays the information exchange is fast, easy and exhibits great variety; social activities are more convenient than ever as the virtual distances have being reduced. These advancements are all thanks to the low attenuation, huge bandwidth and low electromagnetic interference [1] of optical fibres as they have now largely replaced conventional copper wire technology in major communication lines, and act as the dominating information transmission media.

There were several fundamental breakthroughs that led to today's widespread use of optical fibre communications. It first began with the successful demonstration of laser operation in 1960 by T. H. Maiman [2]. Soon after, a few steps were taken towards the real-world deployment of commercially viable optical fibres: 1966 - Kao and Hockham publish on fibre waveguides as a communication medium [3]; 1970 - Corning manufactures first fibre to meet Dr. Kao's specifications [4]; 1975 - World's first live traffic was carried over fibre systems in US and UK [5]. The introduction of wavelength division multiplexing (WDM) technology in 1977 [6] and the Erbium doped fibre amplifier (EDFA) in 1987 [7] then provided an immense boost to the total transmission capacity of fibre communication networks, enabling enormous amount of data to be transmitted across transoceanic distances. Essentially, these pioneering efforts have led us into the current era of worldwide optical communications.

In recent years broadband fibre optic communication technology has been progressing rapidly. There have been continual reports and world records on impressive transmission experiments, field trials, and commercial deployments involving ultra-large capacity and/or extremely long distances [8-14]. The motivation behind such developments in the research and commercial worlds is, without doubt, the explosive demand coming from the customer side.

The global telecommunication industry has been through notable development for the past decade yet still sees no sign of stopping. The data traffic is ever-increasing and the demand for bandwidth continues to grow. According to the Cisco forecast announced in May 2013, the global Internet data traffic in 2012 has already reached 32.2 Exabyte (1 Exabyte = 10^{18} bytes) per month and this number will skyrocket to 93 Exabyte per month by 2017 [15]. Meanwhile, traditional telecom services have been experiencing a new definition: due to the advancement of digital technologies and a common Internet Protocol (IP) platform, the boundaries between conventional telecom (phone), Internet (computer), and television networks are now blurring and various voice, data and video services are integrated into a combined business model (the "triple play"). Such service convergence is creating numerous market demands on the bandwidth hungry IP applications of various sorts which all jointly contribute to the network growth and expansion into the foreseeable future. As shown in Fig. 1.1, it has been predicted that the annual global IP traffic will hit the Zettabyte threshold (1 Zettabyte = 10^{21} bytes) by 2015 and go up to 1.4 Zettabyte per year in 2017.

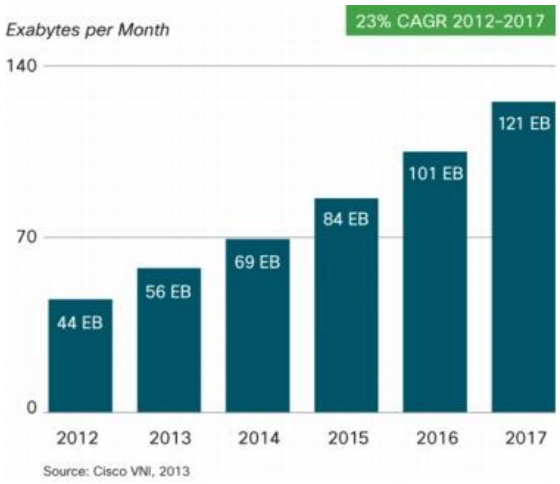

Figure 1.1: Cisco forecasts 120.6 Exabyte per month of IP traffic in 2017 [15].

In light of these trends, the current telecommunication industry is expected to be under pressure soon and will need to look for solutions. This has created a series of research and discussions on the development of advanced photonics techniques, optoelectronic devices, and highly efficient modulation schemes in every segments of the overall communication network [5] [14]. Under the framework of this dissertation the access portion becomes the central element for discussion, and some novel technologies as well as network infrastructure suitable for next generation evolution will be examined.

1.1.2 Communication networks

The overall communication network is an extremely complicated system. A simple geographical division of such a system into several sub-networks could be useful as these individual parts usually operate with different functionalities and distinct requirements [16]. The resultant architecture consists of long haul, metropolitan and access networks and is schematically shown in Fig. 1.2.

The *long haul (core)* networks can be considered as the "backbone" of an overall communication system as they offer long distance data aggregation between cities, countries, and continents. The ultra-long transmissions usually cover hundreds to thousands of kilometres and in some cases the submarine cables could span up to 10,000 km. The network design normally utilises a mesh topology to guarantee robust communication links between major information exchange nodes.

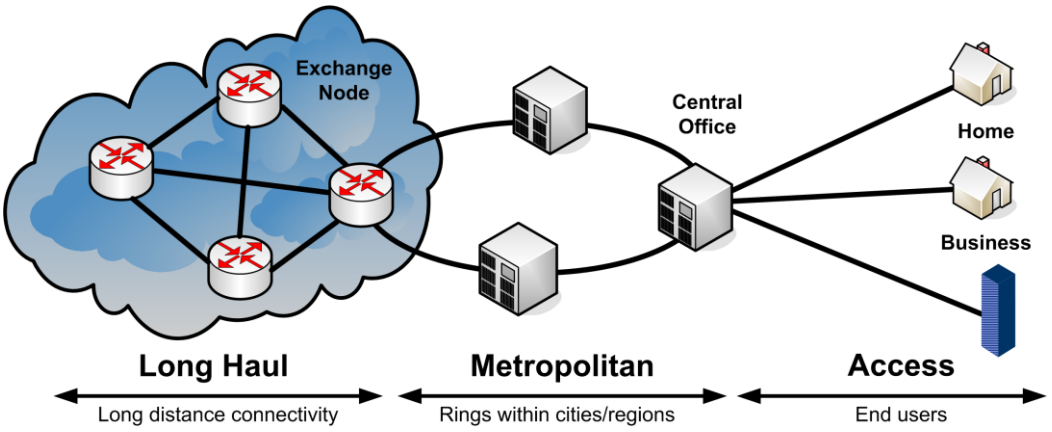

Figure 1.2: Simplified communication network structure. Distances in the figure are only illustrative.

The *metropolitan (metro)* networks provide interconnectivity within a smaller graphical range such as cities and regions. The range of coverage usually varies from tens to hundreds of kilometres, and a ring structure is often adopted to collect traffic from many data sites (central offices). Each central office further spreads out and reaches the far end of the communication network: the user premises. As such, the concept of metro network can sometimes be extended and viewed as the combination of an inter-office metro ring and a metro-access segment [16].

The *access* network, usually referred to as the *"last mile"* (or the "first mile", depending on the direction of communication), represents the final portion of a telecommunication network and provides immediate service distribution to the end users. It extends out to a few or tens of kilometres and links the central offices to the network subscribers (residential or business). The access network can be viewed as the "capillaries" of the general communication network and it usually involves complex architectures with various complicated geographic distributions.

1.1.3 The access bottleneck

The access network is an important ingredient of the telecommunication network as it directly involves the service network consumers. It is also a challenging part of the network design and usually represents a significant limitation to the overall network capacity. The access network has been widely recognised as the "*bottleneck*" since it can easily cause network traffic congestions.

The formation of the access bottleneck can be largely attributed to the drastic improvement of personal information technology. The advancements of personal computers, laptops and

other electronic devices in modern society has produced huge demands on consumer entertainment, e-learning and e-business, thus stimulating a great diversity of multimedia applications such as video on demand (VoD), high definition television (HDTV), voice over IP (VoIP), interactive games, two-way video conferencing etc. The main traffic pattern in the access networks has evolved from simple voice and data centric applications towards the bandwidth exhausting video oriented services and heavily contributes to the global IP traffic. In May 2013, Cisco predicted that 67% of all Internet traffic will be composed of video applications at year 2017 [15]. Dominated by these customer demands, the traffic dynamics in the communication networks are changing: the majority of the network traffic is shifting from the core network towards the metro and access side as service providers try to bring content closer to their customers. According to a Bell Labs study in December 2013, the data traffic in metro-access networks is set for a 560% increase by 2017, with the majority of that traffic terminating in the metro-access portion and less than 25% traversing the core network [17].

For the broadband services delivery, traditional access networks mainly adopt twisted-pair wire based digital subscriber lines (DSL) and hybrid fibre-coaxial (HFC) technologies [18]. These copper based technologies are attractive because they leverage the legacy infrastructure to deliver digital data traffic. The DSL has various standards and they are collectively described by the term xDSL, which utilise traditional telephone lines to provide access bandwidth up to tens of megahertz. The HFC cable network was originally designed by cable television operators and can be used to deliver broadband data services with ~1 GHz bandwidth. However as cable systems are shared-medium networks and a typical network subscriber number ranges between 500 to 2000, the guaranteed bandwidth per user is rather small [18]. Therefore, both DSL and HFC technologies are essentially limited in terms of the available bandwidth and maximum reach, prohibiting the satisfactory delivery of bandwidth intensive triple play services and hindering future development. Although there are other wireless alternatives such as wireless fidelity (Wi-Fi, IEEE: Institute of Electrical and Electronics Engineers standard 802.11) and worldwide interoperability for microwave access (WiMAX, IEEE standard 802.16) providing flexible mobile access solution, these techniques are fundamentally limited by the unreliability of the wireless channel and also have a limited access range.

For future broadband access, optical fibre is one of the most promising candidates. Compared to the rather limited bit-rate-distance product of twisted pair wires and the frequency dependent loss in coaxial cables [19], a standard single mode fibre typically sees < 0.4 dB/km attenuation within the available transmission spectral range (~30 THz) [5]. Therefore fibre access makes high bandwidth service delivery possible over long distances while avoiding the use of serially cascaded power amplifiers in the complicated outdoor environment. Widely recognised as the only future-proof technology [18] [19], optical fibre access has the real potential to overcome the physical media constraints of current copper-based solutions, solve the network traffic congestion in metro/access aggregation, and truly eliminate the bottleneck.

1.2 Optical Access Technology

Similar to most novel technologies, fibre optic communications were first deployed in the long haul and metro networks where telecom service providers usually invest considerable amount of resources. In these networks, cost can be shared amongst hundreds or thousands of subscribers whereas in the access segment, it is more difficult to justify the new deployments due to the relatively smaller number of customers. As an emerging technology, fibre access might be considered as an expensive technical choice and is still facing strong competition from other access solutions [18]. It is reasonable to believe that co-existence will most likely happen for a certain period before the lifetime of current copper access technologies have been reached [20].

Nevertheless, as the global Internet traffic continues to grow from the video-rich services, many service providers have already started moving on to the fibre-to-the-x (FTTx) networks in various parts of the world, where x stands for home, neighbourhood, cabinet, building, premise etc. depending on how close the fibre is to the end user [19]. In February 2013, a statistical report by the FTTH Council Europe (Fig. 1.3) reveals that several countries/regions have already seen higher than 40% of the households deploying the deepest form of fibre access: fibre to the home/building (FTTH/B), where the fibre optic cable directly reaches the building or even inside the home [21]. Meanwhile many other countries are starting or seriously considering joining the optical access market. These figures are believed to be still

increasing, stemming from further cost reduction of photonic components together with the active research and innovation in the area [18].

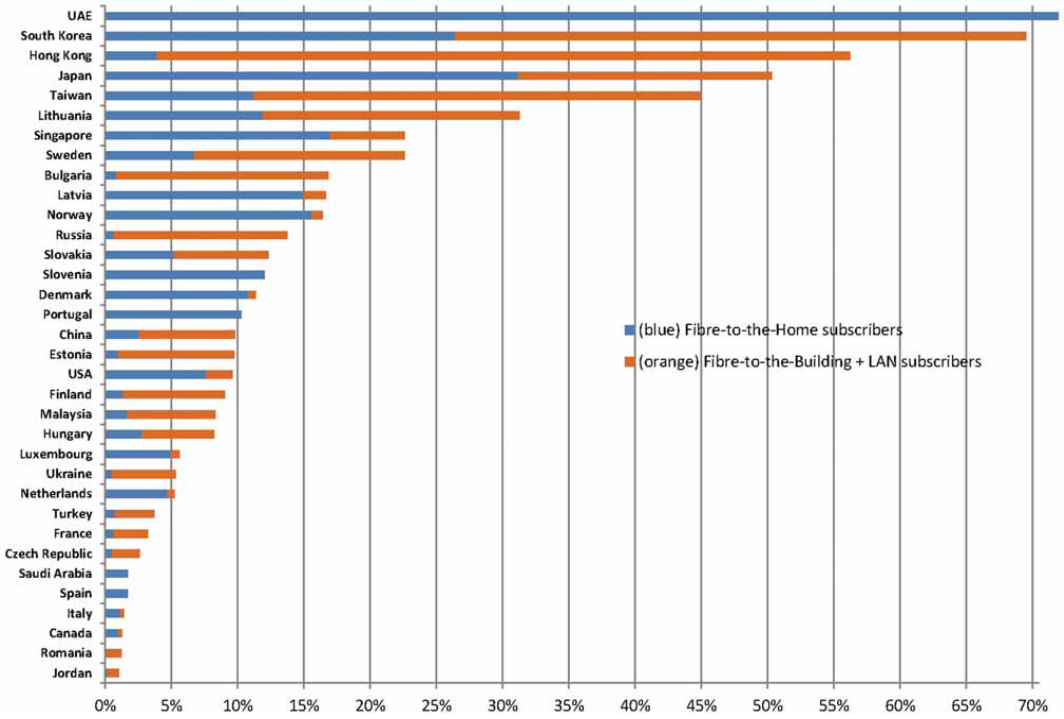

Figure 1.3: FTTH/B global ranking (countries/regions with more than 1% deployment) by the end of 2012 [21].

1.2.1 Passive optical network

The most common network architecture for realising FTTx is the passive optical network (PON) model shown in Fig. 1.4. As the name (passive) implies, there are no active elements at any intermediate point along the optical transmission paths. The active units are located at the end-sides of the communication link, with an optical transceiver device called an optical line terminal (OLT) residing in the central office (CO) to provide the interface between access network and service node, and a number of optical network units (ONUs) either near or inside the user homes (in the latter case an ONU is referred to as ONT: optical network terminal) delivering broadband telecom services through an opto-electronic device. Between the OLT and the ONUs, the number of active elements requiring electrical powering in the outdoor environment is minimised as only passive optical connections exist. The passive optical branching devices (e.g. power splitters or wavelength routers) logically linking the OLT and ONUs are located in a remote node (RN) that is close to the customer premises so that the distributing fibre is of limited length. These branching devices together with the feeder and

distribution fibres are referred to as the optical distribution network (ODN) [18].

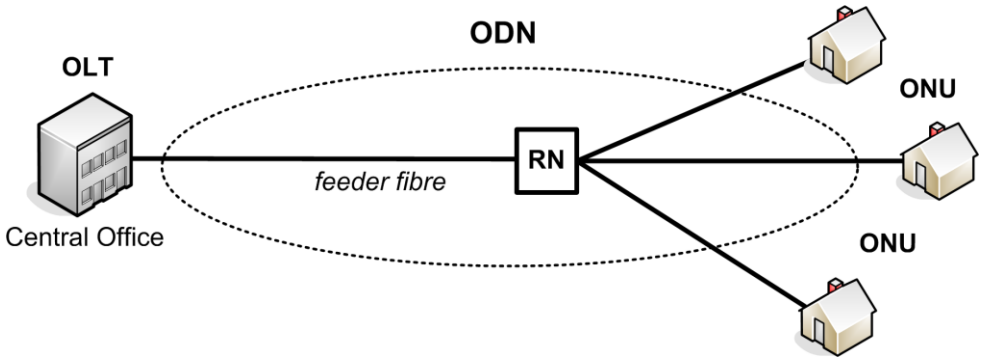

Figure 1.4: A simplified PON infrastructure. Distances in the figure are only illustrative.

The PON technology utilises a point-to-multipoint physical topology. The shared feeder fibre avoids dealing with large numbers of fibres, connectors and optical splices in the network and results in easy termination and space/cost savings in the central office. It also reduces the technical difficulties and maintenance constraints regarding long distance installations of massive components (an ONU can be typically 10 to 20 km from the CO) [22]. In comparison to an active optical network (AON), the PON architecture does not rely on the electrical switching devices at end-sides of the network or the optical-electrical-optical (O-E-O) conversions in the transmission path to manage the signal distributions [23] [24]. However since no routing or buffering is performed to direct the network traffic, certain collision avoiding mechanisms are required in a PON to prevent conflict between different ONU data. A number of techniques have been proposed to guarantee the unobstructed network sharing, examples including time division multiplexing (TDM), wavelength division multiplexing (WDM), orthogonal frequency division multiplexing (OFDM), and optical code division multiplexing (OCDM) [25] [26]. Of these candidates, the TDM and WDM approaches have been recognised as the most feasible solutions for practical PON systems and the TDM-PON has already been standardised [22]. A large amount of effort has been dedicated to the research and development of these two technologies to enable low-cost viable PONs for wide range FTTx services.

1.2.2 Current standard

Currently most commercial PON deployments are utilising the TDM technology. A TDM-PON uses passive optical power splitter(s) to realise the ODN. In such a network, the downstream

information is power split and continuously broadcast to all ONUs; each ONU selects its own portion by an unique identification in the data frame. For the upstream direction, the transmission is in burst-mode: each ONU is individually assigned a unique time slot for the full occupation of the optical bandwidth. The upstream and downstream traffic use two different wavelength bands in order to avoid conflict in the single feeder fibre. From this sense, a TDM-PON also utilises WDM technology. However the term "TDM-PON" or "time division multiple access (TDMA)" [22] specifically refers to the sharing of available bandwidth resource in one direction (downstream or upstream). The operational principle of a TDM-PON is illustrated in Fig. 1.5.

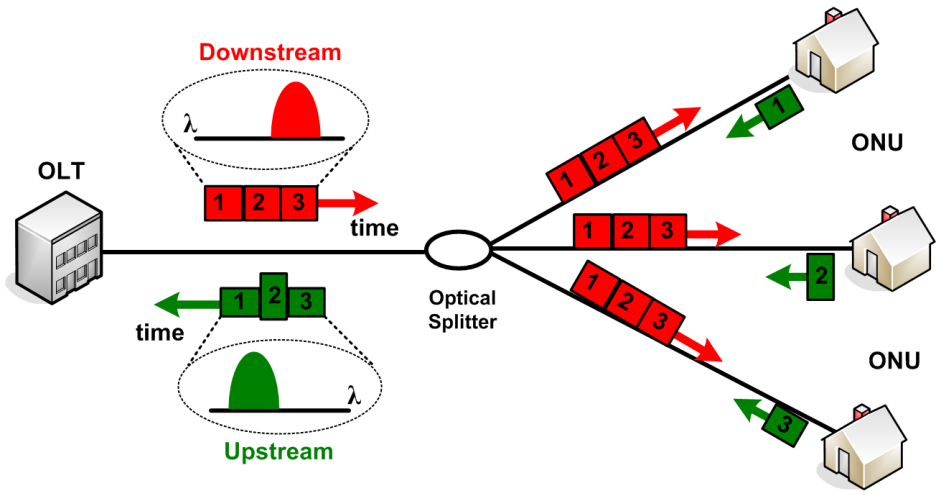

Figure 1.5: TDM-PON operating principle. Distances in the figure are only illustrative.

There are several technical requirements regarding the TDM-PON infrastructure. In the downstream direction, data encryption is needed since all users have access to the broadcast traffic. For the upstream transmission, the OLT has to negotiate with the ONUs and make arrangements between them to avoid packet collision. This involves some complex algorithms to obtain the precise time-delay information between OLT and each ONU (ranging and discovery), as well as an adaptive mechanism for the efficient time-slot assignments amongst ONUs (DBA: dynamic bandwidth allocation) [18]. Due to the burst nature of the upstream transmission, a burst-mode receiver with fast synchronisation ability is needed in the OLT to coordinate multi-user data. Each ONU requires a burst-mode transmitter with high reliability as the malfunctioning of one ONU would cause interference with other ONUs and bring in catastrophic failure for the entire upstream transmission.

The TDM-PON was originally proposed in 1987 under the name "telephony on passive

optical network" [27]. It took several years before some key technologies, such as the low-loss optical splitters and low-cost burst-mode transceivers were developed and became mature [28]. In 1995, the full service access network (FSAN) working group recommended the first TDM-PON model based on the asynchronous transfer mode (ATM) protocol: APON. It was ratified by the International Telecommunication Union (ITU) in 1998 and later redefined in 2005 with extra add-in functionalities [29]. The updated version is called the broadband PON (BPON) and has a nominal line rate up to 1.25 Gb/s for the downstream and a line rate up to 622 Mb/s for the upstream. Due to the ATM nature of the BPON, there are limiting features hindering next-generation upgrades. As such, the gigabit PON (GPON) was proposed by FSAN and ITU in 2003 (current version approved in 2008) [30]. GPON is backward compatible with BPON but further supports the Ethernet protocol [18]. The GPON standard provides line rate of up to 2.4 Gb/s in both downstream and upstream directions although a 1.25 Gb/s upstream is more commonly used [30]. In the meantime, another branch of the study group (Ethernet in the first mile alliance: EFMA) and standards body (IEEE) have been working on the Ethernet version of the high-speed PON system. The result is the Ethernet PON (EPON) standardised by the IEEE 802.3 working group in 2004 [31]. The EPON standard provides symmetric 1.25 Gb/s in both downstream and upstream directions. Currently, both EPON and GPON have become popular FTTx solutions and have been in use in different parts of the world, with EPON dominating the Asian market and GPON deployed mainly in the US [26].

A few years ago, the ITU with FSAN and the IEEE with EFMA both released their updated 10 Gb/s TDM-PON versions to address the explosive growth of Internet services. The standardised solutions are the ITU-T G.987 series XG-PON [32] and the IEEE 802.3av 10G-EPON respectively [33]. XG-PON is an immediate (short-term) solution towards next generation PON (NG-PON) system, providing enhanced security and novel power saving features [26] but also targets full compatibility with legacy PON infrastructures. As a result XG-PON is generally recognised as the next generation PON stage 1 (NG-PON1) [25] [34]. Two phase transmission speeds were identified by the XG-PON standard: 10 Gb/s downstream, 2.5 Gb/s upstream and 10 Gb/s symmetric (namely XG-PON1 and XG-PON2). The 10G-EPON on the other hand, offers symmetric 10 Gb/s transmission, and asymmetric 10 Gb/s

downstream with 1 Gb/s upstream data rates [33].

Recently, field trials have been carried out for both XG-PON and 10G-EPON by several organisations [35] [36]. In 2013, BT and ZTE further demonstrated the first commercial deployment of XG-PON in a live customer environment [37]. Despite these achievements, there are issues associated with these TDM based PON systems. As the bandwidth demand keeps growing and the network requirements become more stringent, some limitations of the TDM technology might be reached. These limiting features stem from the basic properties of the TDM/TDMA technique and are expected to hinder the future evolution of broadband optical access networks [26] [38].

One of the fundamental issues with TDM-PON is that although upstream collision is avoided by time-sharing, the bandwidth resource to each user is also being shared. With a standard PON split ratio of 32 or 64 [29-33], only a few per cent of the channel capacity is actually dedicated to each ONU. The severe loss of the passive power splitter also results in a poor system power budget thus limiting the maximum allowable user number or system range. Meanwhile, with the video-rich multimedia applications now being the prevalent traffic pattern in the access networks peak-hour data traffic has become dominant due to the “prime time” demands. This means that the average Internet traffic has been surpassed [15] and the statistical multiplexing gain in a data centric network is expected to be less useful. As such, the DBA algorithm employed in TDM-PONs to co-ordinate multi-user bandwidth distribution might not suffice for the busy peak-hour traffic. Moreover, with such high pressure on the consumer traffic delivery, whether the network will be able to constantly provide a satisfactory quality of service (QoS) becomes questionable, as a high QoS is a critical factor for the video intense multi-media services. Another issue associated with TDM is that the requirement for the burst-mode transmitter/receiver in the ONU/OLT becomes increasing challenging as data rate grows higher. In particular, since each ONU receiver needs to operate at the aggregated downstream date rate, the receiver bandwidth requirement is much higher compared to its dedicated data rate. This results in a signal-to-noise-ratio (SNR) degradation and also raises cost issues for further upgrade [22].

1.2.3 Next generation access

For future evolution towards next generation access (NGA) networks, the WDM-PON is a

strong candidate to overcome the technical limitations of TDM/TDMA and thereby provide a long-term solution [26]. In the WDM-PON infrastructure, an entirely new network type is adopted and the spectral resource is shared in the wavelength domain even for one transmission direction. Each ONU is assigned a dedicated wavelength pair for the respective upstream and downstream transmission and the wavelength distribution is accomplished through the wavelength router such as an arrayed waveguide grating (AWG) in the ODN, as demonstrated in Fig. 1.6. (Note that as a natural extension, multiple AWGs may be utilised in cascaded fashion to further improve the flexibility and the scalability of the network distribution [18] [38].) One interesting feature with the WDM-PON is that despite the physical point-to-multipoint architecture, the dedicated wavelength pairs actually create a virtual channel between each ONU and the OLT thus providing logical point-to-point connectivity.

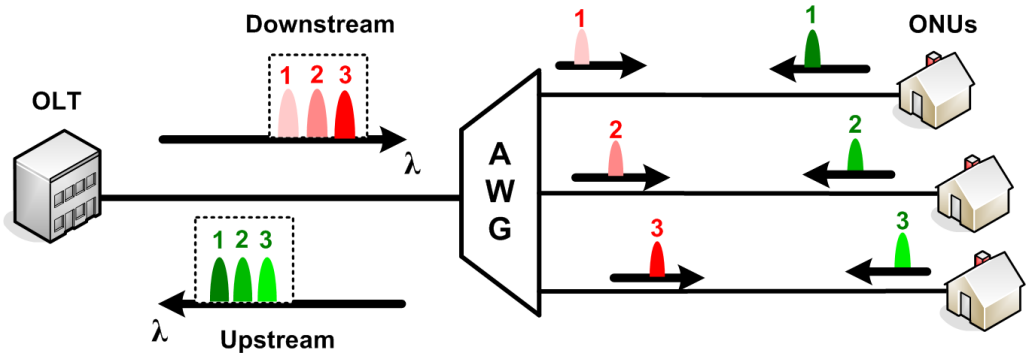

Figure 1.6: WDM-PON configuration. Distances in the figure are only illustrative.

The WDM-PON concept was first proposed in 1986 [39] and it is a powerful way to efficiently share the network bandwidth. Compared to the TDM-PON technology, the WDM channelization uncouples the ONUs from each other, ensuring robust connections between the CO and the users with enhanced security, protocol and bit rate transparency, and at the same time guarantees bandwidth and QoS experience (particularly attractive for latency-sensitive video based services [26]). Since the power splitters are replaced by wavelength routers the ODN loss of a WDM-PON is considerably reduced, translating into a relaxed power budget and resulting in longer transmission distances and/or a higher network user count. In addition, the absence of burst mode transceivers in the ONU/OLT releases the time-sharing management issues of TDMA, providing format agnostic operation and reduced receiver bandwidth requirements at the ONU.

On the other hand, the use of a WDM device (AWG) in the ODN has brought in some

problems for the WDM-PON. First of all, the network broadcast ability has now been lost and so has the DBA capability that shares the unused bandwidth across customers on demand. Secondly, the network agility is gone and the network is now spectrally "locked" or "coloured", meaning that the OLT and the ONUs need to have wavelength specific transmitters (the receivers need not to be wavelength specific as the ODN performs channel selection). The latter issue has been of major concern since under the cost-sensitive access network scenario, dedicating a pair of wavelength unique optoelectronic devices to each remote access location (ONU) could be prohibitive from repair, management and inventory perspective. For a cost-effective solution, the ONU transmitters should avoid fixed wavelength devices and become "colourless": that is, all ONUs should be able to work on any of the operating wavelengths in the system using identical devices to provide cost savings, operations, administration and maintenance simplification [4].

The component cost issue has been a significant barrier for the wide scale implementation of WDM-PON systems. Despite the universal success of WDM technology in long-haul and metro transmissions, there have been no standards defined on WDM-PON at the moment. Pioneering commercial deployment was noticed in Korea [40] and a field trial has recently been conducted in Austria [41] but the economical result still waits to be evaluated. On the whole, WDM-PON has lost its initial competition with TDM-PON technology over the current access market and is waiting for its moment in NGA networks. Despite this, the research work on WDM-PONs has not stagnated. Over the past decade extensive efforts have been devoted to the topics on low-cost ONU and OLT design, creating active investigations and discussions [42-45]. As an overview on these research proposals some basic principles and key issues will be briefly covered, starting from the ONU side.

Colourless ONU

Tunable laser (TL) – each ONU can be equipped with an identical wavelength tunable laser source within a pre-defined transmission band. The TL could be directly or externally modulated depending on the desired system performance/economics trade-off. Candidate TLs include external cavity laser (ECL) [46], multi-section distributed Bragg reflector (DBR) devices [47] [48], tunable distributed feedback (DFB) laser array [49], tunable vertical cavity surface emitting lasers (VCSELs) [50] and VCSEL array [51]. Technical issues with this

approach include the high cost of the TL devices [44] and wavelength stabilisation/alignment between the laser and the AWG [48], as well as the prior knowledge of assigned wavelength for true colourless operation [52].

Broadband light source (BLS) – instead of using a laser, each ONU can modulate a wavelength independent broadband light source and the upstream wavelength assignment is achieved by an AWG in the RN: different AWG ports pass through different spectral portions of the BLS thus defining individual working channel for each user (the technique is therefore known as "spectral slicing" [45]). The BLS approach was actually the first technique proposed as the simple and low-cost ONU transmitter [53]. Possible BLSs include light-emitting diode (LED) [54], super-luminescent diode (SLD) [55], and multimode Fabry-Pérot (FP) laser [56]. Limitations of this approach include poor power budget/short system reach [56], the bandwidth (bit rate) restriction due to the associated dispersion penalty, and increased intensity noise due to spectral filtering [45].

Injection locking (IL) – a multi-longitudinal mode FP laser can be used in the ONU as wavelength agnostic source and injection locked by an external optical signal to achieve single mode operation [57]. The optical injection can be realised by remote seeding from the OLT using: 1) a spectral-sliced incoherent BLS (e.g. amplified spontaneous emission (ASE) source) [58], 2) optically filtered multi-wavelength transmitter such as a mode locked laser (MLL) [59], 3) the modulated downstream signal [60]. Alternatively, injection can be accomplished by self-seeding with the help of a fibre Bragg grating (FBG) that could be placed in the RN [61]. The IL approach has similar advantages as the BLS method in terms of simplicity and low-cost and has been adopted by Korea Telecom for commercial installation [40]. However, backscattering noise from the BLS, and injection related issues such as power requirements, locking range and stability remain to be major points of concern and the ultimate scalability of this technique needs further investigation [62].

Reflective scheme – the use of a reflective device such as a reflective semiconductor optical amplifier (RSOA) or a reflective electroabsorption modulator (REAM) also eliminates altogether the wavelength dependency in the ONU. (The RSOA and REAM can be further integrated together to enjoy the merits of both components [44] [45].) The reflective scheme has raised increasing attention in recent years and the proposed external seeding methods for

upstream modulation include: 1) centralised light source (CLS) in the OLT providing either un-modulated continuous-wave [63], or modulated downstream signal for wavelength-reuse (re-modulation) [64]; 2) self-seeded RSOA by its own spectrally-sliced ASE light with a passive reflective path in the RN [65]. Potential problems that need to be dealt with involve limited modulation bandwidth of RSOA, high requirements on the link budget (for sufficient CLS power) [44], and the complicated multiple interference between downstream and upstream signals (back reflections, Rayleigh and Brillouin backscattering) [66] [67]. Novel techniques addressing some of these issues have been reviewed in [26].

OLT management

Although the ONU has been attracting lots of attention for cost reduction and operational simplification, the symmetrical nature of a WDM-PON suggests that the downstream portion of the network is equally important and the OLT cost and complexity should be carefully considered as well [68]. Since the WDM-PON is designed for virtual point-to-point connections, the OLT equipment can no longer be shared amongst multiple ONUs as in the TDM-PON (where a single high-performance transceiver communicates with multiple ONUs). Hence, the number of optical transceivers in the CO increases thereby increasing the power dissipation of optic/electronic components. Other issues like installation and maintenance of these devices and space management in the CO, have all contributed to the increase in capital and operational expenditures (CapEx and OpEx) for network operators. It has been estimated that approximately 50% of the network cost in a WDM-PON can be assigned to the OLT [69].

An important functionality of the OLT entails the support of multiple user traffic by providing a multi-wavelength optical signal for downstream transmission or for upstream seeding. Obviously, the aforementioned colourless schemes can be exploited to neatly solve the inventory issue. Photonic/hybrid integration [44] [68] [69] then offers a great opportunity to clear up the stacking of discrete devices (multiple lasers, BLSs or reflective components) and their fibre spaghetti, resulting in size and space saving in the CO. Nevertheless, with the use of these discrete components a few potential issues remain of concern (take discrete lasers for example): 1) to maintain the acceptable level of wavelength accuracy and stability dictated by future dense and ultra-dense WDM-PONs (e.g. with channel spacing of 10 GHz or less), each laser would require high precision temperature controller and/or wavelength locker, in

addition to its own biasing circuit; the fabrication, inventory and operation of these lasers (in particular low linewidth lasers for the possible employment of advanced optical modulation formats) as well as the controlling circuits might prove costly and power consuming. 2) given the intention to manipulate emission wavelength or WDM channel spacing for certain applications, the wavelength of each laser needs to be tuned separately hence complicating the system operation.

In comparison, reduced number of optical transmitter components and great ease on temperature/wavelength tracking are expected with the employment of optical frequency comb sources at OLT [59] [70] [71]. By virtue of the intrinsic property of an optical comb source, a number of simultaneous and independent wavelength channels can be generated with desired (sometimes changeable) spacing, and the tuning of the entire wavelength comb can be achieved with just one control [42]. With further improvement from advanced integration technologies, the highly functional optical comb generation can be realised based on a compactly packaged device thus resulting in a reduced physical size/dimension [72]. The superiorities of such an approach are expected to reflect in the reduction of active components required in the OLT, the decrease in device footprint and power consumption, and a simplified system operation, which all eventually attribute to the network cost reduction, and energy and environmental savings.

The investigations on the optical comb source have been going on for decades yet the application in an access network scenario has received relatively little attention. As mentioned above, the employments of comb sources in the optical access networks results in economic benefits and some other advantages. Notably, these advantages are expected to become useful features for future access network evolution. As communication networks keep evolving, one might take one step forward and envision future network consolidations as the access concept being extended towards larger area and the metro/access interface start merging [73-75]. The resulting network requirements will be very similar to those under discussion in current metropolitan scenarios where finer wavelength granularities with enhanced spectral efficiency and network flexibility have caused serious concerns [76] [77]. The interesting properties of the optical comb sources can perfectly fit into such a scalable and elastic networking context, and the potential of an optical comb sources as a multi-carrier transmitter for future

metro-access applications is promising [77-79]. In the following chapters of this dissertation, detailed studies on the optical comb generation and their applications for WDM-PON based NGA networks will be elaborated.

1.3 Evolutionary Path

Thus far the TDM-PON has been the market leader in worldwide optical access deployments and has evolved over several technology generations. The incoming commercial wave, driven by the newly standardised 10 Gb/s capable XG-PON and 10G-EPON, will offer enhanced bandwidth service delivery but still uses TDM/TDMA as technical basis. For future network demands, it is widely agreed that current TDM-PON cannot economically support the high bandwidth, high subscriber density, extended reach, flexibility, and scalability [26] [28]. Therefore a time might eventually come for other novel multiple access technologies to join the market share.

In terms of the technical selection for network migration, WDM-PON is a promising candidate but not the only choice. There have been competitive alternatives under careful evaluation, examples include: orthogonal frequency division multiple access (OFDMA) that provides flexible network resource assignment and highly efficient bandwidth usage through the advancements of digital processing techniques [80], optical code division multiple access (OCDMA) which offers asynchronous transmission with high data confidentiality [81], and a group of hybrid approaches combining different technologies: hybrid time and wavelength division multiplexed PON (TWDM-PON) [82], TDM-OFDM-PON [83], TDM-OCDMA-PON [84], WDM-OFDMA-PON [85], and WDM-OCDMA-PON [86]. With respect to some of these schemes such as OCDMA and OFDMA, although they are technically interesting the complex requirements in terms of unconventional optics or electronics might delay or prevent their practical implementation [25] [26]. During the technical transitions of optical access network systems, cost-effectiveness stands out as one of the key goals; network operators will always move cautiously and try to avoid large modification to the existing network (unless absolutely necessary) through utilising the legacy infrastructure as much as possible. A smooth and less disruptive network upgrade, in terms of both hardware and services, is highly appreciated for network savings and seamless transition.

1.3.1 Seamless upgrade

Among all the migration schemes, the hybrid TWDM-PON has been chosen by FSAN as the primary solution for 40-Gigabit-capable NG-PON2 systems [25] [82]. The selection of TWDM-PON technology has been through careful deliberation, with three other competitors eventually sifted out: 40 Gigabit TDM-PON (XLG-PON), WDM-PON and OFDM-PON [82]. Very recently, the FSAN group and ITU-T have started the standardisation progress on TWDM-PON and the first edition of ITU recommendation was already approved in March 2013 [87]. The TWDM-PON basically stacks several TDM-PON systems utilising the WDM technology (each TDM-PON operating at a different wavelength pair) to increase the overall system capacity. If XG-PON1 were used, 4 wavelength pairs can provide total 40 Gb/s transmission capability in the downstream and 10 Gb/s in the upstream [88]. An example of the basic TWDM-PON network architecture is demonstrated in Fig. 1.7.

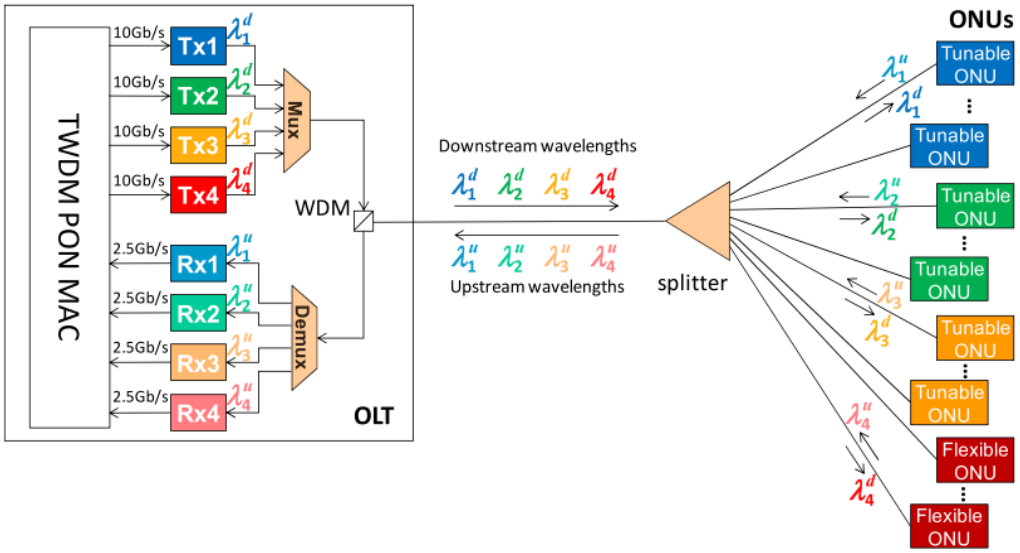

Figure 1.7: A typical TWDM-PON system configuration (4 wavelength pairs) [88].

The hybrid TWDM-PON is a smooth migration step from TDM-PON towards WDM-PON while maintaining some attractive characteristics from both network infrastructures. On the one hand, TWDM-PON retains the flexible power-splitting feature from TDM-PON (an asset hard to replicate in pure WDM-PON) by supporting legacy ODN [87]. This feature enables the re-use of established technical capabilities and protects the major investments made for deploying previous PON generations, avoiding unacceptable service interruption and sustaining co-existence with current systems. On the other hand, the WDM stacking supports:

1) incremental growth of network capacity through gradually populating more TDM/TDMA wavelength pairs (up to 8 pairs [87]), allowing “pay as you grow” on-demand service provisioning; 2) multiple operators sharing one physical network infrastructure. Further enhanced network flexibility can be achieved with the dynamic TWDM-PON architecture [89] (namely the DWA: dynamic wavelength allocation technology [18]) where the ONU wavelength assignment can be changed during communication operations. The DWA enables some useful functionality such as resilience and power-savings for the TWDM-PON system [89].

In a TWDM-PON the OLT side requires some hardware modifications compared to current TDM-PON standards, such as the additional optical transmitters and receivers and the wavelength multiplexer (Mux) and de-multiplexer (Demux) shown in Fig. 1.7. In order to achieve higher system power budget optical amplifiers might be introduced as well [82]. These additional investments (CapEx) are expected to be justified by the increased network throughput and the matter should be trivial. The OLT footprint/energy consumption and management (OpEx), though, might become of concern as several wavelength pairs are now involved in a TWDM-PON system. Moreover, the low-cost colourless ONU requirement forms the real challenging bit of the network design, as each ONU must be able to operate on any of the upstream/downstream wavelengths for easy operation and maintenance. To address these issues, integrated transceiver prototypes have been recently reported for OLT and ONU [88]. The OLT transceiver module utilises electroabsorption modulated lasers (EMLs) and avalanche photodiode (APD) based receiver optical subassemblies (ROSAs), whereas the colourless ONU module contains a thermally tuned directly modulated DFB laser and a tunable filter inside the ROSA. The OLT and ONU transceiver devices are manufactured in enhanced C form factor pluggable (CFP) and small form factor pluggable (SFP+) package respectively [88], demonstrating compact solutions for the network operators and end customers.

The beginning of the NG-PON2 standardisation process and the release of state of the art prototypes are positive signs for the potential commercial deployments and the prospect of TWDM-PON. Of course, these progresses do not necessarily guarantee market acceptance, but they do provide an excellent starting point for examining the realistic cost and performance

requirements that the designers of a fibre access system will be expecting to meet. Furthermore, the important role of such an evolving technology also lies in its potential to unify the diverse access market, which has been caused by the existence of different standardisation bodies and various PON standards. These parallel standards (e.g. GPON versus EPON) and multiple PON generations (e.g. BPON, GPON, and XG-PON) may confuse the emerging fibre access market and delay the deployment cycle, whereas the new standard trend might hopefully provide a perfect merging point to benefit the whole industry. It is also noteworthy that as pioneer example, the Korea Telecom has already installed TWDM-PON system (with RSOA transmitters) for commercial service since March 2009 [90].

1.3.2 Long reach optical access

As another important aspect of the access evolution, extending the physical reach (and/or optical split) of the access network has gained great interest. This entails the increase of the transmission range from a typical 10 or 20 km [30-33] to over 50 km (or even 100 km) in order to improve the overall network integrity [91-103]. By utilising optical access to reach deep into the aggregation network and terminate on a core edge node, the metropolitan ring can be bypassed and all traffic grooming, marshalling and concentration can be performed based on a consolidated platform [73]. The resulting structure concentrates OLTs in fewer COs to serve a larger geographic area, fragmenting the network cost over an increased subscriber count and minimising the network planning. For rural and remote districts with sparse population, the long reach (LR) access networks are particularly suitable to reduce the CapEx and OpEx associated with setting up and running nearby COs through the use of a highly functional centralised PON system [26]. To illustrate the simplified network architecture, Fig. 1.8 shows a converged metro/access aggregation (red solid lines) versus conventional metro ring topology connecting multiple legacy COs (dashed lines).

In the design of a LR access network, the optical power budget is a vital parameter to cope with the increased transmission distance and power splitting ratio. There are several ways to achieve a higher power budget. One option is to employ higher power transmitters and more sensitive receivers; this however, requires modifying the network terminals (OLT and ONUs) and thus is less preferable. Another method depends on the advancement of high forward error

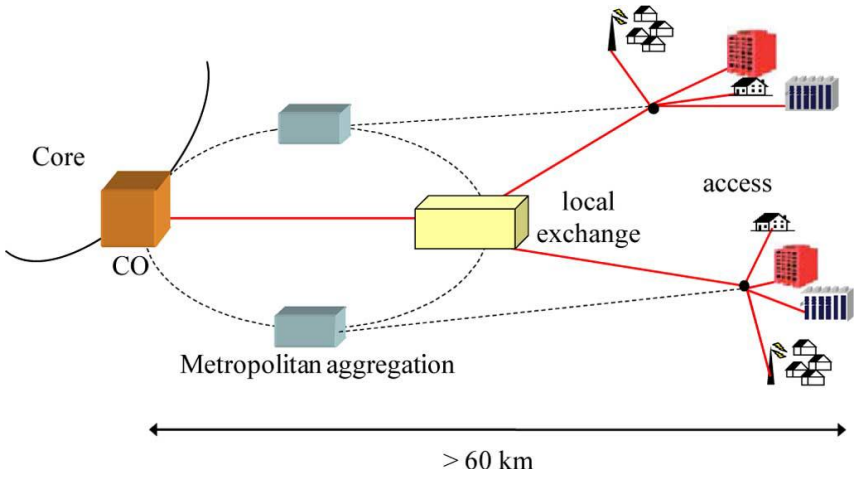

Figure 1.8: Long reach optical access system for network consolidation [26].

correction (FEC) coding gain, which can be of some value but the link budget improvement is rather limited [91]. A more powerful approach is the use of optical amplification techniques, including distributed remote (Raman) amplification [92] or mid-span reach extenders in the ODN [45]; the latter has raised notable research interests since the early 1990s [93-95] with possible candidates including semiconductor optical amplifiers (SOAs), rare-earth doped fibre such as Erbium doped fibre amplifiers (EDFAs), or electronic regeneration (O-E-O).

Indeed, the employment of active mid-span repeaters might move away from the initial engineering principle of a PON system: to keep the ODN passive. Nevertheless, it is believed that the advantages brought about by the LR PON system could potentially leverage these extra hardware deployments and eventually lead to revenue growth (especially for greenfield deployments where fibre connections are constructed for the first time and installation cost is an inescapable fact) [73] [91]. Moreover, if optical amplifiers were used the fibre optics remains transparent to protocol and modulation formats therefore it is still "passive" in a sense that the upper transmission layers are untouched [74]. As the communication network requirements keep developing and low-cost amplifier technologies become mature, the LR PON concept is now under serious consideration and the reach extension of PON systems has been standardised by ITU for GPON and XG-PON recently [96] [97]. The possibility for commercial deployments has also been demonstrated, with a typical GPON system (1:32 split size and 20 km reach) improved to 60 km and 1:128 split through SOA based reach extender prototypes and a 10 Gb/s capable XG-PON1 prototype system upgraded to 100 km reach, 512-way split via mid-span EDFAs [91]. In addition the field trial of a 100 km symmetric rate

10G-EPON was also successfully demonstrated with the use of cascaded SOAs [36].

While reach extension has been proved to be a feasible solution for TDM-PONs, the idea can be equally applied to the hybrid TWDM-PON systems [98] [99]. As for the WDM-PON infrastructures, the low-loss nature of the ODN makes it possible to achieve LR transmissions without any form of mid-span repeaters but at the price of reduced reconfigurability [100-102]. To make up for this expense, digital coherent receivers have gained research attention for LR access applications within recent years [78] [79] [103]. Here, the frequency selectivity of coherent receivers effectively enables dense or ultra-dense WDM-PON schemes running on legacy power splitter based ODNs without the need for narrow band optical filtering [103] [104]. Through proper engineering the tunable laser based local oscillators (LOs) can be further exploited as upstream transmitters [104] [105]. Other advantages attributed to the use of digital coherent receivers are the high sensitivity, transmission impairment compensation (through digital signal processing) and potential high spectral efficiency (by spectrum shaping and the use of advanced modulation formats).

In reality, the main obstacle of introducing digital coherent detection into optical access networks (coherent access) is probably the considerable investment on high performance components (LO, optical hybrid, balanced-photodetectors etc.) that are required in each ONU. Besides, there are major disruptive installations and complex operational issues that need to be addressed in the ONUs and at OLT. These concerns suggest that the coherent access approach, despite its potentials and attractiveness for LR PON applications, might stay in the research and development stage for a while and might not be ready for the commercial deployment in the near future [26]. Looking ahead, with emerging works and continuing advances in photonic/hybrid integration, high speed processors and other relating technologies [103] [105], the cost curve may be eventually dragged down to meet the demand growth and the high CapEx for initial deployments might be finally offset by the low OpEx per user, making the coherent PON solution competitive in the access market and ready to take off.

1.4 Summary

In this chapter the general situation on current and future optical access networks has been reviewed. As the communication networks keep suffocating from the explosive global data

growth, fibre optics is being introduced into the access segment. The current optical access market mainly employs time division multiplexed/time division multiple access passive optical network (TDM/TDMA-PON) therefore key technical features and various standards have been discussed. For upgraded FTTx services and enhanced future proofing the wavelength division multiplexed passive optical network (WDM-PON) has been proposed but faces cost-related issues. The economic and engineering concerns mainly come from two end-sites of the network: 1) at OLT a robust comb source is critical for providing multi-user services; 2) in the ONU cost-effective "colourless" solution must be deployed. Therefore to allow for smooth and practical access upgrade the hybrid TWDM-PON has been selected as the next step migration. Long reach access further provides another attractive direction for future metro/access evolution with a reduced number of network nodes and a consolidated network structure.

References

[1] J. M. Senior, *Optical Fibre Communications: Principles and Practice* (Pearson, 2009).

[2] T. H. Maiman, "Stimulated optical radiation in ruby," Nature **187**, 493 (1960).

[3] K. C. Kao and G. A. Hockham, "Dielectric-fibre surface waveguides for optical frequencies," Proc. IEE **113**, 1151 (1966).

[4] http://www.corning.com/opticalfibre/

[5] H. Venghaus and N. Grote (Editors), *Fibre Optic Communication: Key Devices* (Springer, 2012).

[6] W. J. Tomlinson, "Wavelength multiplexing in multimode optical fibres," Appl. Opt. **16**, 2180 (1977).

[7] R. J. Mears, L. Reekie, I. M. Jauncey, and D. N. Payne, "High-gain rare-earth-doped fibre amplifier at 1.54μm," in *Proc. OFC 1987, WI2*.

[8] M. Salsi, O. Bertran-Pardo, J. Renaudier, W. Idler, H. Mardoyan, P. Tran, G. Charlet, and S. Bigo, "WDM 200Gb/s single-carrier PDM-QPSK transmission over 12,000km," in *Proc. ECOC 2011, Th.13.C.5*.

[9] J. Yu, Z. Dong, H. C. Chien, Z. Jia, X. Li, and N. Chi, "WDM transmission of 108.4-Gbaud PDM-QPSK signals (40×433.6-Gb/s) over 2800-km SMF-28 with EDFA only," in *Proc. ECOC 2012, Mo.2.C.2.*

[10] D. G. Foursa, H. G. Batshon, H. Zhang, M. Mazurczyk, J. X. Cai, O. Sinkin, A. Pilipetskii, G. Mohs, and N. S. Bergano, "44.1 Tb/s transmission over 9,100 km using coded modulation based on 16QAM signals at 4.9 bits/s/Hz spectral efficiency," in *Proc. ECOC 2013, PD3.E.1*.

[11] http://newscenter.verizon.com/corporate/news-articles/2013/08-12-verizon-completes-200g-field-trial/

[12] http://coriant.com/company/press_release.asp?id=1029

[13] http://www.ciena.com/connect/blog/Comcast-and-Ciena-hit-1-Terabit-using-toolbox-of-new-optical-technologies.html

[14] M. Nakazawa, K. Kikichi, T. Miyazaki (Editors), *High Spectral Density Optical Communication Technologies* (Springer, 2010).

[15] http://www.cisco.com/c/en/us/solutions/service-provider/visual-networking-index-vni/index.html

[16] R. Ramaswami, K. N. Sivarajan, and G. H. Sasaki, *Optical Networks: A Practical Perspective* (Morgan Kaufmann, 2010).

[17] http://www.opticalconnectionsnews.com/1/post/2013/12/bell-labs-predicts-560-increase-in-metro-network-traffic-by-2017.htmlhttp://www2.alcatel-lucent.com/blogs/corporate/2013/12/shift-metro-networks-into-high-gear/

[18] L. G. Kazovsky, N. Cheng, W. Shaw, D. Gutierrez, and S. Wong, *Broadband Optical Access Networks* (Wiley, 2011).

[19] C. Lam, *Passive Optical Networks: Principle and Practice* (Academic, 2007).

[20] D. Stoneback and M. Mobility, "From hybrid fibre coax to all-fibre networks", in *Proc. ECOC 2012, Mo.1.B.1.*

[21] http://www.ftthcouncil.eu/documents/Presentations/20130220PressConfLondon_Online.pdf

[22] C. Lee, W. V. Sorin, and B. Y. Kim, "Fibre to the home using a PON infrastructure," J. Lightwave Technol. **24**, 4568 (2006).

[23] C. P. Larsen, A. Gavler, and K. Wang, "Comparison of active and passive optical access networks," in *Proc. Conference on Telecommunications Internet and Media Techno Economics (CTTE 2010).*

[24] M. Forzati and A. Gavler, "Flexible next-generation optical access," in *Proc. International Conference on Transparent Optical Networks (ICTON 2013), We.A1.3.*

[25] P. Vetter, "Next generation optical access technologies," in *Proc. ECOC 2012, Tu.3.G.1.*

[26] E. Wong, "Next-generation broadband access networks and technologies", J. Lightwave

Technol. **30**, 597 (2012).

[27] J. R. Stern, J. W. Balance, D. W. Faulkner, S. Hornung, and D. B. Payne, "Passive optical local networks for telephony applications and beyond," Electron. Lett. **23**, 1255 (1987).

[28] P. P. Iannone and K. C. Reichmann, "Optical access beyond 10 Gb/s PON," in *Proc. ECOC 2010, Tu.3.B.1.*

[29] ITU-T, *Broadband optical access systems based on Passive Optical Networks (PON)*, Recommendation G.983.1 (2005).

[30] ITU-T, *Gigabit-capable Passive Optical Networks (GPON): General characteristics*, Recommendation G.984.1 (2008).

[31] IEEE, *Carrier sense multiple access with collision detection (CSMA/CD) access method and physical layer specifications, Amendment: Media Access Control Parameters, Physical Layers, and Management Parameters for Subscriber Access Networks*, Std. 802.3ah (2004).

[32] ITU-T, *10-Gigabit-capable passive optical networks (XG-PON): General requirements*, Recommendation G.987.1 (2010).

[33] IEEE, *Carrier sense multiple access with collision detection (CSMA/CD) access method and physical layer specifications, Amendment 1: Physical Layer Specifications and Management Parameters for 10 Gb/s Passive Optical Networks*, Std. 802.3av (2009).

[34] H. Nakamura, "NG-PON2 technologies," in *Proc. OFC 2013, NTh4F.5.*

[35] S. Jain, F. Effenberger, A. Szabo, Z. Feng, A. Forcucci, W. Guo, Y. Luo, R. Mapes, Y. Zhang, and V. O' Byrne, "World's first XG-PON field trial," in *Proc. OFC 2010, PDPD6.*

[36] M. Fujiwara, T. Imai, K. Taguchi, K. Suzuki, H. Ishii, and N. Yoshimoto, "Field trial of 79.5-dB loss budget, 100-km reach 10G-EPON system using ALC burst-mode SOAs and EDC," in *Proc. OFC 2012, PDP5D.8.*

[37] http://wwwen.zte.com.cn/en/press_center/news/201306/t20130607_399833.html

[38] K. Grobe and J. P. Elbers, "PON in adolescence: from TDMA to WDM-PON," IEEE Commun. Magazine, **46**, 26 (2008).

[39] D. Payne and J. Stern, “Transparent single-mode fibre optical networks,” J. Lightwave Technol. **LT-4**, 864 (1986).

[40] C. Lee, S. Lee, K. Choi, J. Moon, S. Mun, K. Jeong, J. H. Kim, and B. Kim, “WDM-PON experience in Korea,” J. Opt. Netw. **6**, 451 (2007).

[41] http://www.advaoptical.com/en/newsroom/press-releases-english/20140122.aspx

[42] R. D. Feldman, E. E. Harstead, S. Jiang, T. H. Wood, and M. Zirngibl, “An evaluation of architecture incorporating wavelength division multiplexing for broad-band fibre access,” J. Lightwave. Technol. **16**, 1546 (1998).

[43] F. Ponzini, F. Cavaliere, G. Berrettini, M. Presi, E. Ciaramella, N. Calabretta, and A. Bogoni, “Evolution scenario toward WDM-PON,” J. Opt. Commun. Netw. **1**, C25 (2009).

[44] K. Prince, T. B. Gibbon, R. Rodes, E. Hviid, C. I. Mikkelsen, C. Neumeyr, M. Ortsiefer, E. Ronneberg, J. Rosskopf, P. Ohlen, E. I. Betou, B. Stoltz, E. Goobar, J. Olsson, R. Fletcher, C. Abbott, M. Rask, N. Plappert, G. Vollrath, and I. T. Monroy, “Giga WaM—next-generation WDM-PON enabling Gigabit per-user data bandwidth,” J. Lightwave. Technol. **30**, 1444 (2012).

[45] L. H. Spiekman, “Active devices in passive optical networks,” J. Lightwave. Technol. **31**, 488 (2013).

[46] J. H. Lee, M. Y. Park, C. Y. Kim, S. Cho, W. Lee, G. Jeong, and B. W. Kim, “Tunable external cavity laser based on polymer waveguide platform for WDM access network,” IEEE Photon. Technol. Lett. **17**, 1956 (2005).

[47] M. J. Wale, “Options and trends for PON tunable optical transceivers,” in *Proc. ECOC 2011 Mo.2.C.1.*

[48] K. Grobe, “Access networks based on tunable transmitters,” in *Proc. ECOC 2013 We.1.F.1.*

[49] H. Suzuki, M. Fujiwara, T. Suzuki, N. Yoshimoto, H. Kimura, and M. Tsubokawa, “Wavelength-tunable DWDM-SFP transceiver with a signal monitoring interface and its application to coexistence-type colorless WDM-PON,” in *Proc. ECOC 2007, PD3.4.*

[50] E. Wong, M. Muller, and M. C. Amann, “Colourless operation of short-cavity VCSELs in

C-minus band for TWDM-PONs," Electron. Lett. **49**, 282 (2013).

[51] E. Lee, J. C. Lee, S. Mun, E. Jung, J. H. Lee, and S. S. Lee, "16-channel tunable VCSEL array with 50-GHz channel spacing for TWDM-PON ONUs," in *Proc. ECOC 2013, Tu.1.F.3.*

[52] S. Moon, H. Lee, and C. Lee, "Automatic wavelength allocation method using Rayleigh backscattering for a WDM-PON with tunable lasers," J. Opt. Commun. Netw. **5**, 190 (2013).

[53] S. S. Wagner, H. Kobrinski, T. J. Robe, H. L. Lemberg, and L. S. Smoot, "Experimental demonstration of a passive optical subscriber loop architecture," Electron. Lett. **24**, 344 (1988).

[54] M. Zirngibl, C. H. Joyner, L. W. Stulz, C. Dragone, H. M. Presby, and I. P. Kaminow, "LARNet, a local access router network," IEEE Photon. Technol. Lett. **7**, 215 (1995).

[55] S. S. Wagner and T. E. Chapuran, "Broadband high-density WDM transmission using superluminescent diodes," Electron. Lett. **26**, 696 (1990).

[56] S. L. Woodward, P. P. Iannone, K. C. Reichmann, and N. J. Frigo, "A spectrally sliced PON employing Fabry-Perot lasers," IEEE Photon. Technol. Lett. **10**, 1337 (1998).

[57] H. D. Kim, S. G. Kang, and C. H. Lee, "A low-cost WDM source with an ASE injected Fabry-Perot semiconductor laser," IEEE Photon. Technol. Lett. **12**, 1067 (2000).

[58] S. Park, C. Lee, K. Jeong, H. Park, J. Ahn, and K. Song, "Fibre-to-the-home services based on wavelength-division-multiplexing passive optical network," J. Lightwave Technol. **22**, 2582 (2004).

[59] Q. T. Nguyen, L. Bramerie, P. Besnard, A. Shen, A. Garreau, C. Kazmierski, G. H. Duan, and J. C. Simon, "24 channels colorless WDM-PON with L-band 10 Gb/s downstream and C-band 2.5 Gb/s upstream using multiple-wavelengths seeding sources based on mode-locked lasers," in *Proc. OFC 2010, OThG6.*

[60] L. Y. Chan, C. K. Chan, D. T. K. Tong, F. Tong, and L. K. Chen, "Upstream traffic transmitter using injection-locked Fabry-Perot laser diode as modulator for WDM access networks," Electron. Lett. **38**, 43 (2002).

[61] S. Hann, T. Kim, C. Park, "Direct-modulated upstream signal transmission using a self-injection locked F-P LD for WDM-PON," in *Proc. ECOC 2005, We3.3.3.*

[62] D. J. Shin, Y. C. Keh, J. W. Kwon, E. H. Lee, J. K. Lee, M. K. Park, J. W. Park, Y. K. Oh, S. W. Kim, I. K. Yun, H. C. Shin, D. Heo, J. S. Lee, H. S. Shin, H. S. Kim, S. B. Park, D. K. Jung, S. Hwang, Y. J. Oh, D. H. Jang, and C. S. Shim, "Low-cost WDM-PON with colorless bidirectional transceivers," J. Lightwave Technol. **24**, 158 (2006).

[63] F. Payoux, P. Chanclou, M. Moignard, and R. Brenot, "Gigabit optical access using WDM PON based on spectrum slicing and reflective SOA," in *Proc. ECOC 2005, We.3.3.5.*

[64] H. Takesue and T. Sugie, "Wavelength channel data rewrite using saturated SOA modulator for WDM networks with centralized light sources," J. Lightwave Technol. **21**, 2546 (2003).

[65] E. Wong, K. L. Lee, and T. B. Anderson, "Directly modulated self-seeding reflective semiconductor optical amplifiers as colorless transmitters in wavelength division multiplexed passive optical networks," J. Lightwave Technol. **25**, 67 (2007).

[66] K. Y. Cho, Y. J. Lee, H. Y. Choi, A. Murakami, A. Agata, Y. Takushima, and Y. C. Chung, "Effects of reflections in RSOA-based WDM PON utilizing remodulation technique," J. Lightwave Technol. **27**, 1286 (2009).

[67] C. Arellano, K. Langer, and J. Prat, "Reflections and multiple Rayleigh backscattering in WDM single-fibre loopback-access networks," J. Lightwave Technol. **27**, 12 (2009).

[68] D. W. Smith, "Reducing the optical component cost for future fibre access," in *Proc. ECOC 2009, 4.7.4.*

[69] A. Borghesani, "Reflective based active semiconductor components for next generation optical access networks," in *Proc. ECOC 2010, Mo.1.B.1.*

[70] R. Maher, K. Shi, L. P. Barry, J. O'Carroll, B. Kelly, R. Phelan, J. O'Gorman, and P. M. Anandarajah, "Implementation of a cost-effective optical comb source in a WDM-PON with 10.7 Gb/s data to each ONU and 50km reach," Opt. Express **18**, 15672 (2010).

[71] C. Chen, C. F. Zhang, W. Zhang, W. Jin, and K. Qiu, "Hybrid WDM-OFDMA-PON utilising tunable generation of flat optical comb," Electron. Lett. **49**, 276 (2013).

[72] R. Zhou, P. M. Anandarajah, M. D. G. Pascual, J. O'Carroll, R. Phelan, B. Kelly, and L. P. Barry, "Monolithically integrated 2-section lasers for injection locked gain switched comb generation," in *Proc.OFC 2014, Th3A.3*.

[73] D. B. Payne and R. P. Davey, "The future of fibre access systems?" BT Technol. J. **20**, 104 Oct. (2002).

[74] T. Pfeiffer, "Converged heterogeneous optical metro-access networks," in *Proc. ECOC 2010, Tu.5.B.1*.

[75] D. Breuer, R. Hulsermann, C. Lange, T. Monath, and E. Weis, "Architectural options and challenges for next generation optical access," in *Proc. ECOC 2010, Mo.2.B.1*.

[76] M. Jinno, H. Takara, B. Kozicki, Y. Tsukishima, Y. Sone, and S. Matsuoka, "Spectrum-efficient and scalable elastic optical path network: architecture, benefits, and enabling technologies," IEEE Commun. Magazine, **47**, 66 (2009).

[77] V. Vujicic, R. Zhou, P. M. Anandarajah, J. O'Carroll, and L. P. Barry, "Performance of a semi-Nyquist NRZ-DQPSK system employing a flexible gain-switched multicarrier transmitter," J. Opt. Commun. Netw. **6**, 282 (2014).

[78] P. M. Anandarajah, R. Zhou, R. Maher, D. Lavery, M. Paskov, B. C. Thomsen, S. J. Savory, and L. P. Barry, "Gain-switched multicarrier transmitter in a long-reach UDWDM-PON with a digital coherent receiver," Opt. Lett. **38**, 4797 (2013).

[79] R. Zhou, P. M. Anandarajah, R. Maher, M. Paskov, D. Lavery, B. C. Thomsen, S. J. Savory, and L. P. Barry, "80-km coherent DWDM-PON on 20-GHz grid with injected gain switched comb source," IEEE Photon. Technol. Lett. **26**, 364 (2014).

[80] N. Cvijetic, "OFDM for next-generation optical access networks," J. Lightwave Technol. **30**, 384 (2012)

[81] R. Matsumoto, T. Kodama, S. Shimizu, R. Nomura, K. Omichi, N. Wada, and K. Kitayama, "40G-OCDMA-PON system with an asymmetric structure using a single multi-port and sampled SSFBG encoder/decoders," J. Lightwave Technol. **32**, 1132 (2014).

[82] Y. Luo, X. Zhou, F. Effenberger, X. Yan, G. Peng, Y. Qian, and Y. Ma, "Time- and

wavelength-division multiplexed passive optical network (TWDM-PON) for next-generation PON stage 2 (NG-PON2)," J. Lightwave Technol. **31**, 587 (2013).

[83] H. Yang, J. Li, B. Lin, Y. Wan, Y. Guo, L. Zhu, L. Li, Y. He, and Z. Chen, "DSP-based evolution from conventional TDM-PON to TDM-OFDM-PON," J. Lightwave Technol. **31**, 2735 (2013).

[84] T. B. Osadola, S. K. Idris, I. Glesk, W. C. Kwong, "Improving network scalability using OCDMA over OTDM," in *Proc. OFC 2012, OM3I.4.*

[85] N. Cvijetic, M. Cvijetic, M. Huang, E. Ip, Y. Huang, and T. Wang, "Terabit optical access networks based on WDM-OFDMA-PON," J. Lightwave Technol. **30**, 493 (2012).

[86] K. Kitayama, X. Wang, and N. Wada, "OCDMA over WDM PON – solution path to Gigabit-symmetric FTTH," J. Lightwave Technol. **24**, 1654 (2006).

[87] ITU-T, *40-Gigabit-capable passive optical networks (NG-PON2): General requirements*, Recommendation G.989.1 (2013).

[88] N. Cheng, J. Gao, C. Xu, B. Gao, D. Liu, L. Wang, X. Wu, X. Zhou, H. Lin, and F. Effenberger, "Flexible TWDM PON system with pluggable optical transceiver modules," Opt. Express **22**, 2078 (2014).

[89] J. Kani, "Enabling technologies for future scalable and flexible WDM-PON and WDM/TDM-PON systems," IEEE J. Sel. Topic Quantum Electron. **16**, 1290 (2010).

[90] J. H. Lee, S. Cho, H. Lee, E. Jung, J. Yu, B. Kim, S. Lee, J. Koh, B. Sung, S. Kang, J. Kim, K. Jeong, and S. S. Lee, "First commercial deployment of a colorless Gigabit WDM/TDM hybrid PON system using remote protocol terminator," J. Lightwave Technol. **28**, 344 (2010).

[91] R. P. Davey, D. B. Grossman, M. R. Wiech, D. B. Payne, D. Nesset, A. E. Kelly, A. Rafel, S. Appathurai, and S. Yang, "Long-reach passive optical networks," J. Lightwave Technol. **27**, 273 (2009).

[92] B. Zhu, D. Au, F. Khan, and Y. Li, "Coexistence of 10G-PON and GPON reach extension to 50-km with entirely passive fibre plant," in *Proc. ECOC 2011, Th.13.B.5.*

[93] D. S. Forrester, A. M. Hill, R. A. Lobbett, R. Wyatt, and S. F. Carter, "39.81Gbit/s, 43.8

million-way WDM broadcast network with 527 km range," Electron. Lett. **27**, 2051 (1991).

[94] I. V. Voorde, M. O. Deventer, P. J. M. Peters, P. Crahay, E. Jaunart, A. J. Phillips, J. M. Senior, X. Z. Qiu, J. Vandewege, J. J. M. Binsma, and P. J. Vetter, "Network topologies for SuperPON," in *Proc. OFC 1997, TuK6.*

[95] D. P. Shea and J. E. Mitchell, "A 10-Gb/s 1024-way-split 100-km long-reach optical-access network," J. Lightwave Technol. **25**, 685 (2007).

[96] ITU-T, *Gigabit-capable passive optical networks (GPON): Reach extension*, Recommendation G.984.6 (2008).

[97] ITU-T, *10 Gigabit-capable passive optical networks (XG-PON): Reach extension*, Recommendation G.987.4 (2012).

[98] G. Talli and P. D. Townsend, "Hybrid DWDM-TDM long-reach PON for next-generation optical access," J. Lightwave Technol. **24**, 2827 (2006).

[99] P. Ossieur, C. Antony, A. Naughton, A. M. Clarke, H. Krimmel, X. Yin, X. Qiu, C. Ford, A. Borghesani, D. Moodie, A. Poustie, R. Wyatt, B. Harmon, I. Lealman, G. Maxwell, D. Rogers, D. W. Smith, S. Smolorz, H. Rohde, D. Nesset, R. P. Davey, and P. D. Townsend, "Demonstration of a 32×512 split, 100 km reach, 2×32×10 Gb/s hybrid DWDM-TDMA PON using tunable external cavity lasers in the ONUs," J. Lightwave Technol. **29**, 3705 (2011).

[100] S. M. Lee, S. Mun, M. Kim, and C. Lee, "Demonstration of a long-reach DWDM-PON for consolidation of metro and access networks," J. Lightwave Technol. **25**, 271 (2007).

[101] P. M. Anandarajah, R. Zhou. V. Vujicic, M. D. G. Pascual, E. Martin, and L. P. Barry, "Long reach UDWDM PON with SCM-QPSK modulation and direct detection," in *Proc. OFC 2014, W2A.42.*

[102] H. Iwamura, G. C. Gupta, M. Kashima, H. Tamai, R. Watanabe, T. Ushikubo, and T. Kamijoh, " 42dB loss budget hybrid DWDM-CDM-PON without optical amplifier," in *Proc. OFC 2007, OWL5.*

[103] D. Lavery, R. Maher, D. S. Millar, B. C. Thomsen, P. Bayvel, and S. J. Savory, "Digital

coherent receivers for long-reach optical access networks," J. Lightwave Technol. **31**, 609 (2013).

[104] H. Rohde, S. Smolorz, E. Gottwald, and K. Kloppe, "Next generation optical access: 1Gbit/s for everyone," in *Proc. ECOC 2009, 10.5.5.*

[105] S. Smolorz, E. Gottwald, H. Rohde, D. Smith, and A. Poustie, "Demonstration of a coherent UDWDM-PON with real-time processing," in *Proc. OFC 2011, PDPD4.*

Chapter 2

Optical Comb Generation for Access Applications

Further to the discussions in the previous chapter, wavelength division multiplexed passive optical networking (WDM-PON) is a promising architecture for the future evolution of optical access networks. To enable the realisation of WDM technology in a cost effective manner, a multi-wavelength transmitter at the optical line terminal (OLT) maybe considered to be an important ingredient in terms of component count and power consumption reduction in the central office. A conventional approach is to implement individual laser sources, but it entails additional concerns regarding precise wavelength controls for each channel, leading to increased management and inventory. As the network demand keeps evolving and the spectral utilisation moves towards finer granularity, these matters will become increasingly challenging and novel technologies are highly desired to meet future requirements.

An optical frequency comb source which generates multiple coherent tones is an interesting alternative because a compact physical device (or subsystem arrangement) could provide multi-wavelength emission with simplicity, reliability and low cost. Besides, there are other features of a comb source, that discrete lasers cannot easily offer, that could make them more attractive for employment in future access networks. In this chapter, we begin our discussion with a general review on the basic concept of optical frequency combs and their key parameters. Then, some of the commonly used comb generation techniques and their basic characteristics are introduced, followed by the potential applications of these comb sources in WDM-PON systems. The selected comb generation technologies under discussion can be mainly classified into three categories: mode-locking, electro-optic modulation, and gain switching.

2.1 Optical Frequency Comb

An optical frequency comb, as illustrated in Fig. 2.1, is a lightwave signal consisting of multiple equally spaced spectral elements that are generated within a single spatial mode laser beam output [1]. A salient feature of an optical frequency comb is the precise frequency spacing among all the spectral "teeth" (the spacing is referred to as the FSR: free spectral range) which has been well exploited by various fields of applications such as optical communications, sensing, metrology, and spectroscopy etc. [1]. These applications require, in general, a high degree of coherence between the comb lines and good overall stability of the comb source. Other important comb parameters include the number of comb lines, the power distribution amongst the frequency components and the noise level of each component, the achievable FSR tuning. These attributes are critical in a WDM communication system as they respectively determine the available user count, the performance quality in terms of signal-to-noise-ratio (SNR) penalties amongst different wavelength channels, and the system reconfigurability.

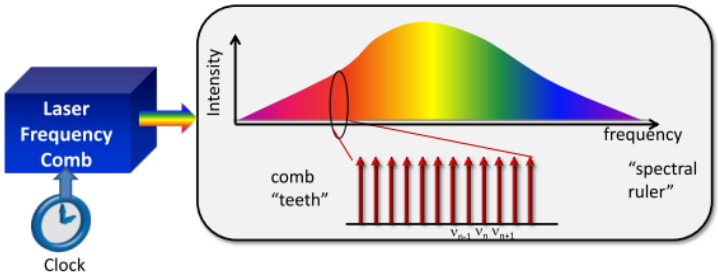

Figure 2.1: Illustrating an optical frequency comb generation [1].

The synthesis of a comb signal is commonly accomplished by stabilising a certain optical comb generator (being a laser component or a set of subsystem devices) to an underlying radio frequency (RF) clock, as indicated in Fig. 2.1. The technical selection of the optical comb generator involves a wide range of available options which include, for example, mode locking, electro-optic modulation, gain switching, Q switching, and parametric process. As such, due to the extensive range of the comb generation technology a detailed review covering all aspects of the topic would be tedious and unnecessary. This chapter therefore focuses selectively on a few technical options and their previous demonstrations in the access networks, whereas many others have been skipped. These selected options (and their potential access applications) are separately discussed in the following sections.

2.2 Mode Locked Laser

Mode-locking (or phase-locking) is a technique that introduces inter-modal phase correlation between the longitudinal modes of a laser resonant cavity [2]. When a fixed phase relationship is achieved amongst the optical modes, short pulse formation occurs with the repetition rate corresponding to the round-trip time of the resonator (or its multiples in the case of harmonic mode-locking [3]). In the frequency domain, the optical spectrum consists of discrete comb lines with constant spacing equal to the pulse train repetition rate, and the beating linewidth yields significantly reduced value compared to an un-locked case.

To achieve mode-locking, the laser can be of various designs. Considering the materials employed the device can be semiconductor or fibre based [2-5]. Regarding the structure, an amplitude modulator or saturable absorber could be placed in the resonant cavity [2]. For the synthesis of the pulse train it can be accomplished by active, passive, or hybrid mode-locking. Depending on the actual device (cavity configuration, material engineering etc.) and the mode-locking method used, the pulse train repetition rate (corresponds to comb line spacing in the frequency domain) and the pulse width (corresponds to the available spectral bandwidth of the frequency comb) may vary significantly [2]. Generally speaking, passive mode-locking is very effective for ultra-short pulse (hence broadband comb) generation without the need for any form of modulation [2]. Recently, semiconductor mode locked lasers (MLLs) employing low dimensional structures like self-assembled quantum dot/quantum dash (QD) devices [6] have gained particular attention for communication applications due to their small footprint and some interesting features [7]. In Fig. 2.2 the comb generated by a mode-locked quantum dash Fabry-Pérot (FP) laser emitting at 1.5 μm window [8] is shown.

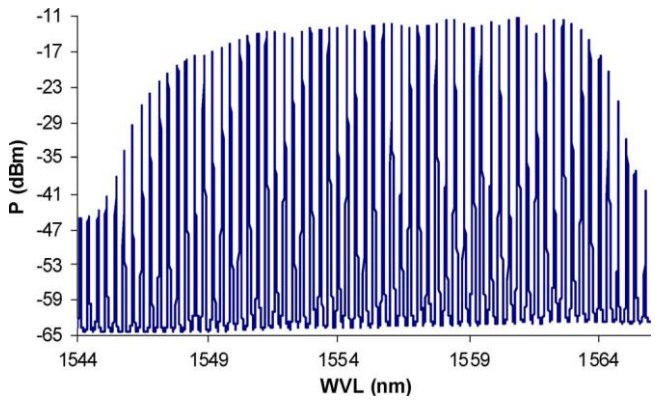

Figure 2.2: Optical spectrum of a FP MLL with 40 GHz comb line spacing [8].

The idea of mode-locking was proposed in 1964 [9]. Within the same year there was the first report on active mode-locking [10]. MLLs have been of research interest for short pulse generation in optical time division multiplexed (OTDM) and optical code division multiplexed (OCDM) systems [11] but with the emerging attention on the WDM technology, they have also been exploited as a multi-wavelength transmitter to replace individual laser sources for easy control and enhanced stability [8] [12]. Lately the use of MLL devices in WDM-PONs for cost reduction and simple wavelength assignment has been proposed [13] [14]. In [14], a bidirectional WDM-PON architecture with two quantum dash MLLs for respective downstream modulation and upstream injection locking (IL) seeding is demonstrated and the proposed system arrangement is shown in Fig. 2.3.

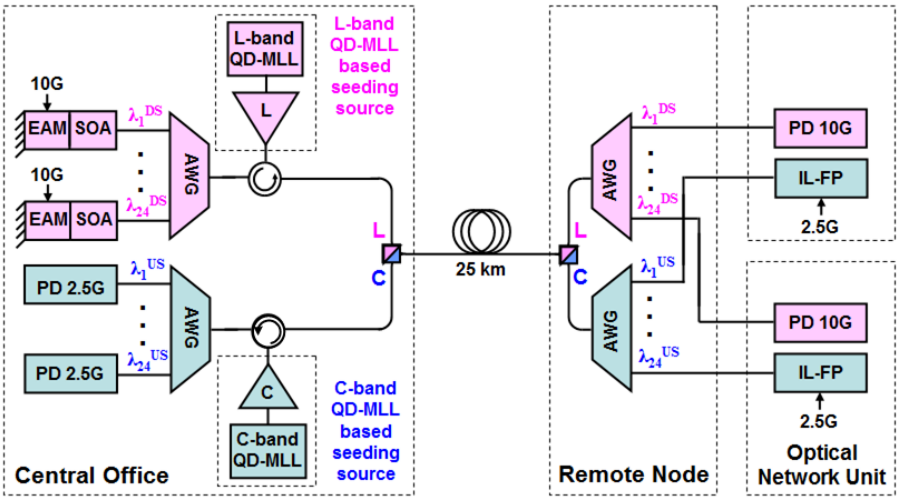

Figure 2.3: A bidirectional WDM-PON system with two QD-MLL comb sources at OLT [14].

For MLL based coherent comb generation, the most significant advantages are the large number of comb lines provided and the potential compact device structure resulting from monolithic integration [15]. However, the sophisticated fabrication of the MLLs usually involves precise cavity design [2], specific band-gap engineering and/or complex material growth [6], thus posing cost-related issues to practical deployment. The flexible tuning ability of the device operation is also limited since the comb line spacing i.e. the free spectral range (FSR) is determined by the cleaved cavity length. Moreover, the noise properties of the device are of concern: 1) the individual modes of a MLL suffer from mode partition noise and result in relative intensity noise (RIN) that needs to be taken care of [14] [16]; 2) optical linewidth of the individual comb tones can be relatively large (usually in tens or hundreds of MHz) unless very complicated structures or optical injection are used [17-19]. The large linewidth hinders

low symbol rate and/or high order modulation formats to be imposed, which might in turn prove disadvantageous for a future access system upgrades towards highly efficient access networking with advance modulation formats [20].

2.3 Electro-Optic Modulation

The idea of exploring external electro-optic (EO) modulation in combination with continuous wave (CW) laser output for optical comb generation can date back to 1972, where a lithium niobate ($LiNbO_3$) phase modulator was placed inside a FP cavity and driven by periodic RF signal for resonance enhanced modulation [21]. This structure illustrated in Fig. 2.4, has been referred to as an optical frequency comb generator (OFCG) and was targeted at various applications [22-24]. An OFCG typically suffers from the loss accumulated by multiple passes of light circulating the FP resonator and the strict requirement for aligning the modulation frequency with the cavity round-trip time. Another obvious drawback is the loss of flexibility in tuning the repetition rate and hence the FSR of the comb. With progress in EO modulator (EOM) technology [25] and the availability of high-power RF amplifiers, modern high-speed modulators with improved modulation bandwidth and reduced drive voltages can be directly driven by large amplitude sinusoidal signal without the need for an optical resonant cavity and repetitive light modulation. This has enabled a series of technical selections for comb generation, such as using one or multiple phase modulators (PMs) [26-32], single or multiple intensity modulators (Mach-Zehnder modulators: MZMs) [33-38], and a variety of their combinations (hybrid amplitude-phase modulation) [39-45].

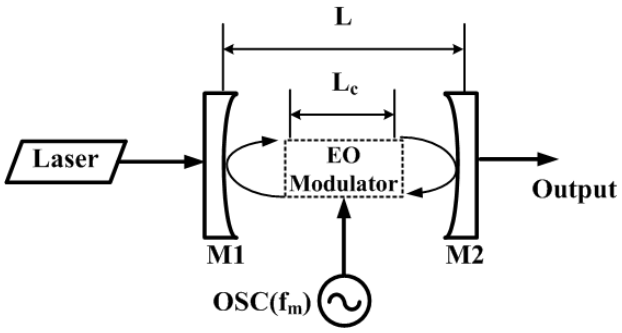

Figure 2.4: Illustration of an OFCG. M1, M2: mirrors for FP cavity, OSC: RF oscillator [23].

On the whole, the hybrid amplitude and phase modulation method provides a good compromise between system complexity and spectral quality, achieving balance in terms of

simplicity, flatness, and tuning flexibility. Compared to the pure PM or MZM cases, it enables utilisation of all the attributes, of both devices, without significantly complicating the setup requirements. Previously, hybrid modulation based comb generation has attracted some interest in terms of its application in optical access networks. In [46], a wired and wireless co-existing WDM-OFDMA-PON downlink transmission system is demonstrated based on PM+MZMs tunable comb generator (TCG). In [47], a carrier-centralized ultra-dense (UD) WDM-PON is proposed where a hybrid modulated (MZM+PM) comb source in the central office (CO) provides remote carrier seeding to the optical network unit (ONU) for highly efficient Nyquist-WDM modulation. The dual- polarisation modulated WDM signal is then transmitted back to the CO for coherent detection.

Unlike the MLLs, EOM comb generators have a large degree of freedom since the operating wavelength and the noise properties are primarily dependent on the external seeding laser. The FSR is also flexible and only limited by the maximum bandwidth of the modulators (and/or the RF amplifiers). Furthermore, manufacturing and cost are no longer major obstacles as current EOM devices are based on a mature technology. However, the insertion loss of the modulators (especially for the MZM case) still proves to be a major disadvantage for this technique. Another potential issue is that these devices are generally built using $LiNbO_3$ and are therefore not suitable for photonic integration. This has been recently addressed by the InP based comb generators [48] [49] but the comb line flatness, using such modulators, requires improvement. Further expansion of the EOM combs have been demonstrated by virtue of highly-nonlinear fibre [50-53] but the increased complexity and high power requirement are expected to hinder them from cost-sensitive optical access applications.

2.4 Gain Switched Laser

Gain switching is a direct modulation technique that emerged around 1980 and was mainly used for short optical pulse generation [54-57]. It can be accomplished by driving a conventional semiconductor laser with RF current pulses from an electrical comb generator (e.g. a step recovery diode) [55] [56] or a sinusoidal synthesiser [57]. To achieve optical pulses much shorter than the electrical driving pulse, the laser relaxation oscillation phenomenon is utilised. The basic idea is to excite only the first oscillation spike at the onset of the laser

operation and cut off the subsequent optical peaks by truncating the electrical driving signal [57]. Through periodically repeating the process, optical short pulse trains with pulse width ~10 ps are achievable [58]. Further pulse compression could result in pulse widths around several picoseconds and a time-bandwidth product approaching the transform-limit [59]. Therefore the gain switching technique has shown its capability as an alternative reliable pulse source for high-speed OTDM systems [59] [60] in addition to MLLs and other pulse generation technologies. More recently, the gain switched laser has demonstrated the potentials in WDM applications hence lent itself towards optical frequency comb generation as well [61].

2.4.1 Operating principle

The theoretical analysis for the gain switching process is usually based on a set of nonlinear rate equations that evaluate the laser dynamics and describe the supply, annihilation (transformation) and creation of carriers and photons inside a laser cavity. With N and S denoting the carrier and photon density, the basic rate equations for a single mode semiconductor laser without considering gain compression effects can be written as [58]:

$$\frac{dN}{dt} = \frac{I(t)}{eV} - \frac{N}{\tau_N} - g(N - N_{tr})S \tag{2.1}$$

$$\frac{dS}{dt} = \Gamma g(N - N_{tr})S - \frac{S}{\tau_P} - \Gamma\beta\frac{N}{\tau_N} \tag{2.2}$$

where $I(t)$ is the time dependent injection current (consists of a dc bias term and a modulating part for gain switching), e is the electronic charge, V is the volume of the laser active region, τ_N and τ_P are the carrier and photon lifetime respectively, g is the gain constant, N_{tr} is the carrier density at transparency, Γ is the confinement factor, and β is the spontaneous emission factor. The physical meanings of the above rate equations are intuitively understandable. On the right-hand side (RHS) of Eq. 2.1, the first term describes the carriers going into the volume of interest, and the second term represents the recombined carriers due to spontaneous emission. The third term, identical with the first term on RHS of Eq. 2.2, is responsible for the stimulated emission. The second and third terms on RHS of Eq. 2.2 are respectively the optical loss in the laser cavity and the portion of the spontaneously emitted photons that are coupled into the laser output. With the nonlinear carrier-photon interaction described by these rate equations, the

formation of short optical pulses highly depends on an appropriate combination of bias current, modulation current and relaxation oscillation conditions (e.g. damping and oscillation frequency) of the laser being used [62]. To understand the gain switched pulse generation process a graphical description of the time evolving carrier (electron) and photon densities is helpful, as that demonstrated in Fig. 2.5.

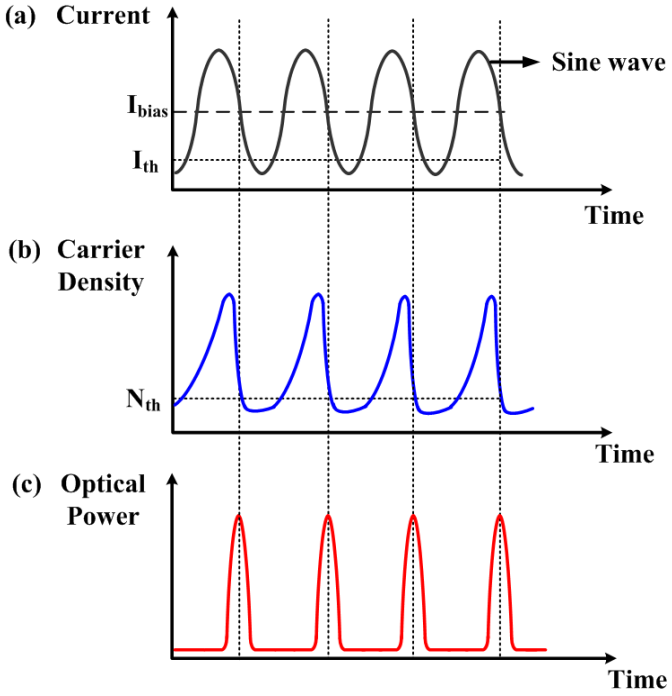

Figure 2.5: Typical evolution of (a) applied current, (b) carrier density, and (c) output optical power for a gain switched laser diode.

From the example shown in Fig. 2.5(a) the laser is biased with a dc current I_{bias} which is above the threshold value (I_{th}). A large amplitude sine wave is applied to the laser as a modulating signal which is also shown in Fig. 2.5(a). The increase of the sinusoidal current from trough to crest builds up the carrier density in the laser cavity to a level much higher than the lasing threshold N_{th}, as demonstrated in Fig. 2.5(b). Then the photon density starts rapidly increasing and quickly depletes the carriers, consequently causing the reduction in photon density and leading to optical pulse emission. Meanwhile the sinusoidal current decreases towards the trough, bringing the laser below threshold, hence preventing the onset of the second and subsequent optical spikes, which are part of the well-known relaxation oscillation phenomenon. Such a process repeats itself and results in an optical pulse train at the laser output.

Because of the direct modulation nature, the gain switched pulses inherently suffer from

frequency chirp due to the time-varying carrier density (hence refractive index) in the laser active region [63]. Moreover the pulses have large timing jitter from the random spontaneous emission character of a laser turn-on event [64]. Both factors potentially contribute to the degradation of generated optical pulses [65]. Previously, frequency chirp in gain switched pulses has been utilised for temporal pulse compression with appropriate dispersion [66] [67] and the turn-on time jitter can be reduced by optimum electrical current [68] [69]. Another effective approach for suppressing both chirp and jitter is the use of optical injection technique [65] [70], which also introduces other benefits to the gain switched laser as will be discussed in more details in the next chapter.

2.4.2 Utility as comb generator

The gain switched lasers have created a large amount of discussion in terms of optical pulse generation for the last few decades with numerous research papers being reported. The notable work using this technique for frequency comb generation, however, only started in 2009 where a novel gain switched discrete mode (DM) laser diode was demonstrated and compared with conventional distributed feedback (DFB) laser [61] (the DM laser diode is essentially a commercially available ridge waveguide Fabry-Pérot (FP) laser device constrained to give single mode emission [71]). In Fig. 2.6, the gain switched DM laser with a bias tee for simultaneous dc biasing and RF modulation for comb generation is demonstrated. The motivation to explore gain switching technique for comb generation was due to the increased interest in the highly efficient WDM systems hence the need for simple, low cost and low noise optical comb sources [72]. Subsequently, the investigation moved on to WDM-PON systems where the gain switched comb source was employed at the OLT to provide phase modulated data to each ONU. In [73], the individual comb lines from a gain switched comb

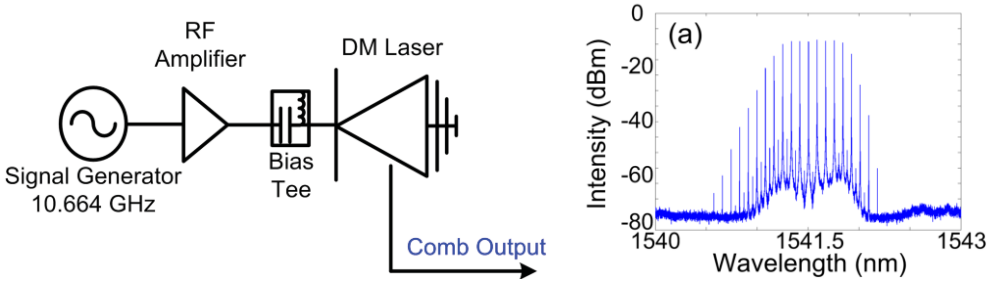

Figure 2.6: Gain switched DM comb source and optical spectrum [72].

source were filtered and encoded with differential phase shift keying (DPSK) modulation for 50 km transmission over standard single mode fibre (SSMF) to the ONUs.

Compared to the other two comb generation schemes discussed in this chapter, the most significant advantage of a gain switched comb source is its cost effectiveness. The gain switching technique requires only commercial off the shelf laser devices as opposed to the delicate design and fabrication of a MLL, and it also offers flexible FSR. There is no additional lossy and expensive component needed such as an EO modulator. The downside of the technique comes from the fixed emission wavelength when DM or DFB lasers are used for gain switching, and the limited spectral bandwidth of the comb source which is typically restricted by the intrinsic modulation bandwidth of a laser diode. Besides, direct modulation induced distortions manifest themselves among the optical comb lines as frequency/phase noise and broadening the optical linewidth [61], potentially result in performance impairments when used for high-speed communication systems. These issues will need to be addressed in order to maximise the utility of a gain switch optical comb source for access network and other applications. Luckily, optical injection seeding provides an excellent platform for achieving simultaneously modulation bandwidth enhancement, noise/nonlinearity suppression, and wavelength selection [65] [74]. A promising fact is that the injection technique lends itself towards highly functional photonics integration, offering the possibility to further reduce device footprint and power consumption [75]. The investigation on the optically injected gain switched optical comb source has formed the essential work of this research thesis and the detailed generation, characterisation and application of such a comb source will be elaborated in the following chapters.

2.5 Summary

Optical frequency comb generation has the potential to benefit various fields of technologies including WDM-PON based next generation optical access networks. In general there are two important attributes that distinguish a comb source from any other multi-wavelength transmitter, namely the strong phase coherence across the spectral bandwidth (stability) and the possibility to tune independently the repetition rate or frequency offset (flexibility). Besides, the substantial economic benefits of using a comb source come from the reduced

number of wavelength lockers and temperature stabilisers, which are necessary for single-mode laser sources and would have added significantly to the complexity and power consumption of the transmitter module. In this chapter three types of comb generators based on distinct working mechanisms have been brought into discussion. Each comb source has its own pros and cons: the MLLs are efficient comb generators but they are costly, complex and in most occasions lack flexibility; the EOMs are highly flexible but intrinsically unstable and usually lossy and bulky; the gain switched lasers offer simplicity and low loss but are limited by the number of comb lines and direct modulation related distortions. As a result, optical injection is proposed to achieve performance enhancement for gain switched comb generators, and making this simple and low cost technology attractive and competitive for future optical access applications.

Reference

[1] N. R. Newbury, E. Baumann, I. Coddington, C. Cromer, J. D. Deschenes, F. R. Giorgetta, G. Rieker, L. Sonderhouse, W. C. Swann, and L. C. Sinclair, "Optical combs for sensor applications," in *Proc. OFC 2014, Th4H.4.*

[2] H. A. Haus, "Mode-locking of lasers," IEEE J. Sel. Topics Quantum Electron. **6**, 1173 (2000).

[3] J. N. Kutz and B. Sandstede, "Theory of passive harmonic mode-locking using waveguide arrays," Opt. Express **16**, 636 (2008).

[4] L. A. Gomes, L. Orsila, T. Jouhti, and O. G. Okhotnikov, "Picosecond SESAM-based Ytterbium mode-locked fibre lasers," IEEE J. Sel. Topics Quantum Electron. **10**, 129 (2004).

[5] S. C. Zeller, L. Krainer, G. J. Spuhler, R. Paschotta, M. Golling, D. Ebling, K. J. Weingarten and U. Keller, "Passively modelocked 50 GHz Er:Yb:glass laser," Electron. Lett. **40** (2004).

[6] F. Lelarge, B. Dagens, J. Renaudier, R. Brenot, A. Accard, F. Dijk, D. Make, O. L. Gouezigou, J. Provost, F. Poingt, J. Landreau, O. Drisse, E. Derouin, B. Rousseau, F. Pommereau, and G. Duan, "Recent advances on InAs/InP quantum dash based semiconductor lasers and optical amplifiers operating at 1.55 μm," IEEE J. Sel. Topics Quantum Electron. **13**, 111 (2007).

[7] R. Rosales, R. T. Watts, K. Merghem, C. Calo, A. Martinez, A. Accard, F. Lelarge, L. P. Barry, and A. Ramdane, "Quantum dash mode locked lasers as optical comb sources for OFDM superchannels," in *Proc. ECOC 2012, Mo.1.E.5.*

[8] A. Akrout, A. Shen, R. Brenot, F. V. Dijk, O. Legouezigou, F. Pommereau, F. Lelarge, A. Ramdane, and G. Duan, "Separate error-free transmission of eight channels at 10 Gb/s using comb generation in a quantum-dash-based mode-locked laser", IEEE Photon. Technol. Lett. **21**, 1746 (2009).

[9] W. E. Lamb, “Theory of an optical maser,” Phys. Rev. **134**, A1429 (1964).

[10] L. E. Hargrove, R. L. Fork, and M. A. Pollack, “Locking of He-Ne laser modes induced by synchronous intracavity modulation,” Appl. Phys. Lett. **5**, 4 (1964).

[11] P. J. Delfyett, S. Gee, M. Choi, H. Izadpanah, W. Lee, S. Ozharar, F. Quinlan, and T. Yilmaz, “Optical frequency combs from semiconductor lasers and applications in ultrawideband signal processing and communications”, J. Lightwave Technol. **24**, 2701 (2006).

[12] H. Yasaka, Y. Yoshikuni, K. Sato, H. Ishii, H. Sanjoh, “Multiwavelength light source with precise frequency spacing using mode-locked semiconductor laser and arrayed waveguide grating filter,” in *Proc. OFC 1996, FB2.*

[13] Z. G. Lu, J. R. Liu, P. J. Poole, S. Raymond, P. J. Barrios, D. Poitras, G. Pakulski, X. P. Zhang, K. Hinzer, and T. J. Hall, “Low noise InAs/InP quantum dot C-band monolithic multiwavelength lasers for WDM-PONs,” in *Proc. OFC 2009, JWA27.*

[14] Q. T. Nguyen, L. Bramerie, P. Besnard, A. Shen, A. Garreau, C. Kazmierski, G. H. Duan, and J. C. Simon, “24 channels colorless WDM-PON with L-band 10 Gb/s downstream and C-band 2.5 Gb/s upstream using multiple-wavelengths seeding sources based on mode-locked lasers”, in *Proc. OFC 2010, OThG6.*

[15] V. Moskalenko, S. Latkowski, T. de Vries, L. M. Augustin, X. J. M. Leijtens, M. K. Smit, E. A. J. M. Bente, “A wide bandwidth coherent optical comb source based on a monolithically integrated mode-locked ring laser,” in *Proc. OFC 2014, Tu2H.3.*

[16] Y. B. M’ Sallen, Q. T. Le, L. Bramerie, Q. Nguyen, E. Borgne, P. Besnard, S. LaRochelle, L. A. Rusch, and J. Simon, “Quantum-dash mode-locked laser source for wavelength-tunable 56 Gbit/s DQPSK,” in *Proc. ECOC 2010, Mo.1.F.4.*

[17] T. Habruseva, S. O’Donoghue, N. Rebrova, F. Kefelian, S. P. hegarty, and G. Huyet, “Optical linewidth of a passively mode-locked semiconductor laser,” Opt. Lett. **34**, 3307 (2009).

[18] I. Ozdur, M. Akbulut, N. Hoghooghi, D. Mandridis, S. Ozharar, F. Quinlan, and P. J. Delfyett, “A semiconductor-based 10-GHz optical comb source with sub 3-fs

shot-noise-limited timing jitter and ~500-Hz comb linewidth," IEEE Photon. Technol. Lett. **22**, 431 (2010).

[19] E. Sooudi, S. Sygletos, A. D. Ellis, G. Huyet, J. G. McInerney, F. Lelarge, K. Merghem, R. Rosales, A. Martinez, A. Ramdane, and S. P. Hegarty, "Optical frequency comb generation using dual-mode injection-locking of quantum-dash mode-locked lasers: properties and applications," IEEE J. Quantum Electron. **48**, 1327 (2012).

[20] N. Yoshimoto, J. Kani, S. Kim, N. Iiyama, and J. Terada, "DSP based optical access approaches for enhancing NG-PON2 systems," IEEE Commun. Mag. **51**, 58 (2013).

[21] T. Kobayashi, T. Sueta, Y. Cho, and Y. Matsuo, "High-repetition-rate optical pulse generator using a Fabry-Perot electro-optic modulator," Appl. Phys. Lett. **21**, 341 (1972).

[22] M. Kourogi, K. Nakagawa, and M. Ohtsu, "Wide-span optical frequency comb generator for accurate optical frequency difference measurement," IEEE J. Quantum Electron. **29**, 2693 (1993).

[23] M. Kourogi, B. Widiyatomoko, Y. Takeuchi, and M. Ohtsu, "Limit of optical-frequency comb generation due to material dispersion", IEEE J. Quantum Electron. **31**, 2120 (1995).

[24] S. Xiao, L. Hollberg, N. R. Newbury, and S. A. Diddams, "Toward a low-jitter 10 GHz pulsed source with an optical frequency comb generator," Opt. Express **16**, 8498 (2008).

[25] M. Doi, M. Sugiyama, K. Tanaka, and M. Kawai, "Advanced $LiNbO_3$ optical modulators for broadband optical communications," IEEE J. Sel. Topics Quantum Electron. **12**, 745 (2006).

[26] S. Ozharar, F. Quinlan, I. Ozdur, S. Gee, and P. J. Delfyett, "Ultraflat optical comb generation by phase-only modulation of continuous-wave light", IEEE Photon. Technol. Lett. **20**, 36 (2008).

[27] J. Zhang, N. Chi, J. Yu, Y. Shao, J. Zhu, B. Huang, and L. Tao, "Generation of coherent and frequency-lock multi-carriers using cascaded phase modulators and recirculating frequency shifter for Tb/s optical communication", Opt. Express, **19**, 12891 (2011).

[28] J. Zhang, J. Yu, N. Chi, Z. Dong, X. Li, Y. Shao, J. Yu, and L. Tao, "Flattened comb generation using only phase modulators driven by fundamental frequency sinusoidal

sources with small frequency offset," Opt. Lett. **38**, 552 (2013).

[29] V. Company, J. Lancis, and P. Andres, "Lossless equalization of frequency combs," Opt. Lett. **33**, 1822 (2008).

[30] T. Yamamoto, T. Komukai, K. Suzuki, and A. Takada, "Multicarrier light source with flattened spectrum using phase modulators and dispersion medium," J. Lightwave Technol. **22**, 4297 (2009).

[31] K. Ho and J. M. Kahn, "Optical frequency comb generator using phase modulation in amplified circulating loop," IEEE Photon. Technol. Lett. **5**, 721 (1993).

[32] S. Bennett, B. Cai, E. Burr, O. Gough, and A. J. Seeds, "1.8-THz bandwidth, zero-frequency error, tunable optical comb generator for DWDM applications," IEEE Photon. Technol. Lett. **11**, 551 (1999).

[33] T. Sakamoto, T. Kawanishi, and M. Izutsu, "Asymptotic formalism for ultraflat optical frequency comb generation using a Mach-Zehnder modulator," Opt. Lett. **32**, 1515 (2007).

[34] T. Sakamoto, T. Kawanishi, and M. Izutsu, "Widely wavelength-tunable ultra-flat frequency comb generation using conventional dual-drive Mach-Zehnder modulator," Electron. Lett. **43** (2007).

[35] A. K. Mishra, R. Schmogrow, I. Tomkos, D. Hillerkuss, C. Koos, W. Freude, and J. Leuthold, "Flexible RF-based comb generator," IEEE Photon. Technol. Lett. **25**, 701 (2013).

[36] T. Healy, F. C. G. Gunning, A. D. Ellis, "Multi-wavelength source using low drive-voltage amplitude modulators for optical communications," Opt. Express **15**, 2981 (2007).

[37] I. L. Gheorma and G. K. Gopalakrishnan, "Flat frequency comb generation with an integrated dual-parallel modulator," IEEE Photon. Technol. Lett. **19**, 1011 (2007).

[38] I. Morohashi, T. Sakamoto, N. Yamamoto, H. Sotobayashi, T. Kawanishi, I. Hosako, "1 THz-bandwidth optical comb generation using Mach-Zehnder-modulator-based flat comb generator with optical feedback loop," in *Proc. OFC 2011, JThA29.*

[39] M. Fujiwara, M. Teshima, J. Kani, H. Suzuki, N. Takachio, and K. Iwatsuki, "Optical

carrier supply module using flattened optical multicarrier generation based on sinusoidal amplitude and phase hybrid modulation," J. Lightwave Technol. **21**, 2705 (2003).

[40] Y. Dou, H. Zhang, and M. Yao, "Improvement of flatness of optical frequency comb based on nonlinear effect of intensity modulator," Opt. Lett. **36**, 2749 (2011).

[41] Y. Xing, Q. Wang, L. Huo, and C. Lou, "Frequency chirp linearization for ultraflat optical frequency comb generation based on group velocity dispersion," Opt. Lett. **38**, 2188 (2013).

[42] R. Wu, V. R. Supradeepa, C. M. Long, D. E. Leaird, A. M. Weiner, "Highly flat and stable optical frequency comb generation using intensity and phase modulators employing quasi-quadratic phase modulation," *IEEE Topic Meeting on Microwave Photonics (MWP), 212 (2010).*

[43] A. J. Metcalf, V. Company, D. E. Leaird, and A. M. Weiner, "High-power broadly tunable electrooptic frequency comb generator," IEEE J. Sel. Topics Quantum Electron. **19**, 3500306 (2013).

[44] C. Huang, Z. Jiang, D. E. Leaird, and A. M. Weiner, "High-rate femtosecond pulse generation via line-by-line processing of phase-modulated CW laser frequency comb," Electron. Lett. **42** (2006).

[45] Z. Jiang, D. E. Leaird, C. Huang, H. Miao, M. Kourogi, K. Imai, and A. M. Weiner, "Spectral line-by-line pulse shaping on an optical frequency comb generator," IEEE J. Quantum Electron. **43**, 1163 (2007).

[46] C. Chen, C. F. Zhang, W. Zhang, W. Jin, and K. Qiu, "Hybrid WDM-OFDMA-PON utilising tunable generation of flat optical comb," Electron. Lett. **49** (2013).

[47] Z. Dong, J. Yu, H. Chien, N. Chi, L. Chen, and G. Chang, "Ultra-dense WDM-PON delivering carrier-centralized Nyquist-WDM uplink with digital coherent detection," Opt. Express **19**, 11100 (2011).

[48] N. Dupuis, C. R. Doerr, L. Zhang, L. Chen, N. J. Sauer, P. Dong, L. L. Buhl, and D. Ahn, "InP-based comb generator for optical OFDM," J. Lightwave Technol. **30**, 466 (2012).

[49] T. Yamamoto, K. hitomi, W. Kobayashi, and H. Yasaka, "Optical frequency comb block

generation by using semiconductor Mach-Zehnder modulator," IEEE Photon. Technol. Lett. **25**, 40 (2013).

[50] T. Ohara, H. Takara, T. Yamamoto, H. Masuda, T. Morioka, M. Abe, and H. Takahashi, "Over-1000-channel ultradense WDM transmission with supercontinuum multicarrier source," J. Lightwave Technol. **24**, 2311 (2006).

[51] C. Huang, S. Park, D. E. Leaird, and A. M. Weiner, "Nonlinearly broadened phase-modulated continuous-wave laser frequency combs characterized using DPSK decoding," Opt. Express **16**, 2520 (2008).

[52] V. R. Supradeepa and A. M. Weiner, "Bandwidth scaling and spectral flatness enhancement of optical frequency combs from phase-modulated continuous-wave lasers using cascaded four-wave mixing," Opt. Lett. **37**, 3066 (2012).

[53] V. Ataie, E. Myslivets, B. P. Kuo, N. Alic, and S. Radic, "Spectrally equalized frequency comb generation in multistage parametric mixer with nonlinear pulse shaping," J. Lightwave Technol. **32**, 840 (2014).

[54] H. Ito, H. Yokoyama, S. Murata, and H. Inaba, "Picosecond optical pulse generation from an R.F. modulated AlGaAs D.H. diode laser," Electron. Lett. **15**, 738 (1979).

[55] C. Lin, P. L. Liu, T. C. Damen, and D. J. Eilenberger, "Simple picosecond pulse generation scheme for injection lasers," Electron. Lett. **16**, 600 (1980).

[56] P. Torphammar and S. T. Eng, "Picosecond pulse generation in semiconductor lasers using resonance oscillation," Electron. Lett. **16**, 587 (1980).

[57] S. Tarucha and K. Otsuka, "Response of semiconductor laser to deep sinusoidal injection current modulation," IEEE J. Quantum Electron. **QE-17**, 810 (1981).

[58] P. Paulus, R. Langenhorst, and D. Jager, "Generation and optimum control of picosecond optical pulses from gain-switched semiconductor lasers," IEEE J. Quantum Electron. **24**, 1519 (1988).

[59] P. M. Anandarajah, A. M. Clarke, C. Guignard, L. Bramerie, L. P. Barry, J. D. Harvey, and J. C. Simon, "System-performance analysis of optimized gain-switched pulse source employed in 40- and 80-Gb/s OTDM systems," J. Lightwave Technol. **25**, 1495 (2007).

[60] L. P. Barry, P. Guignard, J. Debeau, R. Boittin, and M. Bernard, "A high-speed optical star network using TDMA and all-optical demultiplexing techniques," IEEE J. Sel. Areas Commun. **14**, 1030 (1996).

[61] P. M. Anandarajah, K. Shi, J. O' Carroll, A. Kaszubowska, R. Phelan, L. P. Barry, A. D. Ellis, P. Perry, D. Reid, B. Kelly, and J. O'Gorman, "Phase shift keyed systems based on a gain switched laser transmitter," Opt. Express **17**, 12668 (2009).

[62] K. Y. Lau, "Gain switching of semiconductor injection lasers," Appl. Phys. Lett. **52**, 257 (1988).

[63] D. Welford, "A rate equation analysis for the frequency chirp to modulated power ratio of a semiconductor diode laser," IEEE J. Quantum Electron. **QE-21**, 1749 (1985).

[64] K. Obermann, S. Kindt, and K. Petermann, "Turn-on jitter in zero-biased single-mode semiconductor lasers," IEEE Photon. Technol. Lett. **8**, 31 (1996).

[65] P. M. Anandarajah, R. Maher, Y. Q. Xu, S. Latkowski, J. O'Carroll, S. G. Murdoch, R. Phelan, J. O'Gorman, and L. P. Barry, "Generation of coherent multicarrier signals by gain switching of discrete mode lasers," IEEE Photon. J. **3**, 112 (2011).

[66] K. A. Ahmed, H. F. Liu, N. Onodera, P. Lee, R. S. Tucker, and Y. Ogawa, "Nearly transform-limited pulse (3.6ps) generation from gain-switched 1.55μm distributed feedback laser by using fibre compression technique," Electron. Lett. **29**, 54 (1993).

[67] L. Chusseau and C. Kazmierski, "Optimum linear pulse compression of a gain-switched 1.5 μm DFB laser," IEEE Photon. Technol. Lett. **6**, 24 (1994).

[68] A. G. Weber, W. Ronghan, E. H. Bottcher, M. Schell, and D. Bimberg, "Measurement and simulation of the turn-on delay time jitter in gain-switched semiconductor lasers," IEEE J. Quantum Electron. **28**, 441 (1992).

[69] M. Jinno, "Correlated and uncorrelated timing jitter in gain-switched laser diodes," IEEE Photon. Technol. Lett. **5**, 1140 (1993).

[70] J. Dellunde, M. C. Torrent, J. M. Sancho, and M. San Miguel, "Frequency dynamics of gain-switched injection-locked semiconductor lasers," IEEE J. Quantum Electron. **33**, 1537 (1997).

[71] C. Herbert, D. Jones, A. Kaszubowska, B. Kelly, M. Rensing, J. O'Carroll, R. Phelan, P. Anandarajah, P. Perry, L. P. Barry, and J. O'Gorman, "Discrete mode lasers for communication applications," IET Optoelectron. **3**, 1 (2009).

[72] R. Maher, P. M. Anandarajah, S. K. Ibrahim, L. P. Barry, A. D. Ellis, P. Perry, R. Phelan, B. Kelly, and J. O'Gorman, "Low cost comb source in a coherent wavelength division multiplexed system," in *Proc. ECOC 2010, P3.07.*

[73] R. Maher, K. Shi, L. P. Barry, J. O'Carroll, B. Kelly, R. Phelan, J. O'Gorman, and P. M. Anandarajah, "Implementation of a cost-effective optical comb source in a WDM-PON with 10.7Gb/s data to each ONU and 50km reach," Opt. Express **18**, 15672 (2010).

[74] R. Zhou, S. Latkowski, J. O'Carroll, R. Phelan, L. P. Barry, and P. Anandarajah, "40nm wavelength tunable gain-switched optical comb source," Opt. Express **19**, B415 (2011).

[75] R. Zhou, P. M. Anandarajah, D. G. Pascual, J. O'Carroll, R. Phelan, B. Kelly, and L. P. Barry, "Monolithically integrated 2-section lasers for injection locked gain switched comb generation," in *Proc. OFC 2014, Th3A.3.*

Chapter 3

Injected Gain Switched Comb Source

Further to the discussions in the previous chapters, optical frequency combs can be considered to be important components for future high bandwidth, low cost access networks. Chapter 2 presented a few of the most commonly used comb generation technologies amongst the many that exist. This thesis focuses on one of the simple techniques entailing the gain switching (direct modulation) of laser diodes. To further improve the gain switched comb generation performance in terms of spectral bandwidth, noise properties and linearity, optical injection is introduced in this chapter. This can be viewed as one of the novel contributions of this thesis. Hence, this chapter will focus on experimental work entailing the generation and basic characterisation of the injected gain switched comb source.

The chapter is organised as follows. Firstly, a brief overview on optical injection technology will be given. This will include highlighting the numerous benefits brought about by optical injection to a directly modulated/gain switched laser diode, such as resonance frequency enhancement, optical intensity and phase noise reduction, and nonlinear distortion suppression. Other attractive comb source features, brought about by optical injection, are free spectral range flexibility and wavelength tunability. The experimental work that follows highlights, in three different scenarios, the demonstration of one or more of these advantages.

3.1 Optical Injection

Optical injection has a very long history and involves a great variety of complex phenomena. The most attractive phenomenon (due to its wide range applications), injection locking, was originally discovered during mechanically coupled oscillation (clock pendulums), later investigated in electrical resonating systems and finally utilised for lightwave systems [1]. The early work on injection locked semiconductor lasers emerged around 1980 with one of the

main interests, at that time, being optical coherent transmission [2-5]. Subsequently, optical injection locking has been utilised to overcome some of the fundamental limitations of directly modulated semiconductor lasers due to the attractiveness of these low cost optical transmitters [1]. As a special form of direct modulation, the gain switched laser diode naturally benefits from the optical injection and is expected to gain improvement in terms of several important parameters:

Resonance frequency enhancement – the relaxation oscillation of a semiconductor laser originates from the intrinsic oscillating interplay between photon and carrier densities during the turn-on action. The strength and frequency of such resonances are normally determined by the basic laser parameters such as material, device geometry, and bias condition [6]. With optical injection, the laser resonance can be manipulated by different amplitude and phase/frequency alignments of the injecting (master) and the injected (slave) fields [1] [7]. The resulting slave output showing a suppressed [8] or enhanced [9-11] relaxation oscillation are potentially suitable for various systems depending on the particular application. For example, for broadband digital modulation the available 3-dB modulation bandwidth (MBW) is usually of concern and a flat modulation response is preferable [12]. For gain switching, a pronounced resonance peak with extended frequency is beneficial for the sinusoidal (single tone) modulation [13]. Previously, it has been shown that strong optical injection can push the resonance frequency/MBW towards high values way beyond the intrinsic capability of the free running slave laser [7] [14] [15]. The optical injection technique thus becomes a valuable asset for the resonance enhanced gain switched comb generation which exhibits increased (yet flexible) free spectral range (FSR) [16]. The experimental details of such comb sources will be discussed in Section 3.2.

Noise reduction – the noise in a semiconductor laser stems from the quantum nature of light, with dominating contribution by the spontaneous emission during radiative recombination [17]. Laser noise can be usually divided into two categories: intensity (amplitude) noise and frequency (phase) noise. It has been demonstrated that laser intensity noise, commonly quantified by the relative intensity noise (RIN), can be effectively suppressed with suitable light injection [18] [19] due to the reduction in carrier and photon density fluctuations around their equilibrium values. Moreover, intensity noise can also result from a phenomenon known

as the mode partition noise (MPN) which arises from competition/fluctuation of optical gain among multiple longitudinal laser modes [17]. The effect of MPN is the constantly changing power distributions among different modes (although total power is unchanged) hence the degraded stability, especially when subjected to filtering or dispersive propagation, in the laser output (due to the partition or disturbance of the overall equilibrium). As previously reported optical injection can be utilised to reduce MPN and ensure single-mode operation [20]. This feature is highly relevant for the wavelength tunable injected comb generation [21] and the relating experimental work will be described later in Section 3.3. As for the frequency or phase noise, it has been widely recognized that the injection locking technique offers frequency modulation (FM) noise spectrum control from the master to the slave and is able to achieve FM noise/phase jitter suppression and emission linewidth reduction [22-26]. However it is important to point out that this study highlights other issues in the suppressed FM-noise spectrum of the slave laser [24], which are shown to have degrading effects when an injected gain switched comb source is used in phase noise sensitive coherent optical communication systems [27]. In the following sections of this chapter basic optical linewidth characterisation of the comb source will be demonstrated while a more detailed phase noise analysis will be given in the next chapter.

Other benefits – examples of other improvements from optical injection obtained by a modulated slave laser include frequency chirp and nonlinear distortion reduction. Chirp is caused by the simultaneous frequency modulation due to the carrier related refractive index variation of the intensity modulation process and results in spectral broadening [17] [28]. Optical injection reduces carrier fluctuation and suppresses the undesired frequency modulation in the slave cavity hence achieving chirp reduction [29-31]. The issue of laser nonlinearity is related to the nonlinear interaction of carriers and photons in the active region. Such an inherent nonlinear property of the laser diode transfers energy into unwanted harmonics and intermodulation products therefore distorting the laser modulation output [32] [33]. Theoretical and experimental works have shown that coherent light injection can reduce the influence of undesired distortion and improve the laser dynamic behaviour [34-36], by supplementing additional photons from the master to the slave cavity, hence suppressing the nonlinear carrier-photon coupling in the slave laser during large signal modulation. Additional

experimental results are shown in Section 3.4, with the aid of compact comb generation [37], that these enhanced modulation properties can be achieved with injection.

3.2 Resonance Enhanced Comb Source

As pointed out in Chapter 2, one fundamental limitation of a simple gain switched comb source is the restricted modulation bandwidth of the laser. To improve the usefulness of the comb source and achieve a broader selection of FSR, it is desirable to widen the frequency range over which the laser can be gain switched at. As mentioned earlier, this is enabled by optical injection and therefore this section demonstrates results from experimental investigation on resonance enhanced comb generation [16]. The study is based on a commercially available distributed feedback (DFB) slave laser diode (NEL) whose inherent resonance has been increased from 15 GHz to 33 GHz and beyond by strong optical injection from a narrow linewidth tunable laser source (Agilent N7711A).

3.2.1 Laser resonance enhancement

To characterise the frequency response of the slave laser and observe resonance enhancement, an experimental setup is built as shown in Fig. 3.1(a). The slave DFB laser is packaged in an optically un-isolated temperature controlled high-speed butterfly package, with a radio frequency (RF) K-type connector attached enabling direct modulation. The laser exhibits a threshold current of 12.5 mA at room temperature and emits in the 1.5 μm window. The master tunable laser injects light into the slave cavity via a polarisation controller (PC) and a circula-

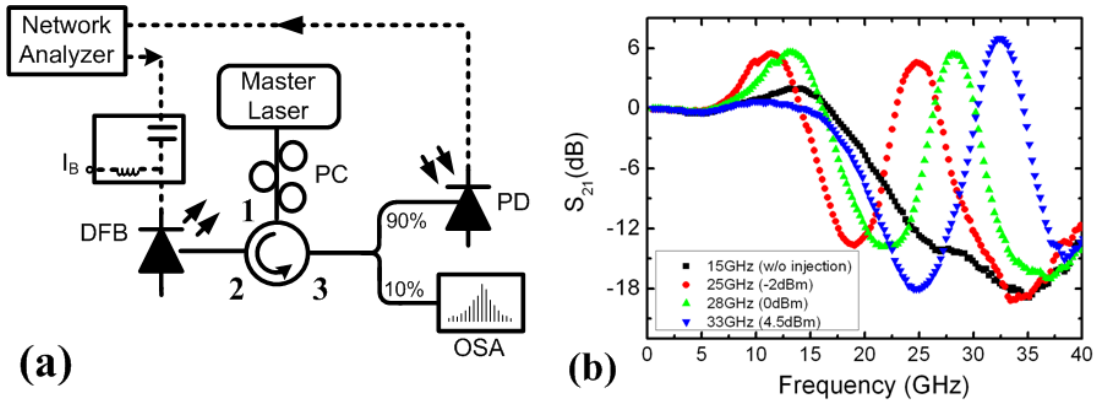

Figure 3.1: (a) Experimental configuration for the frequency response measurement scheme, (b) measurement results of the free-running (w/o injection) and of the externally injected DFB slave laser, with injection powers and enhanced resonance frequencies indicated in the legend.

-tor. The PC is used to align the polarisation state of the injecting light with the optical waveguide of the slave laser, and the circulator allows for unidirectional injection and coupling of the slave light. The master laser wavelength is tuned to a value (λ_{master} = 1545.85 nm) that results in negative wavelength detuning between the master and the free-running slave laser (λ_{slave} = 1546.32 nm, wavelength detuning defined as $\Delta\lambda = \lambda_{master} - \lambda_{slave}$ = -0.47 nm), which is critical for achieving the resonance enhancement [38] as will be discussed later. The slave laser is temperature controlled at 25°C and dc biased at 50 mA ($4I_{th}$) with the aid of a bias-tee.

To analyse the small signal frequency response of the DFB laser with and without injection, a Hewlett Packard Network Analyser System (45 MHz - 50 GHz) is employed to directly modulate the slave laser. Port 3 of the circulator is then passed into a 90/10 coupler with 90% of the signal detected by a 50 GHz photodetector (PD) (u^2t photonics XPDV2120R) and directed back to the network analyser for S parameter (S_{21}) measurement. The 10% tap is used to monitor the optical spectrum of the slave laser, with the aid of a 20 MHz resolution bandwidth optical spectrum analyser (OSA) (APEX AP2443B), to ensure there is at least 35 dB side mode suppression ratio (SMSR) between the emitted (injected) and the residual slave cavity modes. This is to ensure control over the injection process so that stable injection locking is maintained as unstable locking can result in unwanted phenomena such as four-wave mixing or chaos [7].

The modulation response of the DFB laser under fixed wavelength detuning and different injection powers are demonstrated in Fig. 3.1(b), with the injection power (measured at port 2 of the circulator) and the achieved resonance frequency in each case specified in the legend. In the figure, the black squares indicates that the free-running (w/o injection) slave laser has a relaxation oscillation frequency of about 15 GHz and a 3-dB MBW around 19 GHz. The resonance frequency is then enhanced through the injection with injected power increased from -2 dBm to 0 dBm and ultimately 4.5 dBm. This corresponds to an increase in the resonance peak to 25, 28 and 33 GHz respectively, as indicated by the red circles, green triangles (pointing up) and blue triangles (pointing down) in Fig. 3.1(b). Note that for clarity reason only three frequencies are illustrated here but the laser resonance can be continuously tuned by varying the injection power and the RF drive signal, with the upper tuning limit determined by the effective injection power coupled into the slave cavity (as will be explained

later), and the maximum available wavelength detuning range before exciting the neighbouring longitudinal mode of the slave laser [15] [39].

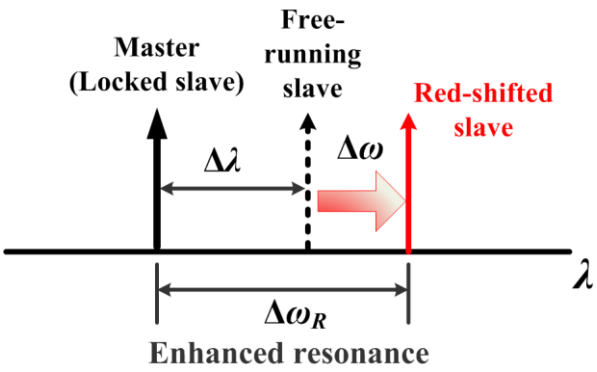

Figure 3.2: Description for the injection induced resonance enhancement. The slave laser is locked to the master despite the existence of its own cavity mode, which is red-shifted by injection. The interaction between the locked and shifted slave modes resonantly enhances the modulation response.

The physical principle of resonance frequency enhancement in externally injected semiconductor lasers has been well studied [1] [38] and can be simply depicted as follows. Firstly, the optical injection reduces the carrier density in the slave cavity by supplying extra photons from the master laser emission. This increases the refractive index and leads to a red-shift in the slave cavity mode from its free-running case [40-42] as illustrated in Fig. 3.2. The angular *frequency* change corresponds to such red-shift can be written as [41]:

$$\Delta\omega = \frac{\alpha}{2} g\left(N - N_{th}\right) \tag{3.1}$$

where α is the linewidth factor [42] that describes the amplitude-phase coupling of the electric field in the cavity and indicates the carrier induced refractive index change, g is the optical modal gain, N is the carrier density in the slave cavity and N_{th} denotes the carrier density at threshold. Note that under external injection the carrier number is reduced from its threshold value hence $(N - N_{th}) < 0$ and $\Delta\omega < 0$.

Under injection locking, the injected master light dominates the optical spectrum and forces the slave to actually emit at the master wavelength. However the intrinsic slave cavity mode (red-shifted by injection) remains active and interferes with the injection locked slave mode [1] [7]. With a negative wavelength detuning ($\Delta\lambda < 0$ as indicated in Fig. 3.2) the interaction between the locked slave and the red-shifted slave can cause various behaviours such as beating phenomenon and intensity pulsations [40-43]. More importantly when the locked slave laser is subjected to direct current modulation, the optical sideband of the locked

mode can be resonantly enhanced by the residual cavity mode [38]. As such, the frequency difference between the locked and shifted slave modes dictates the resonance enhancement $\Delta\omega_R$ [15] as demonstrated in Fig. 3.2. The above described process holds as long as the injection happens within the locking range. The locking range is defined as the range of detuning over which stable locking is achieved, and it is determined by the effective external optical power that could be coupled into the slave laser cavity [1] [7]:

$$-\frac{\omega_0}{2Q}\sqrt{\frac{S_{inj}}{S_0}}\sqrt{1+\alpha^2} < \Delta\omega_{inj} < \frac{\omega_0}{2Q}\sqrt{\frac{S_{inj}}{S_0}} \tag{3.2}$$

where $\Delta\omega_{inj}$ represents the locking range in angular *frequency*; ω_0 and S_0 are the laser frequency and photon density in the slave cavity, α is the linewidth enhancement factor of the slave, S_{inj} is the injecting photon density from the master, and Q is the coupling quality factor of the slave laser cavity [39]. In Eq. 3.2, the upper bound of the *frequency* locking range (hence the lower bound of wavelength locking range) represents the maximum achievable resonance frequency enhancement, $\Delta\omega_{R,Max}$ [15] [39]:

$$\Delta\omega_{R,Max} = \frac{\omega_0}{2Q}\sqrt{\frac{S_{inj}}{S_0}} \tag{3.3}$$

and from Eq. 3.3 $\Delta\omega_{R,Max}$ depends on the external injection power ratio as well as the coupling efficiency (Q factor) of the slave laser cavity.

If the master laser injection locks the slave laser with positive wavelength detuning (the master is at higher wavelength than the free-running slave), the modulation response of the slave laser shows reduced resonance enhancement frequencies (compared to the negative wavelength detuning case as discussed before) and tend to have a less pronounced resonance peak [7]. This is because: 1) the master (locked slave) mode and the red-shifted slave mode are sitting closer together hence a reduced $\Delta\omega_R$ and, 2) the master gains better control and further suppresses the intrinsic slave cavity mode, hence a reduced mode beating due to the larger SMSR [7]. Therefore, it is in general not an ideal region for resonance enhanced gain switching. However the benefit gained by positive wavelength detuning is the improved stability and reduced phase noise of the slave output [24]. As such, careful selection of the injection detuning becomes an interesting topic for discussion and the extensive study on

compromising bandwidth enhancement (requires negative wavelength detuning) for low noise property (favours positive wavelength detuning) [27] will be presented in the next chapter.

3.2.2 Comb generation and characterisation

Subsequent to the small signal modulation response measurement, the DFB slave laser is then gain switched for resonance enhanced comb generation. This is achieved by driving the DFB laser with a large amplified (24 dBm) sinusoidal signal in conjunction with the dc bias (50 mA). The experimental setup is demonstrated in Fig. 3.3. The frequency of the signal generator (SG) and the output power of the master laser are set to match the three chosen FSR shown in Fig. 3.1(b). The generated multi-carrier signal is observed with the OSA and also passed through a wavelength and bandwidth tunable optical band-pass filter (BPF) (Yenista Optics, XTM-50) to select individual comb lines for optical linewidth characterisation, which is accomplished with a delayed self-heterodyne (D-SH) measurement scheme [44].

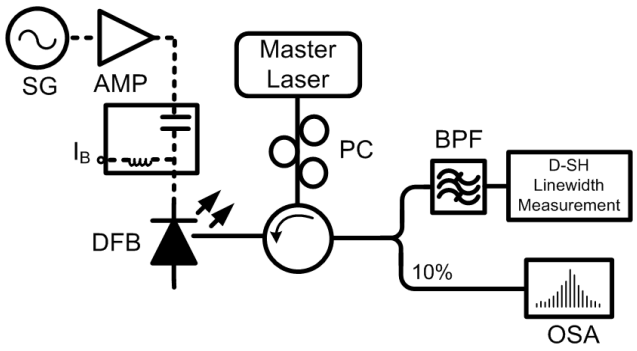

Figure 3.3: Experimental setup of externally injected, gain switched DFB laser for resonance enhanced and FSR flexible comb generation. SG: signal generator, AMP: RF amplifier.

The externally injected gain switched comb generation captured by the high resolution OSA are plotted in Fig. 3.4, with (a), (b) and (c) corresponding to a FSR of 25 GHz, 28 GHz and 33 GHz respectively. In the figure, multiple clearly resolved and phase correlated optical tones showing background noise extinction ratio in excess of 40 dB could be observed, and the tones are offset by an integer multiple of the drive frequency. The comb line numbers generated within a 3-dB spectral envelope in each case are (a) 6 lines (b) 5 lines and (c) 4 lines. It is important to note that the flexible selection of large FSR beyond the capability of the laser's inherent bandwidth limitation is achieved by simply varying the injection power without changing the wavelength detuning. Also as mentioned earlier, even though this

demonstration focuses on a few selected FSR from 25 to 33 GHz it is expected that the technique renders itself for broadband FSR flexibility from ~5 to 40 GHz, and is only limited by the practical bandwidth of the high-power RF amplifier used for gain switching.

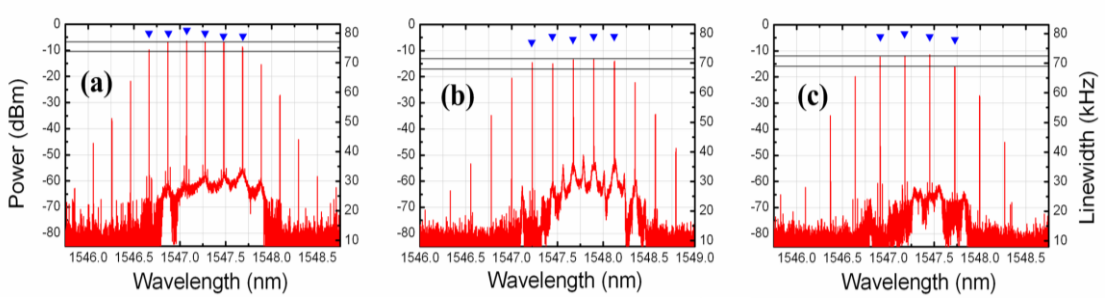

Figure 3.4: Generated combs at the chosen FSR (a) 25 GHz (b) 28 GHz (c) 33 GHz. Superimposed in blue triangles is the optical linewidth of individual comb lines. OSA resolution is 20 MHz.

In Fig. 3.4, the optical linewidth characterised for each comb line and for each of the three FSR combs are shown in the form of blue triangles superimposed on the spectral plot. The individual comb line linewidth of all FSRs associated with the reported comb is measured to be 80 kHz, which is identical to the optical linewidth of the injection master laser measured using the same D-SH setup. This, in comparison with the linewidth of the free-running slave which is estimated to be about 8 MHz when biased at 50 mA (fibre coupled output power of 5.15 dBm), clearly illustrates that the injected slave laser resists the phase fluctuation imposed by its own spontaneous emission and the optical linewidth follows the linewidth of the master laser [22] [24]. Such narrow linewidth obtained from a single injection master but simultaneously transferred to all the comb lines highlights the potential for low-cost implementation of phase noise sensitive advanced modulation formats on each comb tone channel in next generation wavelength division multiplexed passive optical network (WDM-PON) systems [45] [46]. This is one of the subjects for discussion in the next chapter.

3.3 Wavelength Tunable Comb Source

For the conventionally gain switched comb source using discrete mode (DM) laser or injected DFB laser [31], an major limiting factor is the lack of tunability in the central operation wavelength. This is expected to restrict its potential applications for future reconfigurable and agile metro-access networks. In order to introduce wavelength tuning ability to the comb source, an injection locked and gain switched Fabry-Pérot (FP) laser diode [21] is

experimentally investigated in this section. The multi-mode emission of the FP laser offers the possibility to validly select operating wavelength of the optical comb source when subjected to optical injection. The injection, into a particular longitudinal mode, results in single mode emission at that injected mode. Moreover, as mentioned earlier, the injection enhances the gain switched coherent multi-tone signal generation (in terms of improved bandwidth and reduced noise) centred on the injected FP mode. Such a coherent comb generation process can be easily replicated at any given FP mode thereby resulting in wide range (40 nm) wavelength tunability.

Additionally, the viability of this wavelength tunable optical comb source would be further improved if the generated comb line number can be increased on demand. Several options could be employed for increasing the number of comb lines including the nonlinear comb expansion with dispersion compensation fibre and highly nonlinear fibre [31]. In this work however, we utilise a more economic and power saving approach with respect to the targeted optical access application, and explore the electro-optic (EO) modulation technique for coherent comb expansion. Through the experimental demonstration in this section, a single optical phase modulator, driven by the same sinusoidal RF signal used for gain switching, doubles the number of comb lines at all operating wavelengths. It is also noteworthy that this expansion technique is easily scalable by simply increasing the number of modulators being used (and with proper RF driving signals).

3.3.1 Experimental configuration

The schematic configuration of the tunable comb generation is depicted in Fig. 3.5 consisting of an optical part (solid lines) and a RF part (dash lines). The FP slave laser diode used in the experiment is a 200 μm long, commercially available device and is hermetically encased in a high speed butterfly package. The laser emits in the 1.55 μm window and features a threshold current of 8 mA at room temperature. The small signal 3-dB MBW is measured at room temperature to be around 11 GHz when biased at 40 mA ($5I_{th}$). A Hewlett Packard 8168F tunable laser source, an external cavity laser (ECL), acting as the master injects light into the slave laser via a circulator (CIR) and enables the seeding of 20 longitudinal modes of the FP laser thereby achieving single mode operation at each of these selected wavelengths. The wavelength of the master is tuned to match one of the longitudinal modes of the slave and the

injection power to the slave laser measured at port 2 of the circulator varies from 0 to 2 dBm. The slight variation in the injected power is due to the fact that higher injection powers are required to achieve optimum single mode operation around the edges of the FP laser gain curve. A polarisation controller (PC1) is used to align the polarisation state for optical injection.

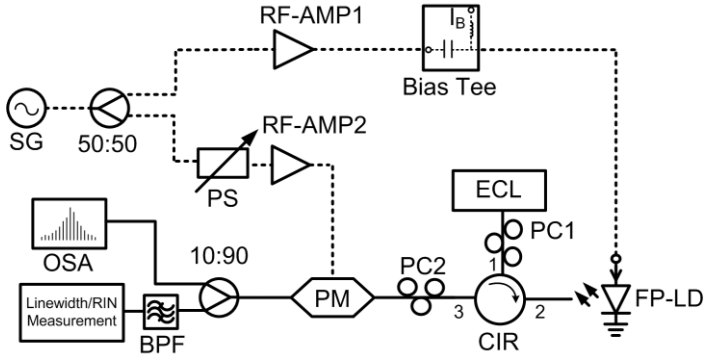

Figure 3.5: Experimental setup for the wavelength tunable comb generation using an externally injected, gain switched FP laser and subsequent comb expansion with an optical phase modulator (PM). SG: signal generator, PS: phase shifter, CIR: optical circulator.

The externally injected slave laser is then gain switched with the aid of a 10 GHz, 24 dBm RF sinusoidal signal in combination with a 40 mA dc current applied via a bias tee, while the FP laser is temperature controlled at 20°C. The resulting optical comb is then put through a 20 GHz EOSPACE low loss phase modulator (PM) for further expansion and shaping of the comb tones. A PC2 is placed at the input of the PM to optimise the state of polarisation. The insertion loss of the PM is about 3 dB over the entire C-band, and the modulation level of the driving signal to the PM is around 18 V, which corresponds to about 4 V_π (V_π ~ 4.5 V at 10 GHz). The PM is driven by an amplified sinusoidal waveform drawn from the same signal generator (SG) used for gain switching, while a RF phase shifter is used to optimise the phase of the applied modulation signal. The output of the PM is split by a 90/10 optical coupler with 10% of the signal being recorded with a 20 MHz resolution APEX AP2443B complex optical spectrum analyser (OSA) and 90% of the signal being sent to the optical linewidth and RIN measurement schemes.

The expansion and shaping of the comb source through a PM can be explained as follows. For each comb line, passing through a sinusoidally modulated PM results in modulation sideband generation at a frequency spacing that is equal to the RF driving signal. With the RF

driving frequency identical to that used for gain switching, the PM modulated sidebands coincide and interact with the neighbouring gain switched comb lines in a constructive or destructive manner, depending on the relative phase relation between the two stages of the RF signal. Hence with proper tuning of PS in Fig. 3.5, the edge comb lines of the gain switched comb could be enhanced resulting in an increased comb line number, and the overall flatness of the output comb can be manipulated.

3.3.2 Comb generation and expansion

Before demonstrating tunable comb generation, the free-running and injection locked spectrum of the FP slave laser under a 40 mA bias current are shown in Fig. 3.6(a) and 3.6(b), respectively. As can be seen from Fig. 3.6(a), the longitudinal mode spacing of the FP laser is approximately 1.7 nm which corresponds to a laser cavity length of 200 μm. By carefully adjusting the polarisation state of the injecting signal from the ECL, precise injection into a particular FP mode results in single mode operation of the slave laser because the injected light enhances the optical gain in this specific FP mode and significantly suppresses all other free-running modes. An exemplary single mode operation case at around 1551 nm with side mode suppression ratio (SMSR) greater than 60 dB is illustrated in Fig. 3.6(b). With the fine tuning of ECL injection over a wide wavelength range, over 20 single mode operation points, with high SMSR, can be realised in the same manner. It is important to note that the FP laser gain curve can be shifted in wavelength by about ±1 nm through temperature tuning, hence achieving quasi-continuous wavelength tunability. The temperature tuning could be also used to ensure that the chosen longitudinal mode is aligned in wavelength with the ITU grid thereby conforming to the required standards.

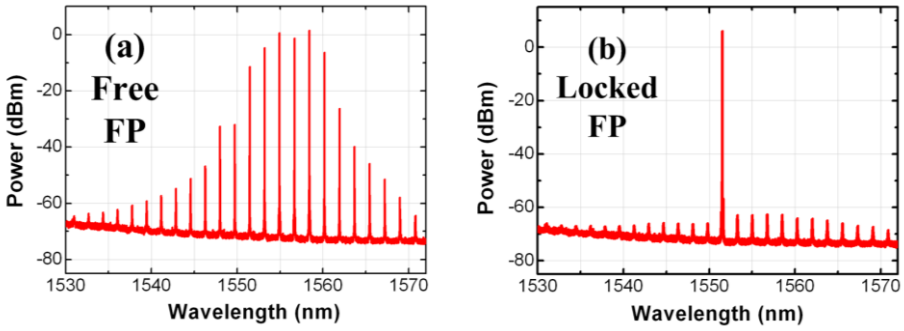

Figure 3.6: Optical spectra (a) free-running FP laser at 40 mA bias, (b) externally injected FP laser. OSA resolution is 20 MHz.

Under injection locking, gain switching of the slave FP laser, at these chosen operating points, results in the generation of highly coherent frequency combs at each of the FP laser modes within the wavelengths of 1530 nm to 1570 nm. These combs consist of 5-8 clearly resolved 10 GHz spaced tones within a 3-dB spectral window all show a carrier to background noise extinction ratio over 50 dB. For the purpose of clarity, some exemplary operating points within the wavelength tuning range are demonstrated in Fig. 3.7(a)-(f). Note that the relatively smaller number of comb lines (5 lines) at around 1530 nm in Fig. 3.7(a) could be attributed to the particular gain profile of the FP laser under given bias and temperature conditions, since these conditions has resulted in reduced modal gain around 1530 nm as shown in Fig. 3.6(a). The reduced optical gain, compared to other FP modes, has caused the slight comb line number reduction in this operating point.

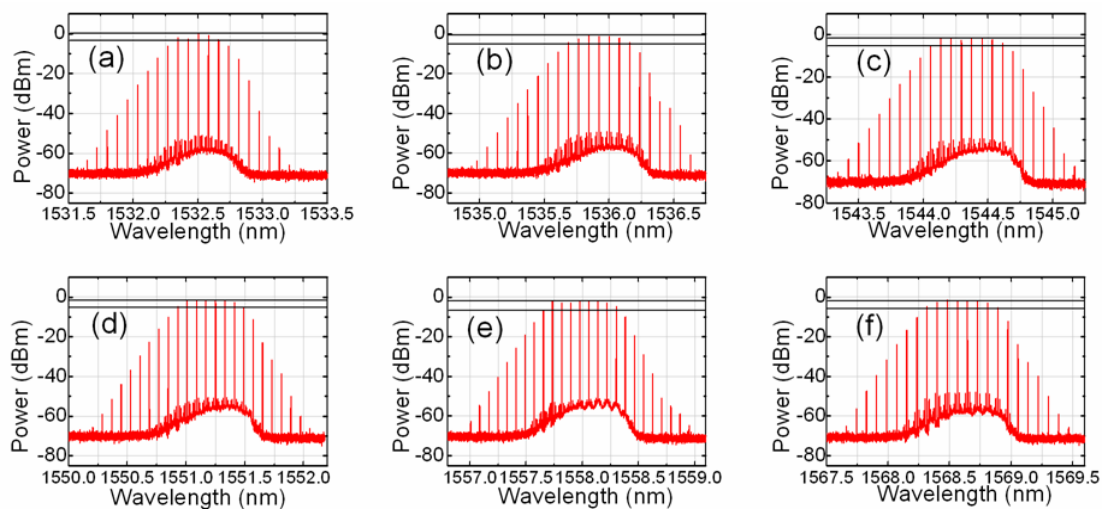

Figure 3.7: Optical spectra of external injected, gain switched optical combs at six selected operating points (a)-(f) from 1530 nm to 1570 nm (40 nm wavelength tuning range). OSA resolution is 20 MHz.

Subsequently, the expansion of the tunable comb when passed through the PM for some of the above demonstrated operating points is presented in Fig. 3.8(a)-(c). The phase modulation proves to be an effective means of improving the comb line number and comb flatness, as in the Fig. 3.8(c) where 16 lines in a 3-dB spectral window can be observed at 1568 nm and very similar results (14 lines and 15 lines respectively) are obtained around 1530 nm - 1540 nm in Fig. 3.8(a) and 3.8(b). The spectra are optimised by tuning the phase shifter only and all other conditions (injection, gain switching) remain unchanged. As such even with the unbalanced gain curve of the FP laser diode, doubled comb line numbers and nicely flattened combs can

be obtained over the entire wavelength tuning range.

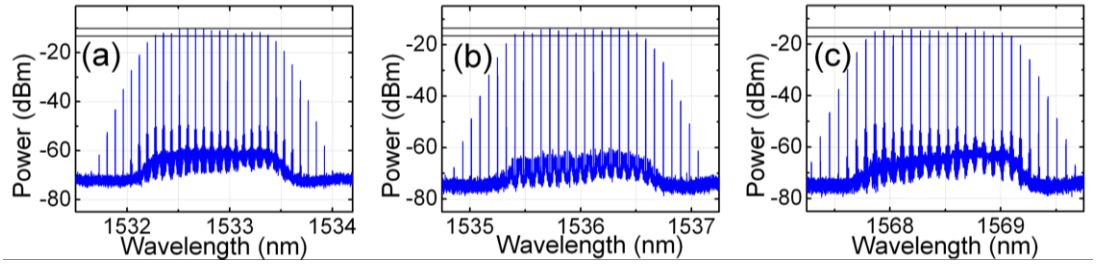

Figure 3.8: Expanded combs from optical phase modulation consisting of 14-16 tones in 3-dB window. OSA resolution is 20 MHz.

3.3.3 Comb line characterisation

After the tunable comb generation and expansion, the signal is sent to a wavelength and bandwidth variable optical band-pass filter (BPF) followed by the linewidth and RIN measurement setups for intensity and phase noise characterisations. The tunable BPF (Alnair Labs, BVF-200 Bandwidth-Variable Tunable Filter) with a minimum 3-dB optical bandwidth of around 12.5 GHz is used to select out individual comb lines from each of the operating points to enable these measurements. The linewidth measurement, using the identical D-SH setup [44] as reported in Section 3.2, has a fibre length of 12 km in the delayed arm which corresponds to a spectral resolution of about 17 kHz. The RIN measurement, which examines the ratio between optical power fluctuation and mean optical power [47], can be accomplished in the electrical domain by capturing the power fluctuations on an electrical spectrum analyser (ESA) (Anritsu MS2668C, 9 kHz - 40 GHz) and the averaged optical power at the output of the photodiode (u^2t photonics XPDV2120R, 50 GHz) [36] [48].

For the optical linewidth measurement, 14 of the operating modes, within the given wavelength tuning range, are chosen. At each of these operating modes, 3 individual comb tones are filtered and measured. The individual comb line optical linewidth is measured to be between 60-90 kHz as shown in Fig. 3.9. The linewidth of the master ECL is also measured for comparison and shown in the same figure, with recorded values of around 75 kHz (±15 kHz variation) across the whole 40 nm wavelength tuning range. These measurement results clearly illustrate that the optical linewidth of the individual comb lines follow the linewidth of the master laser, due to the domination of injection master noise property over the low frequency phase noise behaviour of the slave laser [24].

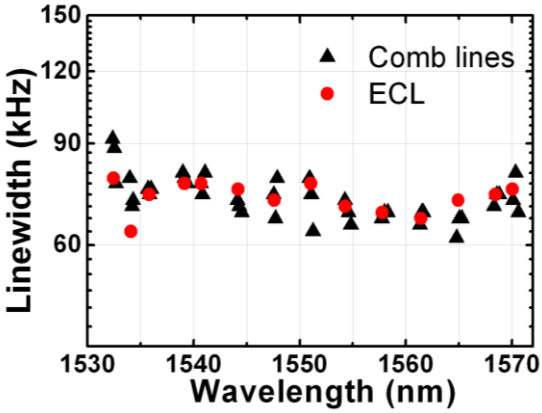

Figure 3.9: Optical linewidth of selected comb lines (black triangle) and that of injection master ECL (red circles) at 14 operating FP modes over the 40 nm wavelength range.

The RIN measurements are carried out at 3 of the operating wavelengths (1530 nm, 1550 nm and 1570 nm). Two different scenarios are verified at each of these operating wavelengths: 1) RIN of the unfiltered comb at the given operating wavelength, and 2) RIN of 3 individually filtered comb lines at each of the operating wavelengths marked as "Line 1" "Line 2" and "Line 3". The achieved results are shown in Fig. 3.10. The averaged RIN (from dc to 10 GHz) for the entire optical comb (all lines), at the 3 operating wavelengths, is around -135 dB/Hz, whereas the RIN values are all below -120 dB/Hz for the 9 filtered comb lines. The reason that the individual comb lines have higher RIN values than the entire comb is because of a phenomenon known as mode partitioning effect, which arises from the competition/fluctuation of optical power among multiple longitudinal modes (in this case comb lines). With the influence from this mode partition noise (MPN), although the overall output spectrum (the whole comb) remains relatively constant due to the overall equilibrium, the individual spectral lines demonstrate considerable fluctuations hence increased RIN values. The slightly lower (-130 dB/Hz) comb line RIN values for the 1530 nm and 1570 nm cases is due to the reduced

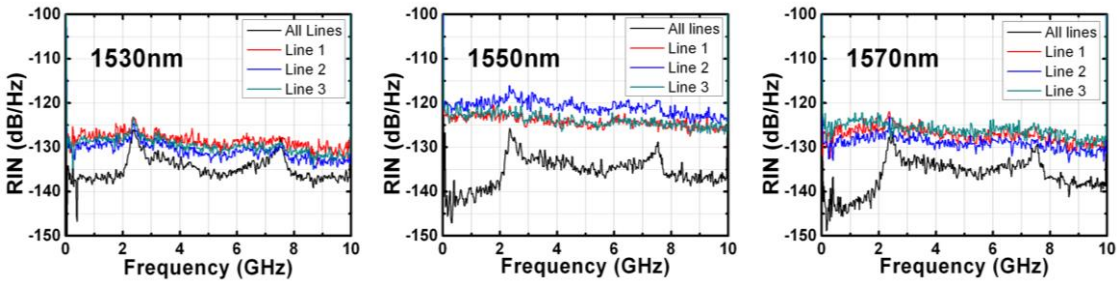

Figure 3.10: RIN measurement of the 3 chosen operating modes and of the filtered comb lines. ESA resolution is 100 kHz.

comb line number at these wavelength (stem from the reduced optical gain at these FP modes). Hence, the power fluctuations in comb lines are relatively lower at these wavelengths. However, the RIN of the individually filtered comb tones is still not much higher than the entire comb even for the 1550 nm case (15 dB difference has been noticed) thus indicating that the effect of mode partition noise is less significant than that in a quantum dash mode locked laser [49].

3.4 Compact Comb Sources

Thus far, the injected gain switched comb generation has been demonstrated with multiple discrete components including the master and slave lasers. A circulator, polarisation controller, and connecting fibres would be the additional passive optical elements required for the successful realisation of this master-slave configuration. Hence, such an experimental arrangement would potentially suffer from various external sources of instability in the injection path, such as polarisation dependence, temperature variation and/or mechanical vibration. Integration of the two lasers (master and slave) would alleviate the aforementioned problems, reduce the insertion losses incurred, reduce the footprint, and improve the overall robustness. As such, monolithic integration offers a simplified solution for the realisation of optically injected and gain switched comb generation, providing significant packaging consolidation, testing simplification, less fibre connections, improved reliability and drastic reduction in space and power consumption of the comb source.

In this section, two different types of monolithically integrated lasers will be demonstrated as compact optical sources for injected gain switched comb generation. One of them is a custom fabricated device that integrates the master and slave discrete mode (DM) lasers on a single all-active chip [36], namely the integrated 2-section DM index patterned laser. The other device explores optical feedback to achieve optical injection, which is based on a commercially available complex coupled DFB laser with an integrated feedback section [50], namely the passive feedback laser (PFL). Exemplary comb generation with injection enhanced properties such as 3-dB MBW, noise and nonlinear distortions will be examined.

3.4.1 Comb generation with integrated 2-section DM laser

Optical injection in the 2-section DM index patterned laser is achieved by building a structure

that places the master and slave DM sections onto a common substrate, so that all photonic couplings occur within the substrate and the function of the master-slave configuration is consolidated into a single physically unique device. This makes the optical injection process simple, cost effective and polarisation independent compared to external optical injection using discrete master and slave lasers. Moreover, monolithic integration offers the possibility of further integrating other elements and making highly functional photonic integrated circuits. A unique feature of this integrated 2-section laser is that it enables multiple applications by improving basic laser parameters such as the RIN, MBW, SMSR, and linearity [36], allowing direct modulation to be used effectively. The waveguide structure requires only a single growth stage and uses optical lithography to realise the ridge [51] hence all the aforementioned positive attributes can be accomplished at a relatively low cost.

The physical structure of the integrated 2-section DM laser used in this work is schematically shown in Fig. 3.11(a). The device is a ridge waveguide laser with a ridge width of 2.5 μm. The laser cavity is 700 μm long and is divided into a master (300 μm) and a slave (400 μm) section, separated by an etched trench that is 2 μm wide. It is worth noting that the current assignment of cavity lengths for the master and slave sections is due to a fabrication error, with the original design targeting at the reversed order (400 μm for the master and 300 μm for the slave). With the method described in [36], index perturbation is introduced in the ridge upper surface for both sections through selectively etched features. These features, in the upper waveguide layers above the active region, define the single-mode emission for each DM

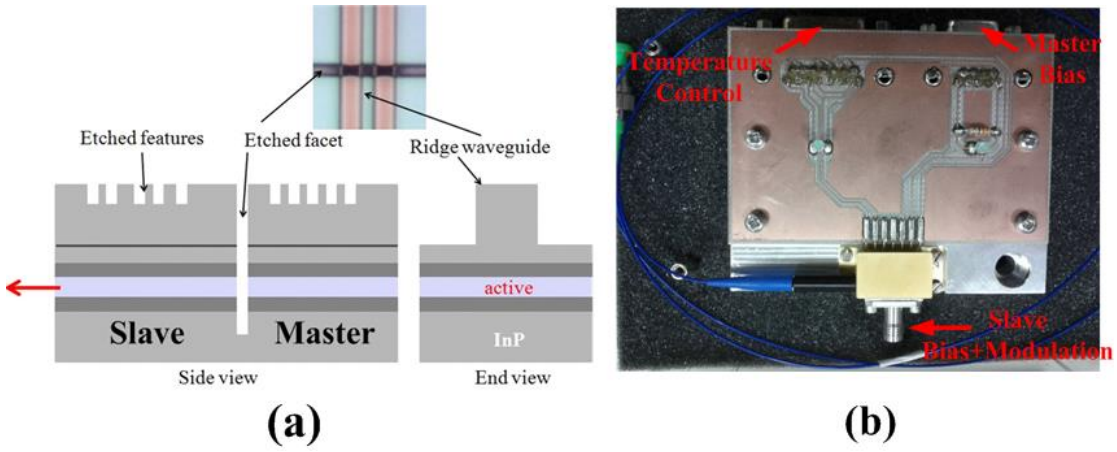

Figure 3.11: Two-section optical injection structure with a DM laser in master section and another DM laser in slave section. (a) Device structure, where a deeply etched trench defines the back and front facets for slave and master. (b) Picture of the packaged device.

section (master and slave) [51]. Additional details on the laser design such as active material and insulations can be found in [36]. The integrated 2-section device is packaged in a temperature controlled butterfly package yielding a room temperature threshold current of 21 mA for the slave section, and linear light-current (L-I) curves for both sections until 100 mA [36]. A picture of the packaged device is shown in Fig. 3.11(b).

With all the aforementioned benefits of the 2-section DM laser [36], the integrated device has the potential to be employed as an ideal candidate for the compact gain switched comb generation. The experimental setup is demonstrated in Fig. 3.12(a). For gain switching the laser, the device is temperature controlled at 20°C and the slave section is biased via a bias tee to allow simultaneous dc bias and modulation. An amplified sinusoidal signal (24 dBm) from the signal generator (SG) in conjunction with the dc current is directly applied to the slave section while the master section is dc biased and tuned to find the optimum optical injection condition. The resulting signals are observed with a high resolution optical spectrum analyser (OSA) and the spectrum resolution is set to 100 MHz.

Before demonstrating the comb generation results, shown in Fig. 3.12(b) is the normalised frequency response of the free-running laser characterised by performing small signal modulation analysis with the aid of a network analyser. In the figure, a 3-dB MBW of approximately 3 GHz (at $2I_{th}$) for the free-running slave section is noticed. However, it can be also seen that the inherent bandwidth of this laser (with slave section emission only) could be improved up to around 10 GHz (about 3 times improvement) by properly biasing the master section (therefore injecting into the slave section).

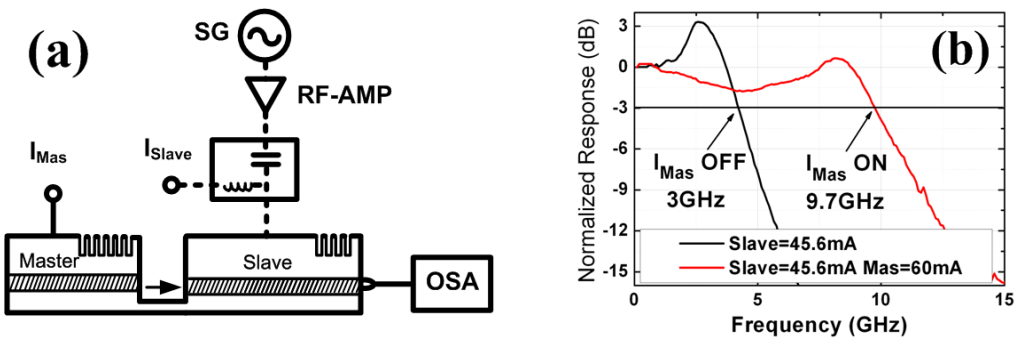

Figure 3.12: (a) Experimental setup for the gain switched comb generation of 2-section DM index patterned laser, (b) small signal MBW measurement results of the device. SG: signal generator.

The results for the comb generation when using the gain switched 2-section DM laser are

demonstrated with two different FSR scenarios. In the first case, the spectra in Fig. 3.13 illustrate the output of the device when the slave section is being gain switched at 5 GHz FSR. In Fig. 3.13(a) the slave section current is 58 mA and the master section is turned off. It can be clearly seen that without optical injection from the master DM section, comb generation is unsuccessful. This is because, the gain switching process imposes abrupt photon density fluctuations in the laser cavity and results in all the cavity modes start to compete for optical gain, therefore the coherent gain in the lasing mode is shared and reduced [31]. This can be viewed more clearly in a larger scale as shown by Fig. 3.13(c), where the neighbouring modes are illustrating similar power level (~5 dB difference) compared to the middle lasing mode. In contrast, Fig. 3.13(b) illustrates the case when the slave section current is kept at the same value while the master section is turned on and the bias current is 20 mA. As a result, comb generation with 9-line flatness is achieved within a 3-dB spectral window. This is due to the fact that the injection from the master enhances the optical gain and the excitation of the lasing mode in slave laser by: 1) reducing the coupling of random spontaneous emission, and 2) suppressing the relative power transferring/fluctuations amongst the cavity modes. The latter improvement can be seen from the zoom out view given by Fig. 3.13(d) where a neighbouring mode suppression of ~40 dB is achieved.

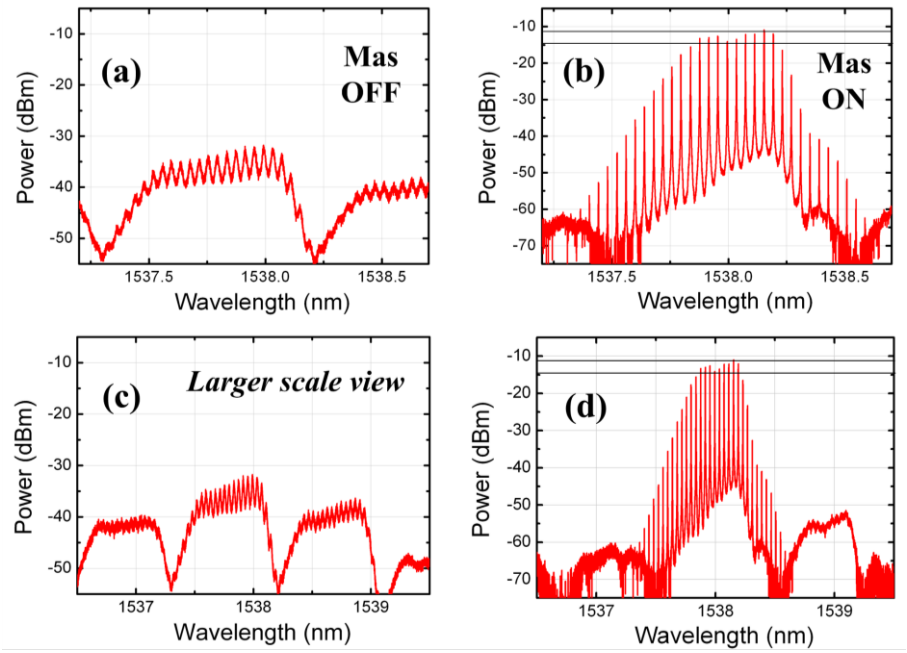

Figure 3.13: Comb generation with 2-section DM laser at 5 GHz FSR, (a) when master section is off and (b) on, respectively, slave/master section currents: 58 mA/20 mA. (c) (d) Zoom out versions. OSA resolution is 100 MHz.

Subsequently, the gain switched comb generation at 10 GHz FSR is demonstrated in the same manner, and the results with master section off and on are shown in Fig. 3.14(a) and (b) respectively. In this FSR scenario the slave and master sections are biased at 46 mA and 19 mA respectively. Fig. 3.14 (a) demonstrates the distorted spectrum when injection from master section is turned off, giving rise to intermediate spurious frequency tones due to a nonlinear phenomenon known as period doubling [52]. For comparison in Fig. 3.14(b), nonlinear distortion has been suppressed through proper injection from the master laser section. The restricted comb line number (3 lines within a 3-dB flatness window) in this case can be attributed to the limited MBW of the current device prototype, since the inherent bandwidth of the laser is restricted to about 3 GHz as shown in Fig. 3.12(b). This is partly due to the relatively long cavity length of the slave section (400 μm) and can be enhanced, with injection to about 10 GHz. Further increasing the injection locked MBW limit is potentially possible with reduced device parasitics and improved device package [6] [53].

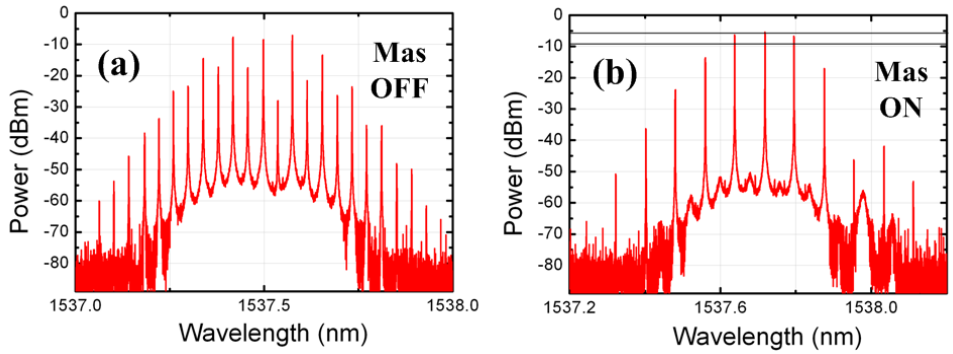

Figure 3.14: Comb generation with 2-section DM laser at 10 GHz FSR, (a) master section off and (b) on, respectively. Slave/master section currents: 46 mA/19 mA. OSA resolution is 100 MHz.

3.4.2 Comb generation with passive feedback laser

The second monolithically integrated laser used for comb generation is a PFL whose physical structure [50] [54] is schematically shown in Fig. 3.15(a). The PFL (chip from Fraunhofer Heinrich Hertz Institute) is also a 2-section device where a passive feedback section is integrated with an active DFB section so that optical phase shift (with some losses) can be obtained by the passive section [55]. The phase shift is critical for providing controlled optical feedback injection to the active section and can be tuned by changing the bias current of the passive section. The device used in this work has a total chip length around 500 μm and is

based on a ridge waveguide structure and strained active quantum well layers. This laser is also encased in a temperature controlled custom designed butterfly package (by Achray Photonics), yielding a threshold current of 8 mA (linear L-I curve until 60 mA) and a room temperature 3-dB bandwidth of approximately 6 GHz (at $3I_{th}$) as shown in Fig. 3.15(b). The passive section current has an allowed operational range of 0-60 mA.

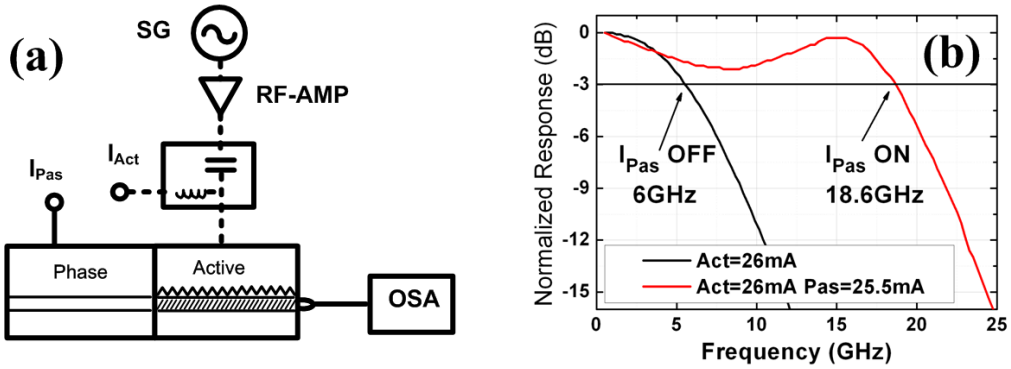

Figure 3.15: (a) Experimental setup for the gain switched comb generation of PFL, (b) small signal MBW measurement results of the device. SG: signal generator.

The PFL has been engineered for the purpose of low cost direct data modulation with enhanced modulation bandwidth in short reach transmission systems [54]. The device design can be viewed as the extended-cavity laser concept with integrated short external cavity [55]. In such a device, the main reason for the MBW/resonance frequency improvement is the beating of two compound-cavity modes that results in additional photon-photon resonance at frequencies much higher than the inherent carrier-photon interaction [50]. Therefore, the physical picture here is very similar to that described in Section 3.2.1. It can be seen from the frequency response characterisation of the PFL device in Fig. 3.15(b) that similar to the 2-section DM laser case, over 3-times MBW improvement can be achieved with this device when the phase section current is appropriately biased.

The PFL device is then gain switched by simultaneously driving the active (DFB) section with a dc current and a sinusoidal modulation signal (24 dBm), as described by Fig. 3.15(a). The laser is temperature controlled at 20°C and the passive section is dc biased and the current is to ensure optimum optical feedback. The output signal is observed with the 100 MHz OSA. For this device, comb generation is demonstrated at 10 GHz and 15 GHz FSR. Firstly illustrated in Fig. 3.16 are the comb generation results corresponding to 10 GHz FSR. Fig. 3.16(a) shows the optical spectrum when the active section is biased at 51 mA and the phase

section has been turned off. Due to the lack of optimal optical feedback from the phase section, nonlinear harmonics between comb tones appear. On the other hand, the optical spectrum in Fig. 3.16(b) illustrates an optical frequency comb with 9 clearly resolved comb lines at 10 GHz FSR that exhibit a spectral ripple of less than 3-dB. This is achieved with the bias current for active section unchanged (51 mA) and the phase current (passive section) chosen at 3 mA.

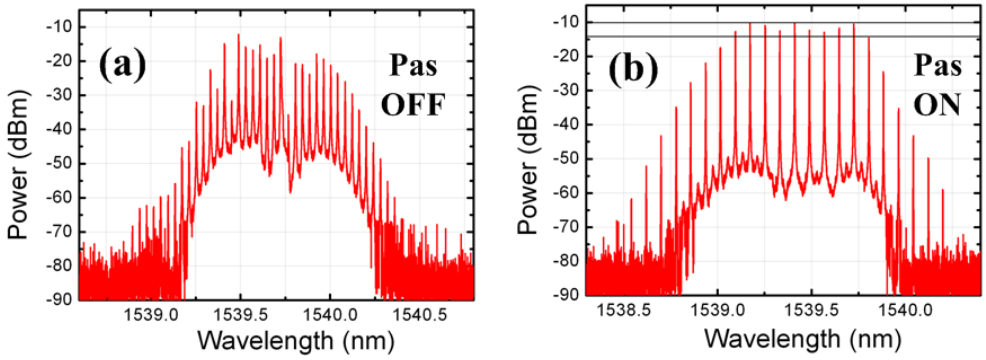

Figure 3.16: Comb generation with PFL device at 10 GHz FSR, (a) passive section off and (b) on, respectively. Active/passive section currents: 51 mA/3 mA. OSA resolution is 100 MHz.

Next, the experimental results for gain switched comb generation at 15 GHz FSR with the PFL device are shown in Fig. 3.17(a) and (b), with the phase current off and on, respectively. For this FSR scenario the active section bias is 65 mA and the passive section bias is 6.5 mA. As can be seen in Fig. 3.17(a), the poor structure of the generated comb signal when only biasing the active section can be attributed to the limited MBW of the device without proper phase feedback, since a maximum of 6 GHz 3-dB bandwidth is achieved at ~$3I_{th}$ as shown by the frequency response measurement result in Fig. 3.15(b). With the passive section biased properly the modulation response could be enhanced up to 18.6 GHz as shown in Fig. 3.15(b).

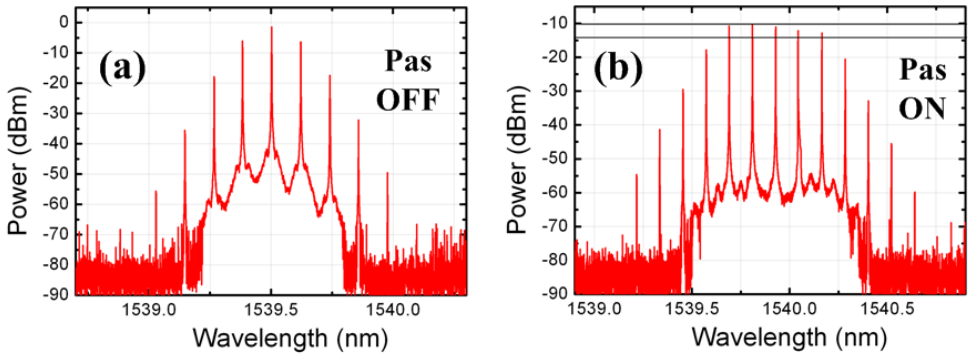

Figure 3.17: Comb generation with PFL device at 15 GHz FSR, (a) passive section off and (b) on, respectively. Active/passive section currents: 65 mA/6.5 mA. OSA resolution is 100 MHz

Hence in this occasion, more comb lines are resulted as demonstrated in Fig. 3.17(b) where a 5-line flat comb (3-dB window) is obtained when passive feedback is on.

3.5 Summary

In this chapter, three types of injected gain switched lasers have been experimentally investigated for frequency comb generation. The first demonstration is a comb source offering enhanced yet flexible FSR, which enables precisely controlled channel spacing that can be easily adapted to suit the desired symbol rate in highly efficient WDM-PON systems. Experimental comb generation at 3 different FSRs: 25, 28, and 33 GHz have been shown, yielding comb line numbers (within a 3-dB spectral window) of 6, 5, and 4 lines for each FSR case respectively. The narrow linewidth of the comb lines (80 kHz, transferred from the injection master) suggests the potential applications involving advanced optical modulation formats. The second comb source exhibiting central wavelength tunability over 40 nm tuning range allows a single WDM multi-carrier transmitter to operate on any specific wavelength channel, thus greatly reduces the network operating costs through sparing and inventory savings. Within the wavelength tuning range, 5~8 comb lines (in a 3-dB spectral window) at 10 GHz FSR have been demonstrated for all the chosen operating points. Furthermore, bandwidth scaling of the tunable comb source has been proven feasible with simple optical phase modulation, which yields doubling of the comb line numbers (14-16 lines) in each demonstrated operating wavelength. The optical linewidth and RIN characterisation results further illustrate the low noise properties of the reported comb source. Finally, the compact optical comb generation utilising gain switching of monolithically integrated 2-section lasers (index patterned 2-section DM laser and passive feedback laser) has shown improved modulation properties (through optimum injection/feedback from the master/phase section) in terms of modulation bandwidth, comb shape, and linearity, hence providing enhanced performance with reduced footprint, improved reliability, and decreased power consumption. As such, the demonstrated compact comb sources having a small form factor and improved power efficiency (through photonics integration) render themselves as simple, robust, and economic solutions to the realisation of highly functional and low cost WDM transmitters.

Reference

[1] E. K. Lau, L. J. Wong, and M. C. Wu, "Enhanced modulation characteristics of optical injection-locked lasers: a tutorial," IEEE J. Sel. Topics Quantum Electron. **15**, 618 (2009).

[2] S. Kobayashi and T. Kimura, "Coherence of injection phase-locked AlGaAs semiconductor laser," Electron. Lett. **16**, 668 (1980).

[3] Y. Yamamoto, "Receiver performance evaluation of various digital optical modulation –demodulation systems in the 0.5-10 μm wavelength region," IEEE J. Quantum Electron. **QE-16**, 1251 (1980).

[4] S. Kobayashi, Y. Yamamoto, and T. Kimura, "Optical FM signal amplification and FM noise reduction in an injection locked AlGaAs semiconductor laser," Electron. Lett. **17**, 849 (1981).

[5] S. Kobayashi and T. Kimura, "Optical phase modulation in an injection locked AlGaAs semiconductor laser," IEEE J. Quantum Electron. **QE-18**, 1662 (1982).

[6] K. Y. Lau and A. Yariv, "Ultra-high speed semiconductor lasers," IEEE J. Quantum Electron. **QE-21**, 121 (1985).

[7] H. K. Sung, E. K. Lau, and M. C. Wu, "Optical properties and modulation characteristics of ultra-strong injection-locked distributed feedback lasers," IEEE J. Sel. Topics Quantum Electron. **13**, 1215 (2007).

[8] R. Lang and K. Kobayashi, "Suppression of the relaxation oscillation in the modulated output of semiconductor lasers," IEEE J. Quantum Electron. **QE-12**, 194 (1976).

[9] J. Wang, M. K. Haldar, L. Li, and F. V. C. Mendis, "Enhancement of modulation bandwidth of laser diodes by injection locking," IEEE Photon. Technol. Lett. **8**, 34 (1996).

[10] T. B. Simpson and J. M. Liu, "Enhanced modulation bandwidth in injection-locked semiconductor lasers," IEEE Photon. Technol. Lett. **9**, 1322 (1997).

[11] X. J. Meng, T. Chau, and M. C. Wu, "Experimental demonstration of modulation

bandwidth enhancement in distributed feedback lasers with external light injection," Electron. Lett. **34**, 2031 (1998).

[12] H. Ghafouri-Shiraz, *The Principles of Semiconductor Laser Diodes and Amplifiers: Analysis and Transmission Line Laser Modelling* (Imperial College Press, 2004).

[13] L. P. Barry, P. Anandarajah, and A. Kaszubowska, "Optical pulse generation at frequencies up to 20 GHz using external-injection seeding of a gain-switched commercial Fabry-Pérot laser," IEEE Photon. Technol. Lett. **13**, 1014 (2001).

[14] L. Chrostowski, B. Faraji, W. Hofmann, M. C. Amann, S. Weczorek, and W. W. Chow, "40 GHz bandwidth and 64 GHz resonance frequency in injection-locked 1.55 μm VCSELs," IEEE J. Sel. Topics Quantum Electron. **13**, 1200 (2007).

[15] E. K. Lau, X. Zhao, H. K. Sung, D. Parekh, C. C. Hasnain, and M. C. Wu, "Strong optical injection-locked semiconductor lasers demonstrating > 100-GHz resonance frequencies and 80-GHz intrinsic bandwidths," Opt. Express. **16**, 6609 (2008).

[16] P. M. Anandarajah, R. Zhou, R. Maher, M. D. G. Pascual, F. Smyth, V. Vujicic, and L. P. Barry, "Flexible optical comb source for super channel systems," in *Proc. OFC 2013, OTh3I.8.*

[17] K. Petermann, *Laser Diode Modulation and Noise* (Kluwer Academic & KTK Scientific, 1988).

[18] N. Schunk and K. Petermann, "Noise analysis of injection-locked semiconductor injection lasers," IEEE J. Quantum Electron. **QE-22**, 642 (1986).

[19] G. Yabre, H. Waardt, H. P. A. Boom, and G. D. Khoe, "Noise characteristics of single-mode semiconductor lasers under external light injection," IEEE J. Quantum Electron. **36**, 385 (2000).

[20] K. Iwashita and K. Nakagawa, "Suppression of mode partition noise by laser diode light injection," IEEE J. Quantum Electron. **QE-18**, 1669 (1982).

[21] R. Zhou, S. Latkowski, J. O'Carroll, R. Phelan, L. Barry, and P. Anandarajah, "40nm wavelength tunable gain-switched optical comb source," Opt. Express **19**, B415 (2011).

[22] P. Gallion, H. Nakajima, G. Debarge, and C. Chabran, "Contribution of spontaneous

emission to the linewidth of an injection-locked semiconductor laser," Electron. Lett. **21**, 626 (1985).

[23] F. Mogensen, H. Olesen, and G. Jacobsen, "FM noise suppression and linewidth reduction in an injection-locked semiconductor laser," Electron. Lett. **21**, 696 (1985).

[24] P. Spano, S. Piazzolla, and M. Tamburrini, "Frequency and intensity noise in injection-locked semiconductor lasers: theory and experiments," IEEE J. Quantum Electron. **QE-22**, 427 (1986).

[25] K. Kikuchi, C. E. Zah, and T. P. Lee, "Amplitude-modulation sideband injection locking characteristics of semiconductor lasers and their application," J. Lightwave Technol. **6**, 1821 (1988).

[26] O. Lidoyne, P. Gallion, and G. Debarge, "Phase jitter in an injection-locked semiconductor laser," Opt. Lett. **15**, 1144 (1990).

[27] R. Zhou, T. N. Huynh, V. Vujicic, P. M. Anandarajah, and L. P. Barry, "Phase noise analysis of injected gain switched comb source for coherent communications," Opt. Express **22**, 8120 (2014).

[28] R. A. Linke, "Transient chirping in single-frequency lasers: Lightwave systems consequences," Electron. Lett. **20**, 472 (1984).

[29] C. Lin and F. Mengel, "Reduction of frequency chirping and dynamic linewidth in high-speed directly modulated semiconductor lasers by injection locking," Electron. Lett. **20**, 1073 (1984).

[30] S. Mohrdiek, H. Burkhard, and H. Walter, "Chirp reduction of directly modulated semiconductor lasers at 10 Gb/s by strong CW light injection," J. Lightwave Technol. **12**, 418 (1994).

[31] P. M. Anandarajah, R. Maher, Y. Q. Xu, S. Latkowski, J. O'Carroll, S. G. Murdoch, R. Phelan, J. O'Gorman, and L. P. Barry, "Generation of coherent multicarrier signals by gain switching of discrete mode lasers," IEEE Photon. J. **3**, 112 (2011).

[32] T. E. Darcie and R. S. Tucker, "Intermodulation and harmonic distortion in InGaAsP lasers," Electron. Lett. **21**, 665 (1985).

[33] W. I. Way, “Large signal nonlinear distortion prediction for a single-mode laser diode under microwave intensity modulation,” J. Lightwave Technol. **LT-5**, 305 (1987).

[34] G. Yabre and J. L. Bihan, “Reduction of nonlinear distortion in directly modulated semiconductor lasers by coherent light injection,” IEEE J. Quantum Electron. **33**, 1132 (1997).

[35] X. J. Meng, T. Chau, and M. C. Wu, “Improved intrinsic dynamic distortions in directly modulated semiconductor lasers by optical injection locking,” IEEE Trans. Microw. Theory Tech. **47**, 1172 (1999).

[36] P. M. Anandarajah, S. Latkowski, C. Browning, R. Zhou, J. O’Carroll, R. Phelan, B. Kelly, J. O’Gorman, and L. P. Barry, “Integrated two-section discrete mode laser,” IEEE Photon. J. **4**, 2085 (2012).

[37] R. Zhou, P. M. Anandarajah, M. D. G. Pascual, J. O’Carroll, R. Phelan, B. Kelly, and L. P. Barry, “Monolithically integrated 2-section lasers for injection locked gain switched comb generation,” in *Proc. OFC 2014, Th3A.3.*

[38] A. Murakami, K. Kawashima, and K. Atsuki, “Cavity resonance shift and bandwidth enhancement in semiconductor lasers with strong light injection,” IEEE J. Quantum Electron. **39**, 1196 (2003).

[39] E. K. Lau, H. K. Sung, and M. C. Wu, “Scaling of resonance frequency for strong injection-locked lasers,” Opt. Lett. **32**, 3373 (2007).

[40] R. Lang, “Injection locking properties of a semiconductor laser,” IEEE J. Quantum Electron. **QE-18**, 976 (1982).

[41] F. Mogensen, H. Olesen, and G. Jacobsen, “Locking conditions and stability properties for a semiconductor laser with external light injection,” IEEE J. Quantum Electron. **QE-21**, 784 (1985).

[42] C. H. Henry, N. A. Olsson, and N. K. Dutta, “Locking range and stability of injection locked 1.54 μm InGaAsP semiconductor lasers,” IEEE J. Quantum Electron. **QE-21**, 1152 (1985).

[43] J. Nishizawa and K. Ishida, “Injection-induced modulation of laser light by the interaction

of laser diodes," IEEE J. Quantum Electron. **QE-11**, 515 (1975).

[44] T. Okoshi, K. Kikuchi, and A. Nakayama, "Novel method for high resolution measurement of laser output spectrum," Electron. Lett. **16**, 630 (1980).

[45] P. M. Anandarajah, R. Zhou, R. Maher, D. Lavery, M. Paskov, B. C. Thomsen, S. J. Savory, and L. P. Barry, "Gain-switched multicarrier transmitter in a long-reach UDWDM-PON with a digital coherent receiver," Opt. Lett. **38**, 4797 (2013).

[46] R. Zhou, P. M. Anandarajah, R. Maher, M. Paskov, D. Lavery, B. C. Thomsen, S. J. Savory, and L. P. Barry, "80-km coherent DWDM-PON on 20-GHz grid with injected gain switched comb source," IEEE Photon. Technol. Lett. **26**, 364 (2014).

[47] R. Hui and M. O'Sullivan, *Fibre Optic Measurement Techniques* (Academic Press, 2009).

[48] Eagleyard Photonics, "Relative Intensity Noise of Distributed Feedback Lasers," http://www.eagleyard.com/fileadmin/downloads/app_notes/App_Note_RIN_1-5.pdf

[49] Y. B. M'Sallem, Q. T. Le, L. Bramerie, Q. T. Nguyen, E. Borgne, P. Besnard, A. Shen, F. Lelarge, S. LaRochelle, L. A. Rusch, and J. C. Simon, "Quantum-dash mode-locked laser as a source for 56-Gb/s DQPSK modulation in WDM multicast applications," IEEE Photon. Technol. Lett. **23**, 453 (2011).

[50] M. Radziunas, A. Glitzky, U. Bandelow, M. Wolfrum, U. Troppenz, J. Kreissl, and W. Rehbein, "Improving the modulation bandwidth in semiconductor lasers by passive feedback", IEEE J. Sel. Top. Quantum Electron. **13**, 136 (2007).

[51] C. Herbert, D. Jones, A. Kaszubowska, B. Kelly, M. Rensing, J. O'Carroll, R. Phelan, P. Anandarajah, P. Perry, L. P. Barry, and J. O'Gorman, "Discrete mode lasers for communication applications," IET Optoelectron. **3**, 1 (2009).

[52] K. K. Chow, C. Shu, Y. M. Yang, and H. F. Liu, "Optical control of period doubling in a gain-switched Fabry-Perot laser diode and its application in all-optical clock division," IEE Proc. Optoelectron. **150**, 239 (2003).

[53] R. S. Tucker, "High-speed modulation of semiconductor lasers," J. Lightwave Technol. **LT-3**, 1180 (1985).

[54] U. Troppenz, J. Kreissl, W. Rehbein, C. Bornholdt, T. Gaertner, M. Radziunas, A. Glitzky,

U. Bandelow, and M. Wolfrum, “40 Gb/s directly modulated InGaAsP passive feedback DFB laser,” in *Proc. ECOC 2006, Th4.5.5.*

[55] O. Brox, S. Bauer, M. Radziunas, M. Wolfrum, J. Sieber, J. Kreissl, B. Sartorius, and H. J. Wunsche, “High-frequency pulsations in DFB lasers with amplified feedback,” IEEE J. Quantum Electron. **39**, 1381 (2003).

Chapter 4

Long Reach Coherent Access Networks with Comb Source

In this chapter, the system performance of an injected gain switched comb source will be experimentally examined in a coherent access network scenario. The coherent access concept exploiting digital coherent receivers has stirred much attention within recent years towards the long reach (LR) optical access network design, which is expected to provide upgraded service yet potentially simplified network structure through metro-access consolidation. The reasons for the attraction of optical coherent receivers in such a network context are mainly attributed to: 1) the superior sensitivity that allows for extended power budget, 2) the high frequency selectivity enabling closely spaced dense/ultra-dense wavelength division multiplexing (D/UDWDM) without the need for narrow band optical filters at receiver side, and 3) the improved optical spectral usage through high order advanced modulation formats.

The employment of advanced optical modulation formats in digital coherent receiver based long reach access networks will pose a stringent requirement on the phase noise property of the WDM transmitter sources. An optical injection locked gain switched comb source, through optical linewidth transfer from a single low noise master laser, has demonstrated the potential to fulfil such a requirement, as presented in Chapter 3. Besides, there also exist other benefits associated with the use of the proposed optical comb source that will become promising in a WDM-PON scenario, as those explained in Chapter 1, Section 1.2.3. As such, this chapter explores the practical suitability of injected gain switched comb sources for use as multi-carrier transmitters in long reach coherent optical access networks. To begin with, the development history and technical advantages of the coherent optical access technology are firstly reviewed. Then, a detailed analytical and experimental phase noise analysis of the comb

source transmitter is carried out in order to complement the simple optical linewidth characterisation results from Chapter 3. Finally, the proposed LR coherent access system performance is characterised with focus placed on achieving a large power budget that enables long transmission distance and/or high network user count. Experimental results consisting of unrepeated 100 km and 80 km downlink distribution networks are successfully demonstrated, with an injected gain switched distributed feedback (DFB) laser implemented at the optical line terminal (OLT) and a digital coherent optical receiver employed at the optical network unit (ONU).

4.1 Coherent Optical Access Technology

Coherent optical transmission, where the frequency, phase, amplitude and polarisation of an optical carrier wave can be all utilised to convey information, was extensively studied during the 1980s [1-5]. Subsequent development of the technology was then stagnated by the predominance of IM-DD systems owing to the introduction of the Erbium doped fibre amplifier (EDFA) around 1990. As a result, research activities on coherent optical communications were interrupted for nearly 20 years until about a decade ago. It was the optical differential quadrature phase shift keying (DQPSK) technology featuring in-phase and quadrature (IQ) modulation and self-homodyne detection [6] that marked the revival of coherent optical communications. Soon afterwards, the resurgence of the "digital coherent demodulation" concept [7] [8] (although first proposed in 1991 [9]) attracted a lot of attention resulting in an upsurge in worldwide research [10]. In a typical digital coherent optical receiver subsystem, an optical front end consisting of a 90° hybrid and photodiodes linearly maps the optical field into a set of electrical signals. The electrical signals are then sampled by analogue-to-digital converters (ADCs) into a set of discrete-time quantised signals for transmission impairment compensation and signal detection [11]. Such a subsystem design reduces the expense of the optical receiver part as there is no need for a complex optical phase locked loop. The processing issues are handed over to the digital electronic subsystem (that can be integrated), which entails the use of mature technologies developed from radio communications. For the past decade, the digital coherent optical receiver has become an engineering milestone for modern fibre optic communications and has brought in notable

success both academically as well as commercially (see for example, [10] [12]).

Lately there have been research activities attempting to bring coherent technology into the passive optical network (PON) systems, motivated by the increasing interests in designing advanced WDM-PON infrastructure [13-18]. In fact, the concept of a coherent optical access was proposed as early as the 1980s and the 1990s (e.g. [19] [20]). However, it was only recently, that the practical feasibility of such a proposal started to look promising thanks mainly to the advancements in digital signal processing (DSP) techniques [13]. In general, the technical significance of deploying a coherent receiver in the access context can be equivalently considered as a WDM receiver with an inbuilt narrow band-pass filter (BPF) and an optical amplifier [15]. The inherent narrow filtering functionality negates the need for WDM filters as required by all other conventional WDM-PON proposals. The optical amplification provided by the coherent gain from the local oscillator (LO) laser offers a high optical power budget that translates into an unrepeated long reach and/or a large split ratio. Moreover, the reception of the full-field of the incoming signal renders additional benefits by creating a platform to: 1) compensate for the linear transmission impairments such as those from chromatic dispersion and polarisation-mode dispersion [11], and 2) better utilise the spectral resource and benefiting future network upgrades through the use of multi-level advanced modulation formats [17]. As such, LR ultra-dense (UD) WDM-PONs with legacy power splitters based optical distribution network (ODN) supporting ~100 km transmission span, ~1000 wavelength splits and high order modulations have become possible [15] [16]. This potentially results in network simplification, installation and OpEx reduction in real estate, equipment and powering through site consolidations [21].

As some examples of current state-of-the-art coherent access technology, the pioneer works reported in [22-24] have demonstrated LR UDWDM coherent PON with real-time capable bidirectional transmissions using optical heterodyne detection. One major advantage of the heterodyne coherent detection is that, while the incoming signal (uplink or downlink) is mixed with the LO and brought down to an intermediate frequency (IF) for electronic processing, part of the LO optical power can be also be employed as the carrier for the other transmission direction. Through such an arrangement, with the LO tuned to the target channel, the other direction is automatically fixed by an offset wavelength (determined by the chosen

IF). The above described principle works for both the OLT and the ONU, hence a fully coherent system can be achieved in a relative cost effective manner with only one optical source in each end-side of the access network [24].

With the heterodyne coherent infrastructure being established, a few other viable technical options remain attractive and provide an ideal opportunity for continued research. Firstly, a natural step forward is to exploit the utility of intradyne coherent receivers which directly assess the in-phase and quadrature signal branches without experiencing an intermediate stage [25-27]. The intradyne receivers effectively reduce the electrical bandwidth requirements compared with their heterodyne counterpart. The downsides of the intradyne receivers are the optical component complexity (as 90° hybrid and more photodiodes are needed), and the additional effort to shift the uplink channel away from the downlink wavelength in order to minimise sensitivity penalties from back reflections [26]. Another possibility for further investigation on coherent LR access networks, as being proposed and studied in this chapter, entails the adoption of an optical frequency comb source at the OLT to offer substantial cost savings through hardware simplification and potential reductions in energy consumption [28] [29]. As such herein, the experimental results originated from such investigations (dedicated to the downlink portion of the network) will be elucidated in Section 4.3. However, to justify the suitability of the multi-carrier source for coherent optical communications, a phase noise characterisation on the injected gain switched comb source [30] is initially carried out and presented in Section 4.2.

4.2 Phase Noise Analysis of Comb Source

In Chapter 3, the spectral linewidth of the injected gain switched comb lines has been characterised and shown to follow that of the master laser (in the order of ~100 kHz). The optical linewidth value has been considered an important criterion indicating phase noise induced bit error rate (BER) penalties in phase modulated coherent communication systems [31]. However, recent studies have demonstrated that the spectral linewidth might not be a sufficient means to fully describe the phase noise property of an optical light source, and a more detailed analysis concerning frequency modulated (FM)-noise spectrum, phase-error variance, and field spectrum of the signal under test can provide a better insight of the phase

noise process as well as its potential influence [32]. Therefore in this section a detailed phase noise characterisation on the individual comb lines of an injected gain switched DFB laser (as presented in Chapter 3, Section 3.2) is given. Initial experimental characterisation is performed via a phase noise measurement method previously developed [33]. The results revealing high frequency FM noise behaviour are then studied with the aid of a simple analytical model [30]. Potential impact of the comb line phase noise on coherent communications is further examined with a self-coherent DQPSK system [34], as well as a digital coherent receiver system employing QPSK and 16 quadrature amplitude modulation (QAM) formats [30].

4.2.1 Experimental characterisation

The experimental setup for the phase noise characterisation of the externally injected gain switched DFB laser is proposed as in Fig. 4.1. The injected gain switched comb generation is achieved with a master-slave configuration. An integrable tunable laser assembly (ITLA) master laser (Furukawa) injects light via an optical circulator to a DFB slave laser (NEL), with a polarisation controller (PC) in the light path to align the polarisation state of the injected light to the optical waveguide of the slave laser. A variable optical attenuator (VOA) controls the injection power to the slave cavity, while the master bias is kept at a constant level throughout the experiment to ensure the consistent phase noise property of the injecting source. Gain switching of the slave DFB laser is achieved by applying an amplified 15 GHz sinusoidal RF signal (24 dBm) in combination with a dc bias current of 40 mA, while the laser is controlled at room temperature. It is worth noting that the 15 GHz FSR is only chosen for demonstration purpose and the FSR of the injected gain switched DFB comb source is widely variable as discussed in the preceding chapter.

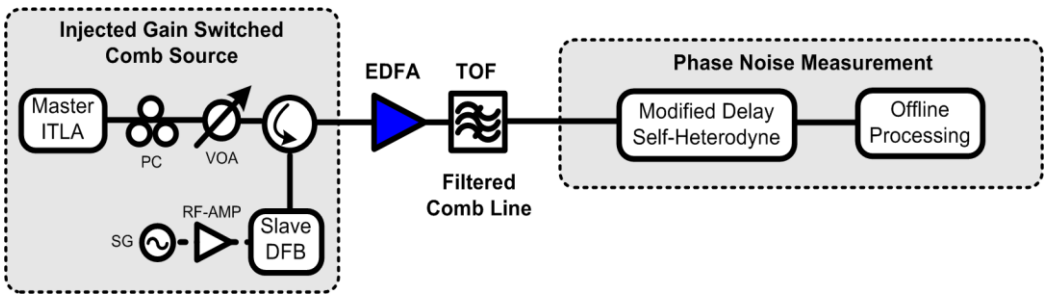

Figure 4.1: Experimental setup for phase noise measurement of injected gain switched comb lines.

The optical comb generation is followed by an Erbium doped fibre amplifier (EDFA)

before being passed to a narrow bandwidth (minimum 3-dB bandwidth: 0.05 nm) tunable optical filter (TOF) (Yenista Optics, XTM-50) to select individual comb lines (one line at a time) for the phase noise characterisation. The phase noise characterisation utilises a modified delayed self-heterodyne (DSH) method based on the harmonic detection principle [33]. The detected signal is captured with a real-time oscilloscope (Agilent infiniium DSO81004B, 10 GHz, 40 GSa/s) and sent for offline processing to recover the complex amplitude of the differential phase error [33]. This allows evaluation of the FM-noise spectrum, which is the power spectral density (PSD) of the instantaneous frequency fluctuations, and the phase-error variance which is the mean-square value of differential phase variation in a given time interval [32].

The injected gain switched comb generation depends highly on the injection conditions, namely the optical injection power and the wavelength detuning between the master and slave laser (some relevant discussions in Chapter 3, Section 3.2.1). By carefully choosing these conditions, optical combs with different noise properties are generated due to the various interactions between the injecting signal and the photons generated in the slave cavity. In this experiment two such conditions are chosen, with the injection power and wavelength detuning ($\Delta\lambda = \lambda_{master} - \lambda_{slave}$) set to (a) 0 dBm, -0.5 nm and (b) 3 dBm, 0.17 nm. The comb in Fig. 4.2(a),

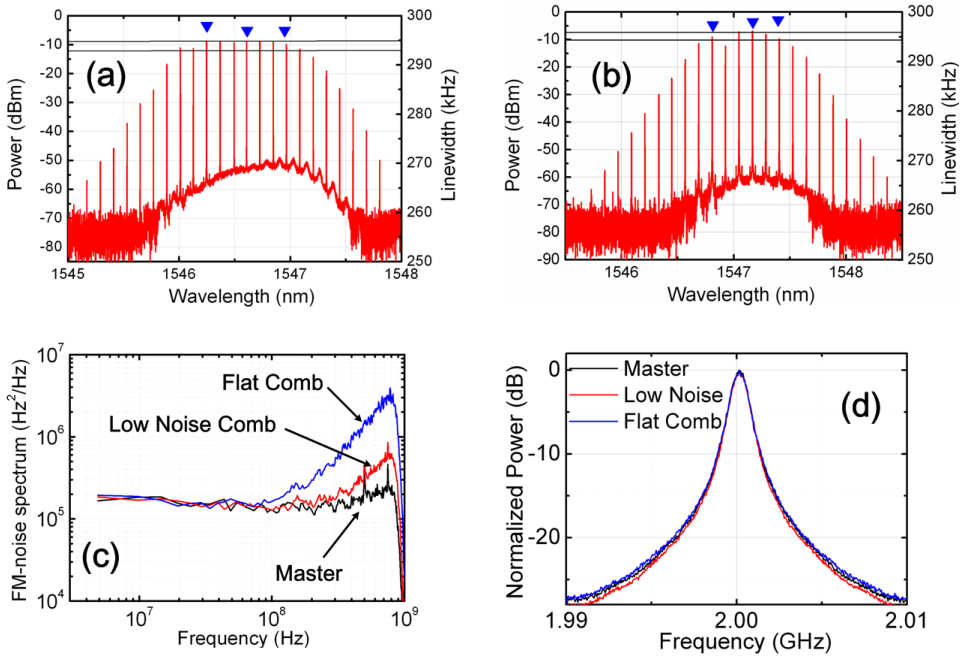

Figure 4.2: Optical spectra (resolution 100 MHz) of (a) “flat comb” (b) “low noise” comb. Optical linewidth measured with conventional DSH method shown on top of comb lines by the blue triangles. (c) FM-noise spectrum of the two combs and that of the master. (d) Averaged DSH lineshape on ESA.

corresponding to injection condition (a), demonstrates 10 clearly resolved comb tones in a 3-dB window and hence referred to as the "*flat comb*". The second comb in Fig. 4.2(b), corresponding to injection condition (b), shows relatively poor flatness compared to the previous case, but has a smaller noise profile under the comb lines; hence named as the "*low noise*" comb. Such naming is verified by the phase noise measurement results (in terms of FM-noise spectrum) shown in Fig. 4.2(c).

In the actual phase noise measurement, we selected three different lines (with similar background noise extinction) from each comb (flat and low noise) and found that comb lines from the same comb source also perform the same. Therefore only one line from each comb is demonstrated in Fig. 4.2(c) for clarity, and they are also compared with the master laser FM-noise spectrum. It is clear in Fig. 4.2(c) that the FM-noise spectrum of the master ITLA (a DFB based laser array) is dominated by white FM noise and shows flat PSD over the frequency range being measured (upper limit ~1 GHz due to digital filtering in the offline processing [33]). The injected slave lines for flat and low noise combs, on the other hand, have identical FM noise PSD to the master at lower frequencies, but both start to deviate from the master at around 100 MHz, and there is a marked increase for the flat comb line at higher frequencies towards ~1 GHz. Such FM noise deviation/increase, however, does not affect the 3-dB optical linewidth, since we also perform a conventional DSH measurement on the injected comb lines and the resulting linewidths all follow the master laser linewidth (~300 kHz), as indicated in Fig. 4.2(a) and 4.2(b) by the blue triangles on top of the selected comb lines. Moreover, the averaged DSH beat signals on the electrical spectrum analyser (ESA) also yield identical spectral lineshape for the flat, low noise combs and the master as evidenced in Fig. 4.2(d). In other words, the high frequency FM noise in the comb lines remains largely unnoticed in a conventional DSH measurement.

These experimental observations in our phase noise measurement agree well with previous study where the slave laser was in a free running condition [35]. The results presented here confirm that insufficient injection (due to low injection power or improper wavelength detuning) leads to an unsuccessful "locking" of the slave FM noise properties to that of the master, at higher frequencies, where the slave FM-noise spectrum is determined by both the master and the slave itself [35]. However, a unique feature for the gain switched slave comb

source compared to its free running case would be the additional phase distortions induced by the unwanted frequency modulation during gain switching (direct modulation) process [36]. Such additional distortions are expected to result in more stringent requirements on the injection conditions and/or more severe deviation in the slave FM-noise spectrum from that of the master laser.

4.2.2 Analytical study

The phase noise property of a free running semiconductor laser can be studied in the form of *frequency noise*, through various noise compositions in the FM-noise spectrum. The most common type of noise component would be the white frequency noise, or the random walk phase noise, which originates from the random fluctuation of spontaneous emission process in laser cavity and typically yields a Lorentzian spectrum lineshape [32]. Other noises that have been investigated include the low frequency FM noise (e.g. *1/f* and $1/f^2$ types of frequency noise [33] [37]), and the relaxation oscillation incurred resonance phase noise (RPN) [38] [39]. Here demonstrated in Fig. 4.2(c), the high frequency FM noise of the injected comb lines shows quite distinct properties from the FM-noise spectrum of a typical free running semiconductor laser. It is worth noting that it should not be confused with the RPN since the relaxation oscillation of this slave DFB laser has been characterised to be over 10 GHz (see Chapter 3, Section 3.2). However, the same methodology that utilises power-law noise analysis for examining the low frequency FM noise [33] [40] can be implemented here to estimate the unusual comb line phase noise. We propose the use of f and f^2 terms to analytically characterise the high frequency FM noise of the injected gain switched comb lines. The analytical model for the comb line FM-noise spectrum can be therefore written as:

$$S_F(f) = S_0 + k_1 f + k_2 f^2 \tag{4.1}$$

where S_0 denotes the flat PSD of the white FM noise component [32] in the slave DFB laser, with $S_0 = \delta f / \pi$ (δf is the 3-dB spectral linewidth and in this work δf = 300 kHz); k_1 and k_2 are constants representing the contribution from f and f^2 noise terms which are caused by the injection. By carefully choosing k_1 and k_2 values (k_1 = 1.7e-5, k_2 = 4.6e-12) it is found that the experimentally characterised comb line FM-noise spectrum can be closely matched by the proposed analytical form in Eq. 4.1, as indicated in Fig. 4.3(a) by the green dash line (only flat

comb is discussed here for clarity). Furthermore, it would be useful to directly assess the time-dependent phase fluctuation in the comb lines by considering the phase-error variance (PEV) [41], which is the mean-square value of the difference between the instantaneous phases at different times separated by an interval τ:

$$\sigma_\phi^{\,2}(\tau) = \left\langle \left[\phi(t+\tau) - \phi(t)\right]^2 \right\rangle \tag{4.2}$$

The PEV can be related to the FM-noise spectrum through [32]:

$$\sigma_\phi^{\,2}(\tau) = 4\int_0^\infty \left(\frac{\sin(\pi f \tau)}{f}\right)^2 S_F(f)\,df \tag{4.3}$$

replacing $S_F(f)$ with Eq. 4.1 and considering a finite frequency range of the actual measurement, Eq. 4.3 can be rewritten as:

$$\sigma_\phi^{\,2}(\tau) = 4S_0\int_{f_L}^{f_U}\frac{\sin^2(\pi f\tau)}{f^2}df + 4k_1\int_{f_L}^{f_U}\frac{\sin^2(\pi f\tau)}{f}df + 4k_2\int_{f_L}^{f_U}\sin^2(\pi f\tau)df \tag{4.4}$$

where f_L and f_U are the lower and upper frequency limits of the measured FM-noise spectrum in Fig. 4.3(a). The three integrals on the right hand side of Eq. 4.4 thus represent the contribution from white, f, and f^2 frequency noise components respectively. By performing each of them individually using similar procedure as in [33], the result yields:

$$\begin{aligned}\sigma_\phi^{\,2}(\tau) = {} & 4\pi S_0\tau\left[\frac{\sin^2(\pi f_L\tau)}{\pi f_L\tau} - \frac{\sin^2(\pi f_U\tau)}{\pi f_U\tau} + \mathrm{Si}(2\pi f_U\tau) - \mathrm{Si}(2\pi f_L\tau)\right] \\ & + 2k_1\left[\ln(\pi f_U\tau) - \ln(\pi f_L\tau) - \mathrm{Ci}(2\pi f_U\tau) + \mathrm{Ci}(2\pi f_L\tau)\right] \\ & + \frac{k_2}{\pi\tau}\left[2\pi f_U\tau - 2\pi f_L\tau - \sin(2\pi f_U\tau) + \sin(2\pi f_L\tau)\right]\end{aligned} \tag{4.5}$$

where $Si(x) = \int_0^x ((\sin t)/t)dt$ is the sine integral function and $Ci(x) = -\int_x^\infty ((\cos t)/t)dt$ is the cosine integral function. We thus plot the calculated PEV of the flat comb from Eq. 4.5 and show in Fig. 4.3(b) by the green dash line.

In Fig. 4.3(b), we also demonstrate the experimental PEV of the flat comb, low noise comb, and the master laser. In the figure, a first observation is the linear increase of the master PEV with respect to the delay time, which is commonly seen for DFB lasers with the presence of only white FM noise [32]. For such case an ideal linear model of $\sigma_\phi^{\,2}(\tau) = 2\pi\delta f\tau$ is widely used[31-33], which can be obtained by letting $k_1 = k_2 = 0$ and assuming $f_L = 0$ and $f_U = \infty$ in

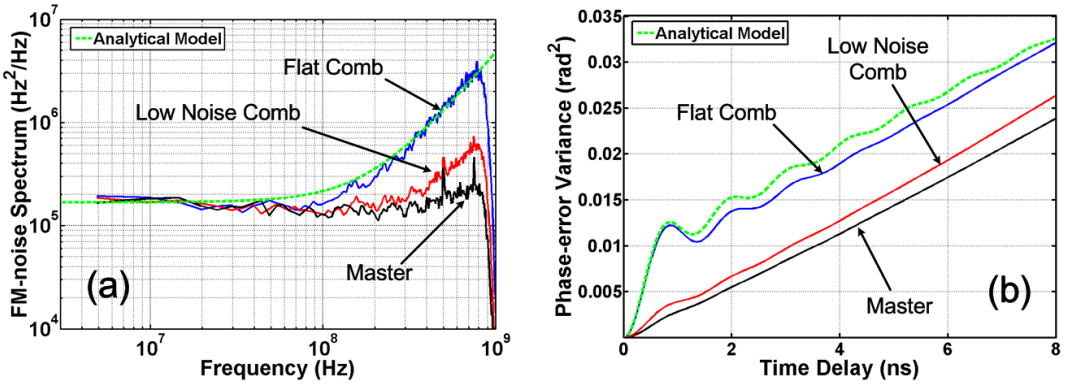

Figure 4.3: Experimental versus calculated results for (a) FM-noise spectrum, (b) phase-error variance.

Eq. 4.4. As for the injected comb lines (both flat and low noise), a very similar linear slope as for the master is recorded at long delay times, thus explaining the identical FM-noise spectrum at low frequencies and the same emission linewidth for the injected comb lines and master laser (the spectral linewidth is typically determined by the low frequency content of the FM-noise spectrum [35]). However, for short term delay times of less than ~4 ns an additional damped oscillatory behaviour is noticed for both combs sources, with the flat comb suffering a severe distortion from the oscillation. Such oscillatory distortion corresponds to the high frequency increase in the FM-noise spectrum and the consequence is that the PEV of the comb lines being upshifted with respect to that of the master. Therefore the comb lines (flat comb in particular) will experience larger phase errors at all delay times compared to the values predicted by the master laser, potentially leading to unexpected errors in coherent communication systems [41].

As such, the experimental and analytical analyses presented here on the FM-noise spectrum and PEV of the injected gain switched comb lines have provided an important guideline as to how to optimise the comb source, in terms of injection power and detuning, towards the desired phase noise versus flatness trade-off. In the following sub-section, we experimentally investigate the performance of these comb lines in coherent optical communication systems operating at 10.7 GBaud and 5 GBaud with different modulation formats, to evaluate the potential influence of the residual high frequency phase noise in the comb line FM-noise spectrum on the performance of a coherent system.

4.2.3 Phase noise impact on coherent systems

The injected gain switched comb lines are tested back-to-back (B2B) in two coherent systems, shown in Fig. 4.4: one uses a digital coherent receiver, and the other a direct detection based DQPSK system (both pre-amplified receivers are beat-noise limited). In the coherent system two modulation formats with different symbol rates are investigated: QPSK at 10.7 GBaud and 16-QAM at 5 GBaud. The direct detection system employs 10.7 GBaud optical DQPSK.

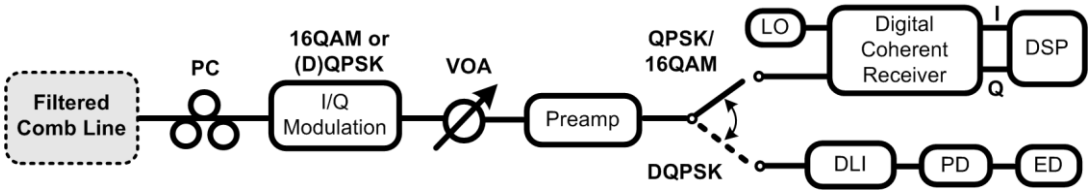

Figure 4.4: Experimental setup for the comb line phase noise impact characterisation. Preamp: optical pre-amplifier, DLI: delay interferometer, PD: photodiode, ED: error detector.

At the transmitter side, the individual comb lines are selected by the same TOF as in Fig. 4.1 to avoid the potential influence from inter-channel crosstalk. A dual-parallel optical I/Q modulator (JDSU) biased at null-point is used for the (D)QPSK modulation (with or without the differential pre-coding), as well as the 16-QAM modulation of the comb lines. Although not shown in the figure, the (D)QPSK drive signal is derived from a pulse pattern generator (PPG) (Anritsu MU181020A, 0.1-12.5 Gbit/s) while the 16-QAM drive signal is generated by an arbitrary waveform generator (Tektronix AWG7102, 10 GSa/s), and in both cases the drive signals are further amplified by a pair of optical modulator drivers (JDSU, H301-1210) before being sent to the I/Q modulator. At the receiver side, the B2B received optical power is controlled by a VOA before going through an optical pre-amplifier which comprises of two stages of an EDFA-filter combination [42]. A polarisation- and phase-diverse 40 GHz compact coherent receiver (PICOMETRIX, CR-40A) is utilised as the coherent optical front-end. Polarisation alignment between the LO and the received signal is achieved via manual tuning of the PC on each light path (not shown in Fig. 4.4). For the 10.7 GBaud QPSK detection an external cavity laser (ECL) (Hewlett Packard 8168F Tunable Laser Source) with ~100 kHz linewidth serves as the LO, and a digital sampling oscilloscope operating at 50 GSa/s (Tektronix DPO71254B, 12.5 GHz bandwidth) captures 1 M samples (correspond to 214 k symbols) of the intradyne I/Q beat signal at the coherent receiver output. Regarding the 5 GBaud 16-QAM we

use a 25 kHz ECL (Agilent N7711A, linewidth from FM-noise spectrum measurement) as the LO, and the sample rate is reduced to 20 GSa/s for capturing 200 k samples (50 k symbols). The QPSK or 16-QAM signal is then sent to offline DSP, which includes the following procedures [42]. First the digital samples are normalised by their root mean square values and I/Q balanced. A non-data-aided frequency correction method [43] then removes the residual intradyne frequency offset between the LO and the incoming signal, and a 20-symbol training sequence is employed to achieve symbol synchronisation. Finally the signal is down-sampled and sent to decision-directed carrier phase estimation, which is based on a one-tap finite impulse response (FIR) filter and the least mean square (LMS) algorithm [44]. In terms of the 10.7 GBaud DQPSK reception, an optical 1-bit delay line interferometer (DLI) (Kylia) is used for the de-modulation. It is followed by a single-ended photodetector (PD) (NORTEL, PP-10G) and then an error detector (ED) (Anritsu MU181040A, 0.1-12.5 Gbit/s) which is placed within the same bit error rate tester (BERT, Anritsu MP1800A Signal Quality Analyzer) as the PPG.

The system performance of the comb lines (3 lines from the flat comb and 3 lines from the low noise comb) are illustrated in Fig. 4.5, in terms of BER versus received optical power. Fig. 4.5(a) shows that in the digital coherent receiver based system, the residual phase noise in the flat and low noise comb lines have no visible influence on the BER performance of the 10.7 GBaud QPSK system when compared to the master laser. In terms of the 5 GBaud 16-QAM system an overall error floor-like behaviour is noticed, since the system requirement on phase noise/linewidth is much more stringent in this case (due to the increased modulation order and

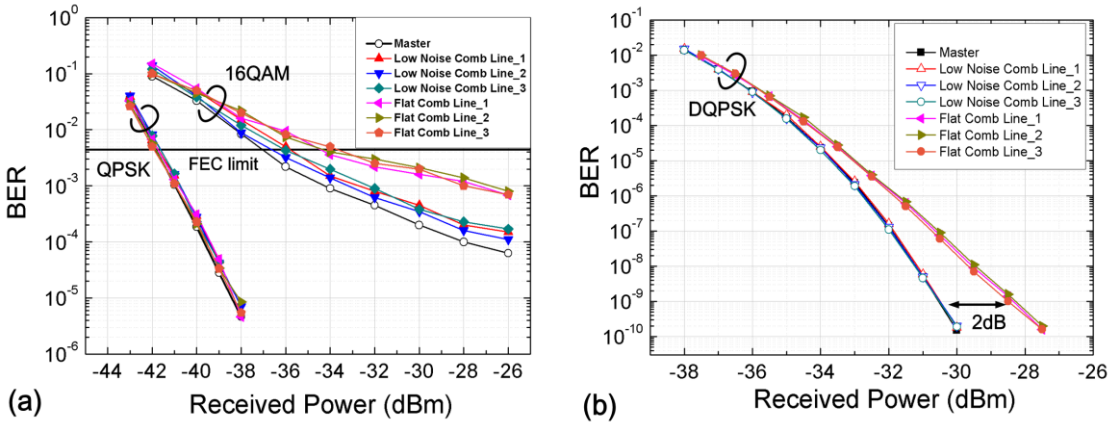

Figure 4.5: BER versus received power for master, flat comb and low noise comb in different coherent systems: (a) 10.7 GBaud QPSK and 5 GBaud 16-QAM with digital coherent receiver, (b) 10.7 GBaud optical DQPSK with DLI and single-ended direct detection receiver.

the reduced symbol rate). Besides, both low noise and flat comb sources demonstrate degraded performance compared to the master laser. At a forward error correction (FEC) limit of 4.4e-3 (assuming 7% overhead [45]) the penalties are 1 dB and 3 dB for the low noise and flat comb respectively. As such, the low noise comb shows similar performance with the master while the flat comb demonstrates a higher penalty. Therefore in a high order modulated digital coherent system operating at low baud rates, certain trade-off should be made in the comb line flatness to reduce the system impact from the excess phase noise increase in injected comb lines.

Next, the 10.7 GBaud optical DQPSK system results are shown in Fig. 4.5(b) with BER calculated from the average of I and Q channels. In this case the low noise comb lines yield identical performance with the master but for the flat comb, there is a notable performance degradation which leads to a 2 dB penalty at a BER of 10^{-9}. In order to find out the potential contribution from intensity noise to this 2 dB penalty, we also perform a 10.7 GBaud on off keying (OOK) modulation experiment, using the same sources (master, low noise and flat comb) and the same single-ended direct detection receiver (PD+ED). The results for OOK B2B system are shown in Fig. 4.6 and demonstrate the same BER performance between the three sources. Therefore we conclude that the power penalty in the directly detected optical DQPSK system for the flat comb is only due to the residual comb line phase noise at the higher frequency ranges of the FM-noise spectrum.

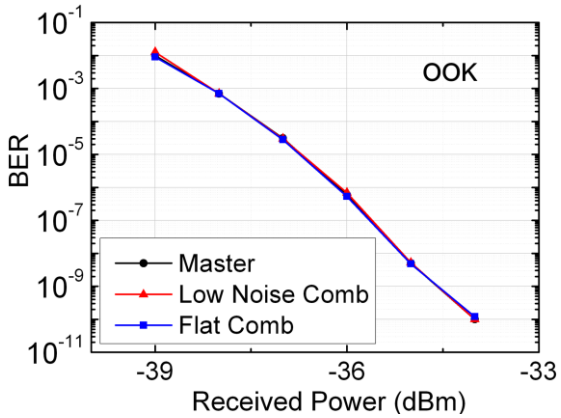

Figure 4.6: BER versus received power for master, flat comb and low noise comb in a 10.7 GBaud directly detected OOK system.

To summarise, a study of the phase noise characteristics of an injected gain switched DFB comb source was carried out followed by the demonstration of the impact of comb line phase noise on coherent communication systems. Experimental study shows that residual phase noise

can exist in the comb lines due to certain injection conditions, which stay unnoticed in optical linewidth values but can be observed through a detailed phase noise characterisation process. A power-law FM noise model is proposed to analytically describe the residual phase noise and we also derived the analytical expression of the PEV. To test the influence of the comb line phase noise in coherent communications two types of coherent systems working with different modulation formats operating at 5 GBaud and 10.7 GBaud are employed. The results suggest the potential of the injected gain switched comb source while also highlighting the possible limitations caused by the residual comb line phase noise, which needs to be accounted for by optimized optical injection at the transmitter or further reducing the combined linewidth of master + LO (thus down-shifts the overall PEV curve). These analyses will become useful guidelines during system implementations of the injected gain switched comb source for use as multi-carrier WDM transmitters.

4.3 Long Reach Coherent Access Systems

In this section, focus is placed on achieving unamplified long distance transmission in highly sensitive digital coherent receiver based optical access networks. The proposed structure is based on a LR D/UDWDM-PON with an injected gain switched DFB comb source at the OLT and a digital coherent receiver at the ONU. In a typical D/UDWDM scenario, the narrow channel spacing would require the frequency spacing between the OLT optical carriers to be kept extremely stable to minimise the potential inter-channel interference. One of the benefits of employing a comb source as opposed to individual lasers is the alleviation of rigorous frequency stabilisation and/or guard band requirements associated with laser temperature and wavelength control. Moreover, the flexible FSR of the proposed comb source facilitates wide range channel spacing selections to accommodate different PON systems. On the other hand, the superior sensitivity offered by the digital coherent receiver in the ONU allows for system performance potentially approximating the theoretical shot noise limit [46], a feature that other types of systems prove unable to provide. Therefore, here we utilise all the advantages afforded by the injected gain switched comb source and digital coherent receiver, and focus our investigation on the downlink portion of a LR (> 50 km) coherent optical access network. The proposed network architecture is schematically shown in Fig. 4.7.

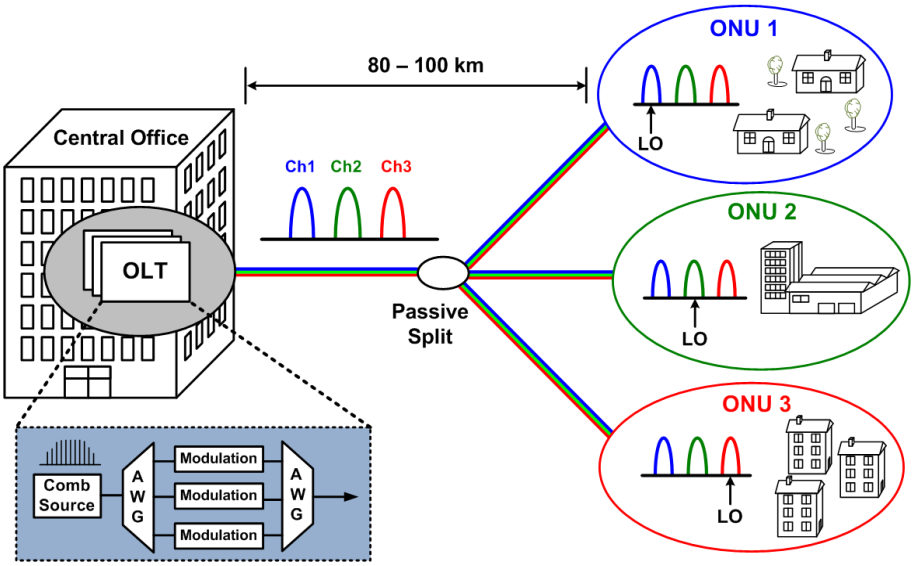

Figure 4.7: Proposed architecture of the downlink LR DWDM-PON based on OLT multi-carrier transmitters and ONU coherent receivers. Distances in the figure are only illustrative.

In the illustrated network scenario of Fig. 4.7, each OLT line card within the central office consists of a simple and robust multi-carrier transmitter based on an externally injected gain switched DFB comb source. The individual channels of the comb source are separated by an arrayed waveguide grating (AWG) and sent for independent user data modulation (only 3 channels are demonstrated here for simplicity), before being re-combined by another AWG to form the D/UDWDM downlink signal which has a channel spacing < 25 GHz. The modulation format and operating bit rate on each of the comb lines are determined by the spectrum availability and specific system requirements; in this work we employ a highly efficient polarisation division multiplexed (PDM) QPSK format operating at 10 Gb/s [28] and PDM-16QAM format operating at 40 Gb/s [29]. As for the passive distribution of the WDM channels, legacy optical power splitters can be reused to maintain the same broadcasting feature as in the time division multiplexed (TDM) PONs; there is no need for a "coloured" component (AWG) in the distribution network since the LO in each ONU can be tuned to the target channel for simultaneous filtering and down-conversion [22-29], as illustrated in Fig. 4.7. The network span ranges from 80 to 100 km without any form of mid-span or remote node amplification, allowing high capacity media rich services from the consolidated central offices delivered to the far side of the network where various end-users (residential homes, business buildings, universities etc.) reside. Two experimental works based on the above described network structure are presented as follows. They include a 100 km LR UDWDM-PON

downlink system using PDM-QPSK, and an 80 km LR DWDM-PON downlink with PDM-16QAM.

4.3.1 100 km downlink system with PDM-QPSK

The first experimental demonstration involves a 100 km, 10 GHz spaced 7 × 10 Gb/s LR UDWDM-PON downlink scenario and a schematic of the experimental set-up is given in Fig. 4.8. The comb source at the OLT is realised by employing an injected gain switched DFB laser (NEL). Gain switching is achieved by driving the laser diode with a large amplified sinusoidal signal (24 dBm at 10 GHz) in conjunction with a dc bias current of 50 mA, while the laser is temperature controlled at 25°C. An ECL with a linewidth of ~200 kHz and an output power of 6 dBm is used to inject into the gain switched DFB laser. The external injection ensures the transfer of the ECL low linewidth (master) to each of the gain switched DFB laser (slave) comb tones, and also guarantees that the FM noise property of the slave comb tones remain suitable for QPSK modulation (as discussed in the preceding section). The injected gain switched comb, as illustrated in Fig. 4.9(a), yields 15 clearly resolved phase correlated optical tones within a 3-dB spectral envelope with each of the tones offset by an integer multiple of the drive frequency (10 GHz). Power equalization and outer sideband rejection are achieved by passing the comb signal through a programmable optical filter (Finisar WaveShaper). This results in the seven chosen tones exhibiting a spectral flatness of 1 dB with the unwanted outer sidebands suppressed to about 15 dB as illustrated in Fig. 4.9(b). An EDFA is also employed at the comb source output to overcome the loss of optical filtering.

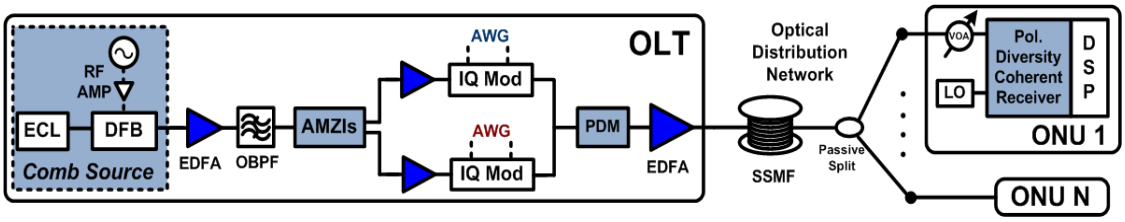

Figure 4.8: Experimental configuration of the 100 km PDM-QPSK downlink LR UDWDM-PON. OBPF: optical band-pass filter, AWG: arbitrary waveform generator, IQ Mod: IQ modulator, PDM: polarisation division multiplexing, SSMF: standard single mode fibre, VOA: variable optical attenuator.

In a practical system, each OLT line card would consist of an optical comb source, an arrayed waveguide grating to filter out the required sidebands, an array of modulators to independently encode the data on to each of the optical comb tones, and another arrayed

waveguide grating to recombine them together as described in Fig. 4.7. However, in this experiment the comb is passed through a dis-interleaver based on an asymmetric Mach-Zehnder interferometer (AMZI), with a free spectral range of 20 GHz, to separate the comb into odd and even channels. This is to ensure that the data information between the neighbouring comb line channels is de-correlated. Both the odd and even channels are subsequently passed through a second dis-interleaver stage to improve the extinction ratio to 40 dB, as shown in Fig 4.9(c) and 4.9(d). The odd (1, 3, 5, 7) and even (2, 4, 6) channels are individually modulated with 3 GBaud QPSK data signals using two dual parallel Mach-Zehnder (IQ) modulators. Successively, the two 3 GBaud QPSK signals are optically amplified and combined before being passed through a polarisation multiplexing emulation stage, thus generating a 7-channel 3 GBaud PDM-QPSK signal. This corresponds to a 10 Gb/s data rate (PDM-QPSK = 4 bits/symbol) plus 20% overhead reserved for hard decision FEC coding, which theoretically corrects the BER from 1.5×10^{-2} to below 10^{-15} [47]. The performance of the WDM PDM-QPSK signal is initially analysed in a back-to-back scenario and subsequently after transmission over 100 km of standard single mode fibre (SSMF). An EDFA at the transmitter sets the power per channel to about 3 dBm prior to being launched to the receiver. The total loss between the OLT and the ONU yields the loss budget, which then determines the maximum number of subscribers and the maximum transmission distance that can be afforded by the LR PON [16]. In the experiment, a variable optical attenuator (VOA) is used at the receiver end to mimic the total loss of the passive splits. At the ONU, the signal is detected using a phase and polarisation diverse coherent receiver [11]. An ECL is used as the LO (output amplified to 14 dBm) and the emission frequency is tuned to match the required wavelength channel. The received signal is then digitised by a digital sampling oscilloscope (Tektronix DSO-50 GSa/s with an effective number of bits (ENOB) of 5), resampled to 6 GSa/s to give 2 samples per symbol and the BER of the coherently received signal is recorded offline using MATLAB [11] [48]. Subsequently, the performance of the LR UDWDM-PON downlink system is verified by recording the BER as a function of the received power under the two mentioned scenarios (back-to-back and 100 km SSMF transmission). The received optical channel powers are measured using a calibrated optical spectrum analyser (OSA, ADVANTEST Q8384).

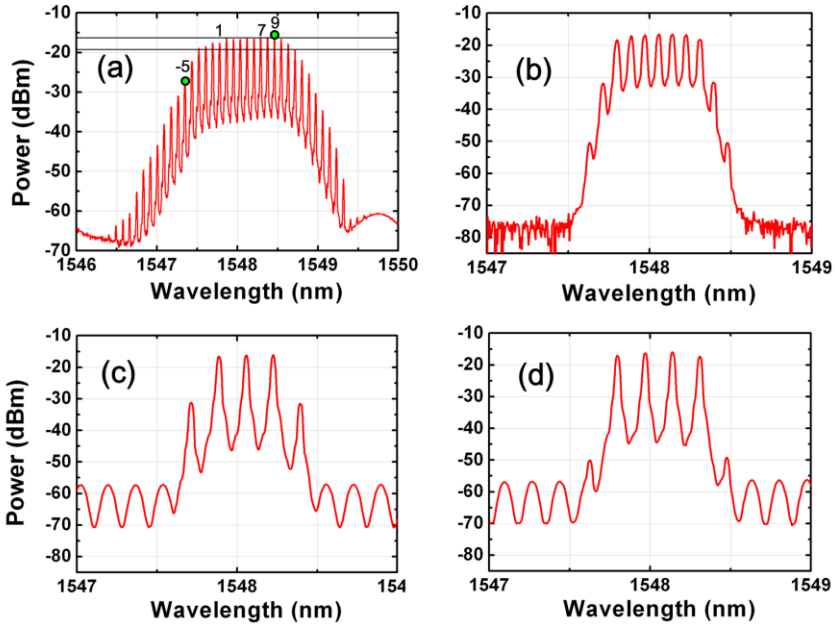

Figure 4.9: Optical spectra of (a) Gain switched comb with CH -5 and CH 9 denoted by a filled circles, (b) filtered output of the comb source with the seven chosen comb tones, (c) even comb tones, and (d) odd comb tones. The OSA resolution is set to 0.02 nm for (a) and 0.05 nm for (b)-(d).

Benchmarking of the comb source's performance is achieved by comparing it against a single channel source employed in a back-to-back configuration. The single channel source is realised by using the master ECL that is used to injection lock the gain switched DFB laser. It needs to be mentioned that all sensitivity and power penalty values quoted have been taken at the FEC limit. Figure 4.10(a) shows the BER performance of the single channel case and all seven comb channels in the back-to-back scenario. The seven comb tones (CH1-CH7) deliver very similar levels of performance with a receiver sensitivity of about -44.4 dBm for the best comb channel and -44 dBm for the worst comb channel. Hence, the power penalty between the best and the worst performing channels is 0.4 dB. In addition, the worst performing comb channel shows a 0.8 dB penalty in comparison to the single channel case. This penalty could be attributed to introduction of coherent crosstalk and in-band noise. The BER as a function of the received power for all seven optical tones, after the 100 km SSMF transmission, are plotted in Fig. 4.10(b). Here again, as can be seen from this plot, all the seven comb tones yields very similar performance with a 0.8 dB penalty between the single channel and the worst performing comb channel. With a worst-case receiver sensitivity of -44 dBm and a per channel launched power of 3 dBm, the proposed system could transmit over 100 km and afford a split ratio of 1:256 which then leaves a power margin of 3 dB (total 47 dB loss budget).

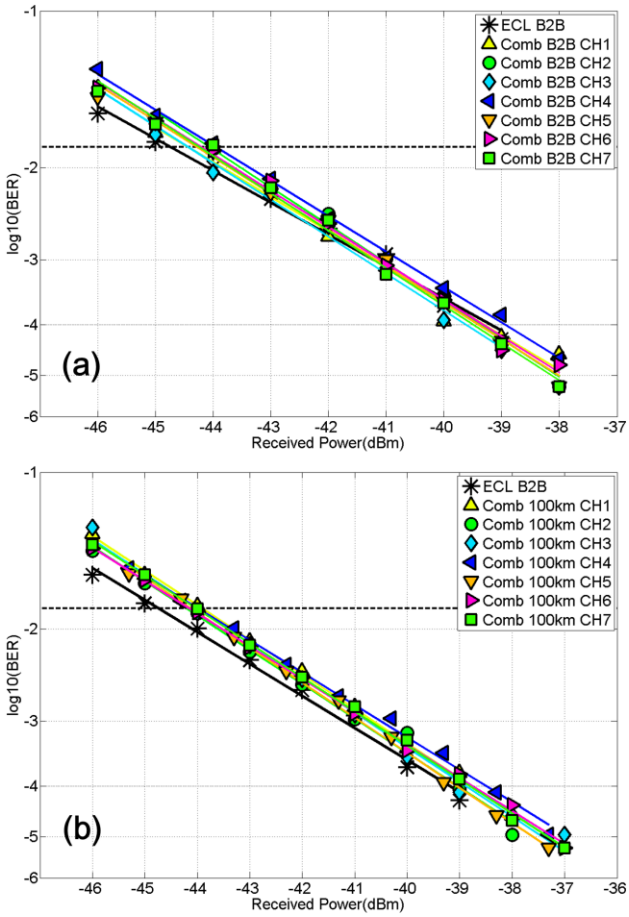

Figure 4.10: BER versus received optical power of the 7-channel 3 GBaud PDM-QPSK: (a) back-to-back performance, and (b) 100 km performance. The single channel (ECL) in back-to-back case is for benchmarking the performance of the comb source.

In order to demonstrate that all the comb lines from the externally injected gain switched laser portray similar phase noise properties, we verify the performance of two channels placed outside the filtered region of the generated comb. The chosen channels are marked by filled green circles in Fig. 4.9(a) on top of the comb lines and are labelled as channel CH -5 and CH 9. The BER as a function of the received power for these two comb tones and the single channel case are plotted in Fig. 4.11. The figure clearly shows that these two outer channels exhibit similar performance in comparison to the initially filtered seven comb channels. CH -5 and CH 9 exhibit receiver sensitivities of -44.5 dBm and -44.2 dBm, respectively. A penalty of 0.5 dB is incurred between CH 9 and the single channel (ECL) case.

As such, in this demonstration we have experimentally shown the feasibility of using an optical comb source at the OLT for downlink transmission in a 10 Gb/s per channel coherent LR UDWDM-PON. The comb source is realized using an externally injected gain switched DFB laser that yielded seven 10 GHz spaced coherent optical carriers. The external injection

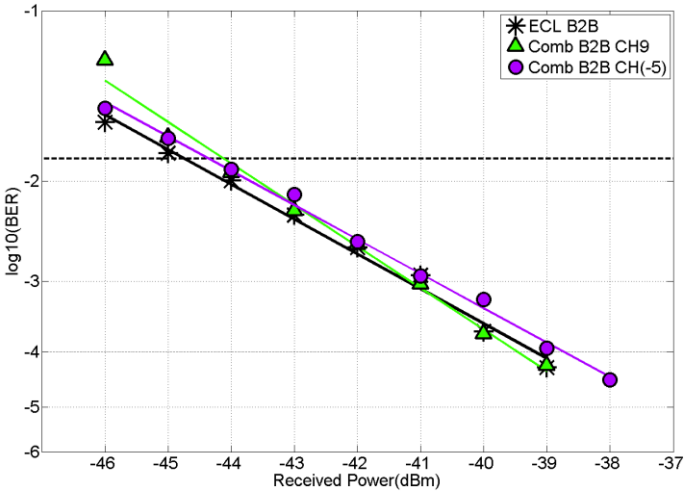

Figure 4.11: BER as a function of received optical power: back-to-back performance of the 2 extreme channels modulated with 3 GBaud PDM-QPSK. The single channel (ECL) is shown as benchmark.

ensured that the phase noise of each of the optical tones is low enough to enable the modulation of 3 GBaud QPSK data. Experimental work has verified the technique to be capable of transmitting a 7-channel 3 GBaud PDM-QPSK WDM signal over 100 km of SSMF. The results obtained have shown about a 0.4 dB sensitivity penalty between the best and the worst performing comb channels, together with a 0.8 dB penalty variation in system performance between the single channel case and the worst comb channel. Hence, this seven channel 10 Gb/s LR UDWDM PON downstream transmission (70 Gb/s) achieves a loss budget of 47 dB, thus enabling 100 km of SSMF transmission and a 1:256 passive split (3 dB margin). The use of such an optical multicarrier source at the OLT offers simplicity, low cost and energy efficiency. The use of a coherent receiver at each ONU compromises on cost, but in return offers improved receiver sensitivity and frequency selectivity, thereby enabling larger split ratios, longer reach and reduced network complexity.

4.3.2 80 km downlink system with PDM-16QAM

In the second experimental demonstration of this section we investigate the feasibility of achieving higher data rate per channel through the implementation of an 80 km, 20 GHz spaced 6 × 40 Gb/s LR DWDM PON downlink system. The experimental setup is identical to that shown in Fig. 4.8 except for the use of different settings as stated below. At the OLT, gain switching of the DFB laser is achieved by driving the laser diode with amplified sinusoidal signal at a frequency of 20 GHz together with a dc bias current of 40 mA. External light from the ECL with 5 dBm optical power and 25 kHz optical linewidth (Agilent N7711A, linewidth

from FM-noise spectrum measurement) injects into the DFB laser cavity to ensure the effective locking for phase noise suppression/linewidth transfer. The resulting low linewidth optical comb with 20 GHz spacing is shown in Fig. 4.12(a). The spacing between the channels can be easily tuned via the RF drive signal, as demonstrated in the previous chapter.

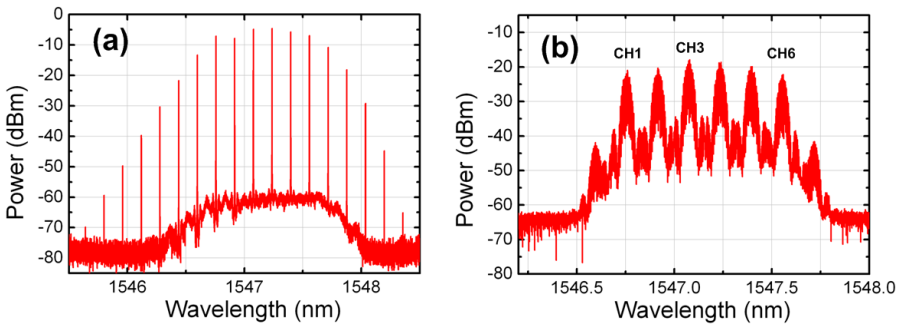

Figure 4.12: Optical spectra, with a 20 MHz resolution, of (a) Injected gain switched comb source with 20 GHz FSR and 25 kHz optical linewidth on each comb line. Note that the FSR is tunable. (b) 6-channel DWDM-PDM-16QAM signal corresponding to the comb in (a).

In this demonstration we use the OBPF to select 6 optical channels (within a 3-dB flatness spectral window) from the optical comb source. The data modulations for the odd and even channels are 6 GBaud 16-QAM signals, which are then recombined before entering a PDM emulator. The PDM emulation is achieved by separating the polarisation states of the input signal with a polarisation beam splitter, and introducing an optical delay-line stage in one of the paths for de-correlation before recombining them together using a polarisation beam combiner. As a result, a 6-channel, 20 GHz spaced DWDM-PDM-16QAM optical signal is generated as shown in Fig. 4.12(b), with each channel carrying 8 bits/symbol. This corresponds to a transmission rate per channel of 40 Gb/s with the 20% hard decision FEC coding overhead.

The transmission span in the experiment consists of 80 km standard single mode fibre (SSMF). In the ONU the LO is provided by an ECL with 200 kHz linewidth and tuned to each channel for the detection of the DWDM signal. The digitised signal at the coherent receiver output is down sampled to 12 GSa/s to give 2 samples per symbol. In the DSP modules, a radially directed equaliser (RDE) with 11 taps is used after pre-convergence with a constant modulus algorithm (CMA) [11]. Then frequency offset is removed before a carrier phase estimation using a decision directed algorithm [49]. Finally the hard decisions, symbol decoding and bit error counting is performed.

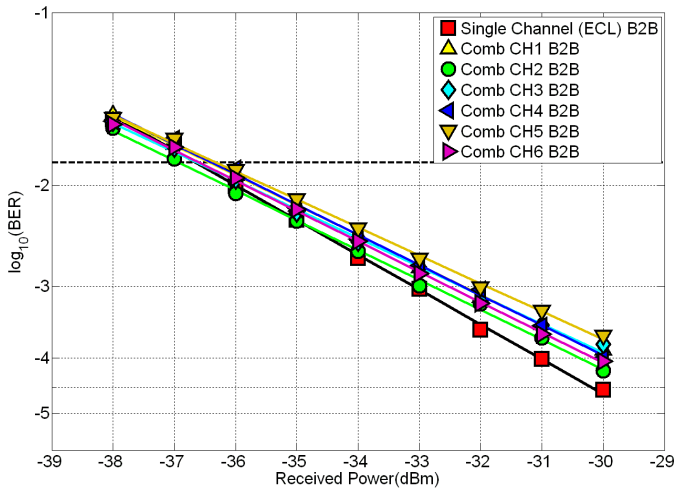

Figure 4.13: Back-to-back (B2B) sensitivity measurements of the 20 GHz spaced 6-channel DWDM-PDM-16QAM signal, and that of the injection master ECL.

Fig. 4.13 shows the back-to-back performance of the downlink channels, with 6 comb line channels (CH1 - CH6) as indicated in Fig. 4.12(b). From the results in Fig. 4.13, only small sensitivity penalties are observed between the single channel ECL and the DWDM signals. At the FEC limit of 1.5×10^{-2} BER, the power penalty between the worst performing back-to-back comb line channel (CH5) and the ECL is less than 0.3 dB. Such a result for the 6 GBaud DWDM-PDM-16QAM signal clearly demonstrates the excellent performance of the comb line channels due to the simultaneous linewidth transfer/phase noise reduction from the injection master ECL.

To continue our investigation, the 80 km SMF transmission performance of the LR DWDM channels at the FEC limit (BER of 1.5×10^{-2}) is examined and shown in Fig. 4.14. In the figure, the required optical power for each channel to achieve a BER of 1.5×10^{-2} is plotted as the red stars. From these results, the worst performing comb line (CH4 and Ch5) yields a received power of -35.6 dBm at the FEC limit. For the best performing comb line (CH2) the required optical power is -36.4 dBm. As such, a 0.8 dB difference in the best and worst performing channels is observed for the LR DWDM signal. In addition, we further evaluate the transmission penalties of individual channels due to the 80 km SMF, and the results are also recorded in Fig. 4.14 (the blue circles). Such evaluation illustrates the sensitivity degradation of each channel due to the fibre transmission, when they are compared to their respective back-to-back cases. It can be noticed in Fig. 4.14 that the transmission power penalty measured at the FEC limit yields a maximum value of 0.8 dB for the worst case channel CH3, and a minimum of 0.4 dB for the

best case channel CH6. Other channels demonstrate similar penalties in the range of 0.5-0.8 dB. In general the centre channels (CH3, CH4 and CH5) suffer slightly higher penalties as opposed to the others.

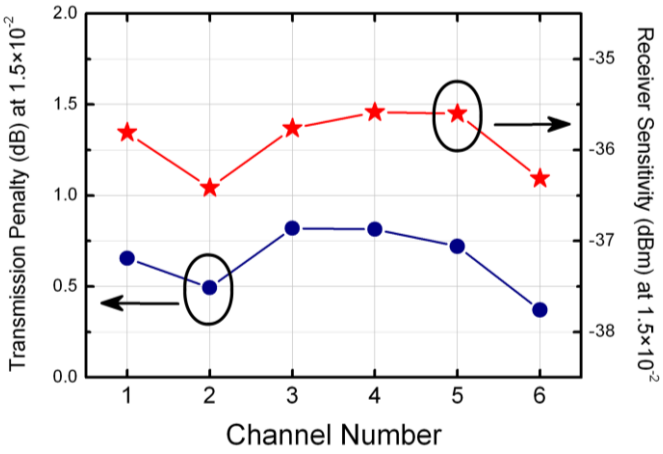

Figure 4.14: Transmission penalties (circles) and the receiver sensitivities (stars) at FEC limit for each LR DWDM channel over 80 km SMF. Centre channels (CH3, CH4 and CH5) demonstrate slightly worse performance in both scenarios, with the inter-channel difference less than 1 dB for both cases.

For the 80 km fibre transmission of LR DWDM-PDM-16QAM signal we record a worst-case receiver sensitivity of -35.6 dBm (54 photons/bit) at the FEC limit of 1.5×10^{-2} BER. Such high sensitivity for the low operating symbol rate (6 GBaud) and the high order (PDM-16QAM) modulation signal is due to the low linewidth/phase noise optical comb source at the OLT, and the use of a digital coherent receiver together with a high FEC overhead at the receiver end. With a total transmission power of 13 dBm and therefore per channel launch power of 5 dBm, the -35.6 dBm sensitivity corresponds to a system loss budget of 40 dB (the loss budget is defined as the sum of all losses incurred between the OLT and an ONU [16]).

In order to investigate the possibility of further enhancing the spectral usage, we also perform measurements with a reduced channel spacing of 15 GHz for the DWDM downlink signal. As proof-of-concept exploration, we have only taken the measurement result with one middle channel (CH3) on 15 GHz channel spacing in a B2B case, as demonstrated in Fig. 4.15 by the red stars. For comparison, the B2B performance of CH3 with 20 GHz spacing and that of the single channel ECL B2B (both from Fig. 4.13) are re-plotted in the figure. It should be noted that the modulation format, symbol rate and all other system conditions remain unchanged. As can be seen from Fig. 4.15, for the reduced spacing of CH3 an error-floor starts to appear at BER

lower than 1e-3, which can be mainly attributed to the inter-channel crosstalk from neighbouring channels owing to the reduced guard band. At the FEC limit however, there is no penalty compared to the 20 GHz spacing case or to the single channel ECL. This clearly suggests the potential of employing such a reduced spacing, by virtue of the high FEC overhead, for enhanced spectral efficiency of the proposed DWDM-PON downlink system. The ultimate system performance, in terms of other wavelength channels and the receiver sensitivity under fibre transmission, remain topics for future investigation.

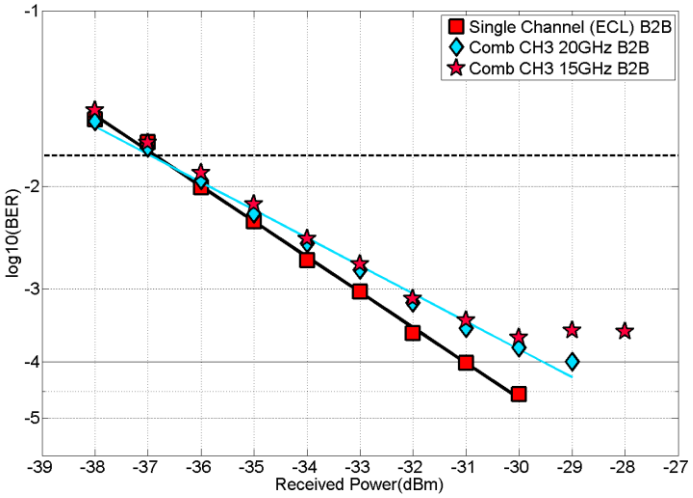

Figure 4.15: Back-to-back (B2B) sensitivity measurements of CH3 with 15 GHz and 20 GHz channel spacing, and that of the injection master ECL.

As a conclusion of the current demonstration, we have implemented a high capacity LR DWDM-PON, with the externally injected gain switched DFB comb source at the OLT and the coherent receiver at the ONU. We transmitted 20 GHz spaced highly coherent 6-channel DWDM-PDM-16QAM signal each at 6 GBaud over 80 km SMF. We have found 0.8 dB transmission penalty for the worst performing channel, together with a 0.8 dB variation in the receiver sensitivities between all the transmitted channels. This downstream 6 × 40 Gb/s transmission of the LR DWDM-PON has achieved a loss budget of 40 dB for 5 dBm per channel launch power. The experiment is demonstrated without any mid-span repeaters. Moreover based on the work presented here, a potential improvement has been suggested to offer improved spectral efficiency to the DWDM-PON system by reducing the channel spacing down to 15 GHz. Its feasibility has been experimentally verified with one wavelength channel in a B2B scenario. Additional research options could be considered include further reduction of channel spacing (e.g. 12.5 GHz) and/or implementing aggressive filtering techniques such as the Nyquist filters

[50]. The latter option is expected to offer the mitigation of potential inter-channel crosstalk and crosstalk induced by back reflections (considering bidirectional transmission), as well as the possible inter-channel nonlinearities such as four-wave mixing (FWM) and cross phase modulation (XPM).

4.4 Summary

Digital coherent optical receivers have revolutionised the long-haul (core) network for the past decade or so, largely due to its linear field detection principle which benefits channel impairments mitigation and complex (spectrally efficient) optical modulation. It is envisioned that the coherent optical transmission technology will follow the trend in the long-haul market and become equally disruptive for the consolidated, high volume metro-access area, albeit for different attractions such as high sensitivity and high frequency selectivity. This chapter outlined some existing efforts on the long reach coherent optical access networks, and further proposed and studied the utility of novel injected gain switched optical comb source in such a network context. The research has been carried out via two stages: 1) phase noise property of the comb source is characterised, through FM noise and phase-error variance analysis, demonstrating how residual comb line phase noise may degrade the performance of coherent optical communications; 2) system investigation focus on downlink portion of the long reach coherent access network through the use of intradyne digital coherent receiver. Experimental results featuring an unamplified 100 km, 10 GHz spaced 7 × 10 Gb/s UDWDM PON and an unamplified 80 km, 20 GHz spaced 6 × 40 Gb/s DWDM PON downlink systems illustrate the potential of the injected gain switched comb source in the proposed network architecture, achieving system loss budget of 47 dB and 40 dB respectively.

Reference

[1] S. Saito, Y. Yamamoto, and T. Kimura, "Optical heterodyne detection of directly frequency modulated semiconductor laser signals," Electron. Lett. **16**, 826 (1980).

[2] T. Okoshi, "Recent progress in heterodyne/coherent optical-fibre communications," J. Lightwave Technol. **LT-2**, 341 (1984).

[3] L. G. Kazovsky, "Balanced phase-locked loops for optical homodyne receivers: performance analysis, design considerations, and laser linewidth requirements," J. Lightwave Technol. **LT-4**, 182 (1986).

[4] T. Kimura, "Coherent optical fibre transmission," J. Lightwave Technol. **LT-5**, 414 (1987).

[5] L. G. Kazovsky, "Phase- and polarization-diversity coherent optical techniques," J. Lightwave Tehcnol. **7**, 279 (1989).

[6] R. A. Griffin and A. C. Carter, "Optical differential quadrature phase-shift key (oDQPSK) for high capacity optical transmission," in *Proc. OFC 2002, WX6.*

[7] M. G. Taylor, "Coherent detection method using DSP for demodulation of signal and subsequent equalization of propagation impairments," IEEE Photon. Technol. Lett. **16**, 674 (2004).

[8] R. Noe, "Phase noise-tolerant synchronous QPSK/BPSK baseband-type intradyne receiver concept with feedforward carrier recovery," J. Lightwave Technol. **23**, 802 (2005).

[9] F. Derr, "Optical QPSK transmission system with novel digital receiver concept," Electron. Lett. **27**, 2177 (1991).

[10] M. Nakazawa, K. Kikichi, T. Miyazaki (Editors), *High Spectral Density Optical Communication Technologies* (Springer, 2010).

[11] S. J. Savory, "Digital coherent optical receivers: algorithms and subsystems," IEEE J. Sel. Topics Quantum Electron. **16**, 1164 (2010).

[12] http://www.opticalconnectionsnews.com/latest-news/acacia-unveils-first-100g-coherent-pluggable-module

[13] S. Naikawa, N. Sakurai, K. Kumozaki, and T. Imai, "Coherent WDM-PON based on heterodyne detection with digital signal processing for simple ONU structure," in *Proc. ECOC 2006, Tu3.5.7.*

[14] S. P. Jung, Y. Takushima, K. Y. Cho, S. J. Park, and Y. C. Chung, "Demonstration of RSOA-based WDM PON employing self-homodyne receiver with high reflection tolerance," in *Proc. OFC 2009, JWA69.*

[15] H. Rohde, S. Smolorz, E. Gottwald, and K. Kloppe, "Next generation optical access: 1 Gbit/s for everyone," in *Proc. ECOC 2009, 10.5.5.*

[16] D. Lavery, M. Ionescu, S. Makovejs, E. Torrengo, and S. J. Savory, "A long-reach ultra-dense 10 Gbit/s WDM-PON using a digital coherent receiver," Opt. Express **18**, 25855 (2010).

[17] N. Iiyama, J. Kani, J. Terada, and N. Yoshimoto, "Two-phased capacity upgrade method for NG-PON2 with hierarchical star 8-QAM and square 16-QAM," in *Proc. OFC 2013, OM3H.2.*

[18] M. F. Huang, D. Qian, and N. Cvijetic, "A novel symmetric lightwave centralized WDM-OFDM-PON architecture with OFDM-remodulated ONUs and a coherent receiver OLT," in *Proc. ECOC 2011, Tu.5.C1.*

[19] E. J. Bachus, R. P. Braun, W. Eutin, E. Grobmann, H. Foisel, K. Heimes, B. Strebel, "Coherent optical-fibre subscriber line," Electron. Lett. **21**, 1203 (1985).

[20] E. J. Bachus, T. Almeida, P. Demeester, G. Depovere, A. Ebberg, M. R. Ferreira, G. D. Khoe, O. Koning, R. Marsden, J. Rawsthorne, and N. Wauters, "Coherent optical systems implemented for business traffic routing and access: the RACE COBRA project," J. Lightwave Technol. **14**, 1309 (1996).

[21] T. Pfeiffer, "Converged heterogeneous optical metro-access networks," in *Proc. ECOC 2010, Tu.5.B.1.*

[22] H. Rohde, S. Smolorz, J. S. Wey, and E. Gottwald, "Coherent optical access networks," in

Proc. OFC 2011, OTuB1.

[23] S. Smolorz, E. Gottwald, H. Rohde, D. Smith, and A. Poustie, "Demonstration of a coherent UDWDM-PON with real-time processing," in *Proc. OFC 2011, PDPD4.*

[24] H. Rohde, E. Gottwald, A. Teixeira, J. D. Reis, A. Shahpari, K. Pulverer, and J. S. Wey, "Coherent ultra dense WDM technology for next generation optical metro and access networks," J. Lightwave Technol. **32**, 2041 (2014).

[25] D. Lavery, E. Torrengo, and S. J. Savory, "Bidirectional 10 Gbit/s long-reach WDM-PON using digital coherent receivers," in *Proc. OFC 2011, OTuB4.*

[26] D. Lavery, C. Behrens, and S. J. Savory, "On the impact of backreflections in a bidirectional 10 Gbit/s coherent WDM-PON," in *Proc. OFC 2012, OTh1F.3.*

[27] D. Lavery, R. Maher, D. S. Millar, B. C. Thomsen, P. Bayvel, and S. J. Savory, "Digital coherent receivers for long-reach optical access networks," J. Lightwave Technol. **31**, 609 (2013).

[28] P. M. Anandarajah, R. Zhou, R. Maher, D. Lavery, M. Paskov, B. C. Thomsen, S. J. Savory, and L. P. Barry, "Gain-switched multicarrier transmitter in a long-reach UDWDM-PON with a digital coherent receiver," Opt. Lett. **38**, 4797 (2013).

[29] R. Zhou, P. M. Anandarajah, R. Maher, M. Paskov, D. Lavery, B. C. Thomsen, S. J. Savory, and L. P. Barry, "80-km coherent DWDM-PON on 20-GHz grid with injected gain switched comb source," IEEE Photon. Technol. Lett. **26**, 364 (2014).

[30] R. Zhou, T. N. Huynh, V. Vujicic, P. M. Anandarajah, and L. P. Barry, "Phase noise analysis of injected gain switched comb source for coherent communications," Opt. Express **22**, 8120 (2014).

[31] L. G. Kazovsky, G. Kalogerakis, and W. T. Shaw, "Homodyne phase-shift-keying systems: past challenges and future opportunities," J. Lightwave Technol. **24**, 4876 (2006).

[32] K. Kikuchi, "Characterization of semiconductor-laser phase noise and estimation of bit-error rate performance with low-speed offline digital coherent receivers," Opt. Express **20**, 5291 (2012).

[33] T. N. Huynh, L. Nguyen, and L. P. Barry, "Phase noise characterization of SGDBR lasers

using phase modulation detection method with delayed self-heterodyne measurements," J. Lightwave Technol. **31**, 1300 (2013).

[34] R. Zhou, V. Vujicic, T. N. Huynh, P. M. Anandarajah, and L. P. Barry, "Effective phase noise suppression in externally injected gain switched comb source for coherent optical communications," in *Proc. ECOC 2013, P.2.5.*

[35] P. Spano, S. Piazzolla, and M. Tamburrini, "Frequency and intensity noise in injection-locked semiconductor lasers: theory and experiments," IEEE J. Quantum Electron. **QE22**, 427 (1986).

[36] K. Petermann, *Laser Diode Modulation and Noise* (Kluwer Academic & KTK Scientific, 1988).

[37] K. Kikuchi and T. Okoshi, "Measurement of spectra of and correlation between FM and AM noises in GaAlAs lasers," Electron. Lett. **19**, 812 (1983).

[38] B. Daino, P. Spano, M. Tamburrini, and S. Piazzolla, "Phase noise and spectral line shape in semiconductor lasers," IEEE J. Quantum Electron. **QE-19**, 266 (1983).

[39] C. H. Henry, "Phase noise in semiconductor lasers," J. Lightwave Technol. **LT-4**, 298 (1986).

[40] K. Kikuchi and T. Okoshi, "Dependence of semiconductor laser linewidth on measurement time: evidence of predominance of 1/f noise," Electron. Lett. **21**, 1011 (1985).

[41] K. Kikuchi, T. Okoshi, M. Nagamatsu, and N. Henmi, "Degradation of bit-error rate in coherent optical communications due to spectral spread of the transmitter and the local oscillator," J. Lightwave Technol. **LT-2**, 1024 (1984).

[42] T. N. Huynh, F. Smyth, L. Nguyen, and L. P. Barry, "Effects of phase noise of monolithic tunable laser on coherent communication systems," Opt. Express **20**, B244 (2012).

[43] T. Nakagawa, M. Matsui, T. Kobayashi, K. Ishihara, R. Kudo, M. Mizoguchi, and Y. Miyamoto, "Non-data-aided wide-range frequency offset estimator for QAM optical coherent receivers," in *Proc. OFC 2011, OMJ1.*

[44] Y. Mori, C. Zhang, K. Igarashi, K. Katoh, and K. Kikuchi, "Unrepeated 200-km

transmission of 40-Gbit/s 16-QAM signals using digital coherent receiver," Opt. Express **17**, 1435 (2009).

[45] M. Scholten, T. Coe, and J. Dillard, "Continuously-interleaved BCH (CI-BCH) FEC delivers best in class NECG for 40G and 100G metro applications," in *Proc. OFC 2010, NTuB3.*

[46] K. Kikuchi and S. Tsukamoto, "Evaluation of sensitivity of the digital coherent receiver," J. Lightwave Technol. **26**, 1817 (2008).

[47] F. Chang, K. Onohara, and T. Mizuochi, "Forward error correction for 100 G transport networks," IEEE Commun. Magazine, **48**, S48 (2010).

[48] S. J. Savory, "Digital filters for coherent optical receivers," Opt. Express, **16**, 804 (2008).

[49] T. Pfau, S. Hoffmann, and R. Noe, "Hardware-efficient coherent digital receiver concept with feedforward carrier recovery for M-QAM constellations," J. Lightwave Technol. **27**, 989 (2009).

[50] J. D. Reis, A. Shahpari, R. Ferreira, S. Ziaie, D. M. Neves, M. Lima, and A. L. Teixeira, "Terabit+ (192× 10 Gb/s) Nyquist shaped UDWDM coherent PON with upstream and downstream over a 12.8 nm band," J. Lightwave Technol. **32**, 729 (2014).

Chapter 5

Direct Detection Based Access Networks with Comb Source

In the previous chapter, the performance of an injected gain switched comb source was experimentally investigated in a coherent access network (downlink) scenario. The combination of a low noise comb source at the optical line terminal (OLT) and a digital coherent optical receiver at each optical network unit (ONU) has enabled high order modulation signal to be delivered to the end-users. This chapter explores the utilisation of simple direct detection architecture for receiving downlink user data encoded with spectrally efficient modulation formats. This is supported by a gain switched multi-carrier transmitter with or without injection at the OLT, and a pilot tone aided optical scalar detection at the ONU. Such a simple but novel scheme, forming another contribution of this thesis, negates the need for low linewidth/phase noise transmitter and local oscillator (LO) lasers in the network, as well as a coherent optical front-end in each user premise. In addition, it overcomes the difficulties associated with the constant optical frequency/phase tracking in the ONU by greatly enhancing the system phase noise tolerance. Hence, the proposed network architecture can be considered as an attractive alternative to the coherent access solution by supporting high capacity wavelength division multiplexed-passive optical networking (WDM-PON) with simplicity, cost and energy savings.

In this chapter, three different pilot tone aided direct detection scenarios, defined by different spectral arrangements between the pilot tone and the data signal, are demonstrated and examined through WDM-PON downlink experiments. Following an explanatory section identifying the distinct features, these three schemes will be each investigated in a dedicated section.

5.1 Pilot Tone Aided Direct Detection

Next generation optical access networks utilising WDM-PON architectures will be in favour of employing advanced optical modulation formats like quadrature phase shift keying (QPSK) and quadrature amplitude modulation (QAM) for improved spectral efficiency. To retrieve the information on these complex modulated signals, optical coherent detection technology is an effective solution as experimentally verified in the preceding chapter (Section 4.3). In such a scenario the phase noise property, of both the transmitter and the LO laser sources, is a critical property that needs to be maintained at a reasonably low level for acceptable system performance (Section 4.2). Regarding the conventional direct detection based receiver structure with a single photodiode (PD) the optical phase information is lost upon a square-law power detection process. However, the complex (amplitude and phase) optical data can be instead coherently recovered in the electrical domain as is well known in radio over fibre (RoF) [1] and subcarrier multiplexed systems [2]. A significant advantage in these systems is that the high stability and the low noise property of the widely available radio frequency (RF) oscillators, which outperform their optical counterparts, can be well exploited. Hence, the system dependence on the optical phase (frequency) noise of the transmitter and LO lasers can be greatly eased.

Another convenient feature of transferring coherent detection into the electrical domain is that more matured RF electronic devices can be used rather than the optical components. The direct benefit involves cost reduction associated with the 90° optical hybrid (for intradyne/homodyne systems), the low linewidth/phase noise wavelength tunable lasers, and several pairs of balanced photodiodes that need to be implemented at the user end in a coherent optical access case. Meanwhile, the process of optical carrier recovery (frequency and phase estimation) [3] can be bypassed therefore the use of complicated optical phase-lock loops (OPLLs) or real-time digital frequency/phase tracking can be avoided. Nevertheless there exists some performance trade-off/limitations compared to the coherent access solution, such as the reduced receiver sensitivity (absence of optical gain from the LO) and the lack of network agility (explained below).

In this chapter we explore the use of direct detection/electrical coherent principle, and propose a WDM-PON downlink scheme capable of delivering high order optical modulation

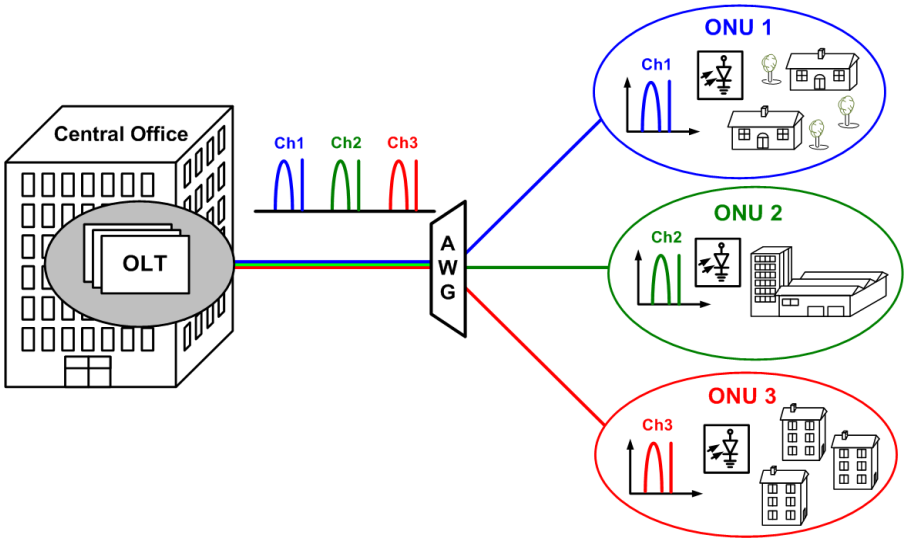

Figure 5.1: Proposed pilot tone aided direct detection scheme for a downlink WDM-PON.

formats using a single PD receiver infrastructure. The network scheme (as shown in Fig. 5.1) entails the use of an arrayed waveguide grating (AWG) based optical distribution network (ODN) infrastructure, and a "pilot tone" signal which is generated at the transmitter side and sent together with the modulated data signal. At the OLT, the pilot tone is derived from the same optical source as the modulated data but separated by an appropriate intermediate frequency (IF). At the remote node, the AWG selects the data + pilot pairs and distributes each pair to an ONU (note that network agility is lost due to the "coloured" ODN). Upon detection at the ONU, the phase modulated data mixes with the pilot tone creating a copy of the data at the selected IF. This heterodyne beating at the PD output containing complex modulation information is independent of the optical linewidth of transmitter light source as the phase noise in pilot and data signal cancel each other out during the beating process (as they are coherent with each other).

As mentioned earlier the pilot aided direct detection scheme can be realised with a few different spectral arrangements in relation to how the pilot tone is generated. Three arrangements that have been experimentally verified and will be discussed in this chapter are graphically illustrated in Fig. 5.2. As shown in the figure, a straightforward approach for the insertion of the pilot tone, is to utilise alternate/neighbouring comb tones as the pilot signal (the "*optical pilot*" scheme). Experimental results successfully demonstrating 50 km unamplified downlink dense WDM-PON transmission with this method [4] will be given in Section 5.2. However, the optical pilot scheme restricts the available number of user channels

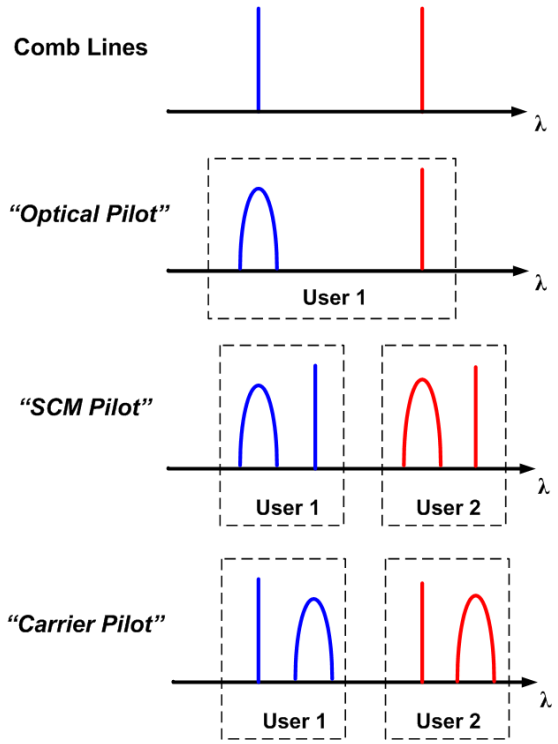

Figure 5.2: Different pilot tone schemes with various spectral arrangements between pilot and data.

as half of the comb lines will need to be reserved as the un-modulated pilots. Therefore we also propose a "*subcarrier multiplexed (SCM) pilot*" scheme, where a RF tone is used as the pilot. This is then SCM on to the optical comb line, which is used for data modulation. This scheme is capable of utilising all the comb tones and a 25 km downlink transmission experiment will be presented in Section 5.3. Finally, we investigate a third scheme by modulating the QPSK data onto a RF subcarrier and exploit the comb line carrier as the pilot tone (the "*carrier pilot*" scheme). This scenario essentially has the same comb tone usage as the SCM pilot case but the wavelength allocation of pilot and data has been exchanged. The relating experimental results consisting of a 100 km downlink unrepeated long reach (LR) ultra-dense (UD) WDM-PON [5] will be reported in Section 5.4.

5.2 Optical Pilot Tone Scheme

This section elaborates on the "optical pilot" scheme where a simple gain switched discrete mode (DM) laser based comb source [6] is implemented at the OLT, and the phase correlated alternate optical comb tones are utilised as the pilot tones. A 50 km DWDM-PON downlink system is demonstrated with simple direct detection in the ONUs for receiving an error free, low symbol rate (2.5 GBaud) QPSK signal. Note that in this experiment, the use of an

un-injected gain switched comb source at the OLT demonstrates the linewidth independence of the proposed direct detection scheme since the DM comb source typically yields a 3-dB comb line linewidth of around 3-5 MHz [7] [8]. Such a linewidth value for the optical carriers, combining with the low operating baud rate of the optical QPSK modulation signal would produce a large linewidth-to-symbol-rate ratio and bring in considerable penalties to the digital coherent received based systems [3] [9]. Hence without the use of the proposed pilot tone aided detection, the demonstrated system would have proven prohibitive for a coherent access scenario.

5.2.1 Experimental configuration

The experimental setup of the optical pilot tone scheme is schematically presented in Fig. 5.3. Gain switching of the DM laser with an amplified 10.663 GHz sinusoidal signal in conjunction with a dc bias current (I_B = 54.7 mA) results in a series of seven clearly resolved phase correlated sidebands (3-dB of the spectral envelope peak) offset by an integer multiple of the drive frequency. Power equalisation and outer sideband rejection is achieved by passing the comb signal through an optical band-pass filter (OBPF 1) with both tunable bandwidth and wavelength. This results in the unwanted outer sidebands being suppressed to about 15 dB below the 6 chosen comb tones, and also yields comb flatness within a 1 dB margin as shown in Fig. 5.4(a). This signal is subsequently optically amplified using an Erbium doped fibre am-

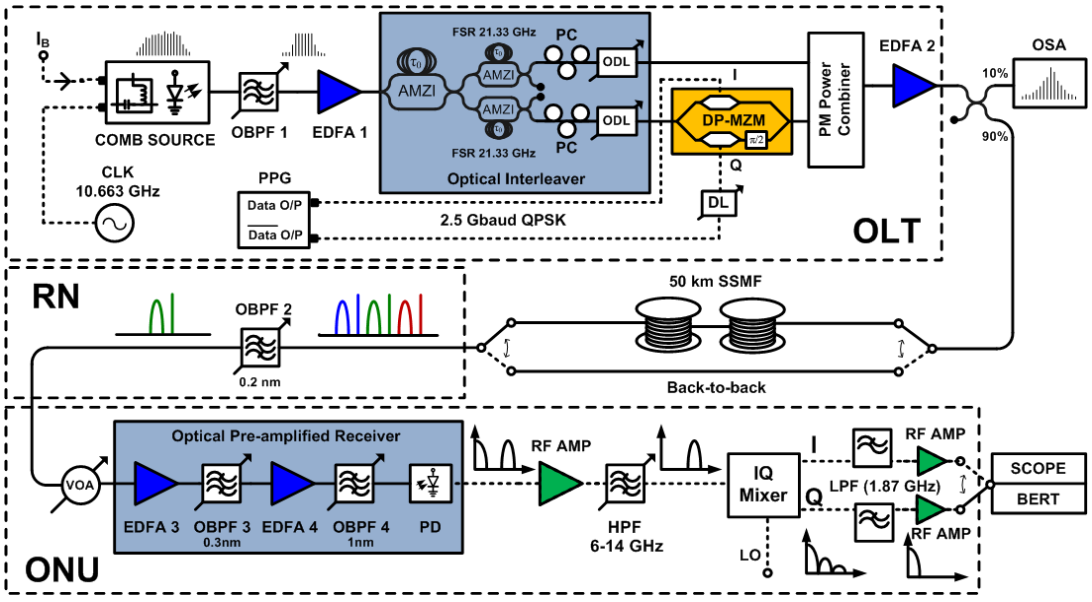

Figure 5.3: Experimental configuration of the 2.5 GBaud QPSK downlink DWDM-PON employing a gain switched DM comb source at the OLT and optical pilot tone aided direct detection at ONU.

-plifier (EDFA 1) to overcome the loss of the optical filter.

The selected comb lines are then passed through an asymmetric Mach Zehnder interferometer (AMZI) based optical dis-interleaver stage, which has a free spectral range (FSR) of 21.33 GHz, to separate the comb tones into even (-2, 0 and 2) and odd (-1, 1 and 3) channels. Both, the odd and even channels are passed through a second stage dis-interleaver (consisting of two identical AMZIs with a FSR of 21.33 GHz) to improve the extinction ratio to about 40 dB. The two sets of channels (one set for data and the other for pilots) are then passed through polarisation controllers (PC) and optical delay lines (ODLs). The ODLs are used to match the path length of the two arms of the interferometer. The 3 odd comb tones (-1, 1 and 3) are modulated with 2.5 Gb/s non-return to zero (NRZ) electrical data and delayed inverse data patterns, with a pseudorandom binary sequence (PRBS) length of 2^7-1, using a dual parallel Mach Zehnder modulator (DP-MZM). The data and inverse data streams from a pulse pattern generator (PPG) are de-correlated (11 bit delay) and bit-aligned with the aid of different electrical cable lengths and a RF delay line (DL). These two de-correlated data signals are then used to drive the in-phase (I) and quadrature (Q) inputs of the DP-MZM to achieve a 2.5 GBaud optical QPSK signal. The second output of the dis-interleaver (3 even comb tones: -2, 0 and 2) is un-modulated (reserved as pilots) and passively multiplexed with the 3 data channels with the aid of a polarisation maintaining coupler. A 10% optical tap is passed into a standard optical spectrum analyser (OSA) with a resolution of 0.02 nm, to enable

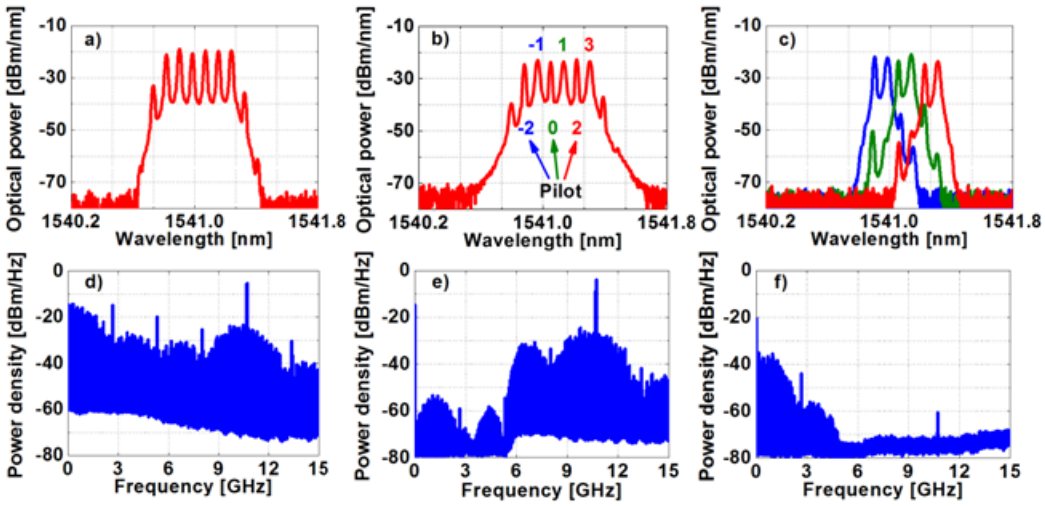

Figure 5.4: Optical spectra recorded at 10% tap of: a) filtered output of the comb source, b) output of the OLT, c) channels filtered out individually with corresponding pilot tone at RN. Electrical spectra acquired in the ONU at: d) the output of the PD, e) filtered output after the HPF, f) filtered output of LPF after down conversion.

monitoring of the signals at the output of the OLT.

The multiplexed signal consisting of three 2.5 GBaud QPSK channels and three pilot tones, as shown in Fig. 5.4 (b), is then transmitted first directly (back-to-back) and subsequently through the 50 km feeder fibre to the remote node (RN). An OBPF 2, at the RN, with a 3-dB bandwidth of ~25 GHz is used to pick out one of the data channels together with an adjacent pilot tone. The output from the RN with the filter tuned to pick out the three different pairs (one pair at a time) is presented in Fig. 5.4(c). In a practical system the tunable filter would be replaced by an AWG, where each output port would route a pair of signals (data and pilot tone) to the designated ONU (user premise).

At the receiver side, a variable optical attenuator (VOA) is used to vary the input power falling on an optically pre-amplified receiver (due to the lack of availability of an appropriate avalanche photodetector at the time of experiment) to measure bit error rate (BER) as a function of received power. The receiver consists of an EDFA (3) acting as a pre-amplifier, a 0.3 nm tunable OBPF 3, a second booster EDFA (4) in automatic power control mode, a 1 nm OBPF 4 and a 40 GHz PD. The detected signal is amplified before being high pass filtered (HPF, 6.3 GHz low frequency cut-off) to reject the detected baseband data and harmonics. This is followed by an electrical I/Q mixer for demodulation and a pair of low-pass filters (LPFs, 1.87 GHz cut-off frequency) to reject the remaining RF signal and electrical LO. A broadband data amplifier is used to boost the baseband signal prior to the error detector (BERT: bit error rate tester) and oscilloscope. Electrical spectra at various parts of the receiver (at the output of the PD, filtered output after the HPF, and I/Q down-converted and filtered output of LPF) are shown in Fig. 5.4 (d)-(f).

5.2.2 Results and discussion

The performance of the optical pilot tone based DWDM-PON system (downlink) is verified by carrying out BER measurements for two different scenarios: back-to-back (B2B) and 50 km standard single mode fibre (SSMF) transmission. The resulting BER (average of I & Q) versus received power recorded for each of the three optical data channels is shown in Fig. 5.5. The red circles, green diamonds and blue triangles denote the performance of the centre, right and left channels, respectively, in a B2B scenario. As can be seen in the figure, error-free operation (BER of 1e-9) for the outer channels is achieved at -33 dBm and for the middle channel at -32

dBm. The 1 dB penalty in the case of the middle channel can be mainly attributed to the non-ideal optical filtering at the RN (leakage of adjacent channels). For the sake of clarity, the performance of only the middle channel when transmitted over 50 km of SSMF is shown in Fig. 5.5 and is denoted by the black squares. The fibre transmission of the central channel results in a further 1 dB penalty (relative to the B2B performance of the central channel at 1e-9) yielding error-free operation at -31 dBm of received power. The outer channels (left and right) both portrayed a receiver sensitivity of -32 dBm at BER of 1e-9 under 50 km transmission (not shown in the figure). Examples of received eye-diagrams are shown as insets in Fig. 5.5, which correspond to both I and Q data recovered from the middle channel for B2B (a and b) and SSMF transmission (c and d) scenarios. These results clearly demonstrate the feasibility of the proposed linewidth insensitive optical pilot tone aided direct detection scheme for a low baud rate (2.5 GBaud) optical QPSK in a long distance (50 km) DWDM-PON scenario. However, apart from the basic limitations mentioned in the previous section a particular drawback of the optical pilot tone scheme is that it uses dedicated comb tones as the pilots, and results in a reduced network user number. In the following sections, we experimentally investigate two variation schemes to address this issue.

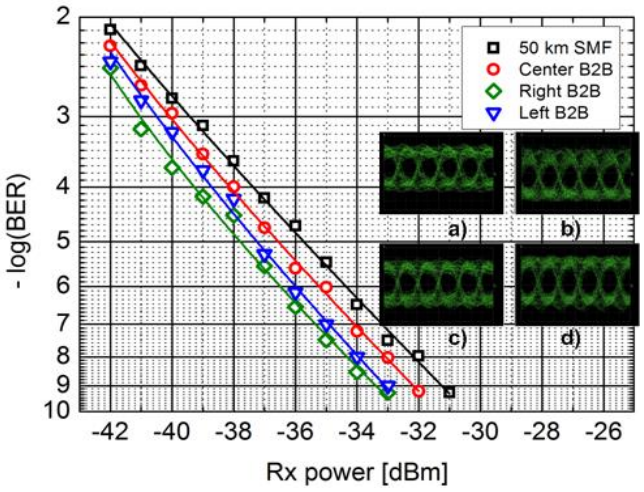

Figure 5.5: BER versus received power for 3 individual channels for the B2B scenario and for the centre channel after transmission through 50 km of SSMF. Insets show received eye diagrams of I and Q signals recorded for the centre channel in B2B (a & b) and 50 km transmission (c & d).

5.3 SCM Pilot Tone Scheme

In this section, we propose a novel “SCM pilot” technique to effectively double the network user number compared to the optical pilot tone scheme. This is achieved by passive electrical

coupling of a RF tone with the complex baseband data prior to optical I/Q modulation. Experimental work on a 25 km DWDM-PON downlink transmission with 2.5 GBaud QPSK is accomplished with an externally injected gain switched distributed feedback (DFB) comb source [6] at the OLT, and a direct detection receiver in the ONU. The optical linewidth transferred from the injection master (another DFB laser) to the comb lines yields a 3-dB value of 10 MHz (measured by a delayed self-heterodyne (DSH) [10] setup), hence again proving the superior phase noise tolerance of the proposed pilot tone aided detection scheme.

5.3.1 Experimental configuration

The experimental setup for the SCM pilot tone scheme is schematically depicted in Fig. 5.6, with only the OLT part shown. The OLT features an externally injected gain switched DFB laser based optical coherent comb source providing 7 optical carriers (OC) spaced by 20 GHz as illustrated in Fig. 5.7(a). The optical signal is amplified with an EDFA 1 and fed to a DP-MZM via a 5 nm OBPF 1 and a PC. The output of the DP-MZM is then amplified again (EDFA 2) prior to launching the signal out of the OLT. Two 2.5 Gb/s NRZ signals (data and inverse data), with a PRBS pattern length of 2^{15}-1, are derived from a PPG and each passed through a low pass filter (LPF) to suppress the high frequency side-lobes. An 8 GHz sinusoidal signal (RF pilot), derived from a signal generator, is split into two paths and coupled with the two data streams that are used to drive the DP-MZM. Electrical attenuators in the setup are used to balance the amplitudes of the data and pilot tones at the OLT, and minimising the reflections from the passive combining stages. An electrical DL 1 in one data path de-correlates and bit-wise aligns the data patterns, and another DL 2 introduces a phase shift in the pilot path to allow one of the optical subcarrier tones to be suppressed (as in Fig. 5.7(b)). The resulting optical signal is a 2.5 GBaud optical QPSK signal on each of the optical carriers

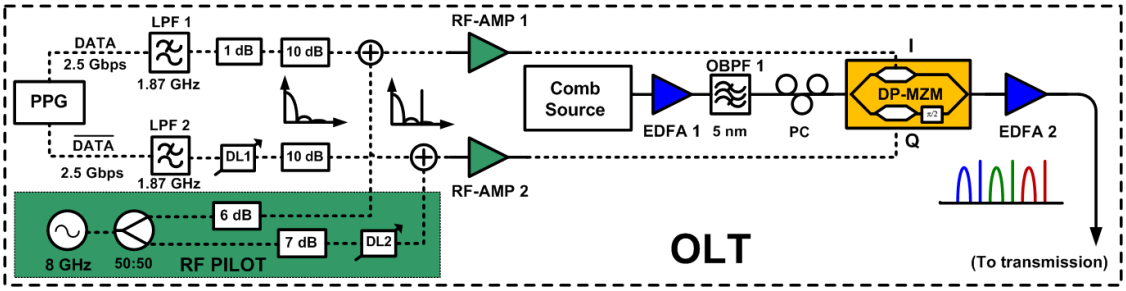

Figure 5.6: OLT configuration of the 2.5 GBaud QPSK downlink DWDM-PON employing injected gain switched comb source at OLT and SCM pilot tone aided direct detection in ONU.

(comb tones) with a single sideband SCM pilot tone placed 8 GHz away from the comb tone. The optical spectrum of this signal is shown in Fig. 5.7(c). Note that the 8 GHz RF tone for pilot generation is to guarantee the sufficient guard band between baseband data and the pilot, and the frequency of this RF tone can be varied depending on the desired spectral efficiency versus performance trade-off.

The rest of the setup is identical with that presented in Fig. 5.3, except for the different experimental settings as explained below. The transmission distance in this experiment is 25 km. A tunable OBPF at RN with 3-dB bandwidth of 0.1 nm selects one data channel together with the corresponding SCM pilot tone (tone at shorter wavelength), as illustrated in Fig. 5.7(d); note that the residual tone on the longer wavelength side of the data is the leakage pilot tone from adjacent channel due to imperfect optical filtering. At the ONU, the filter bandwidth for both OBPFs in the optical pre-amp is 2 nm, and the PD bandwidth is 10 GHz.

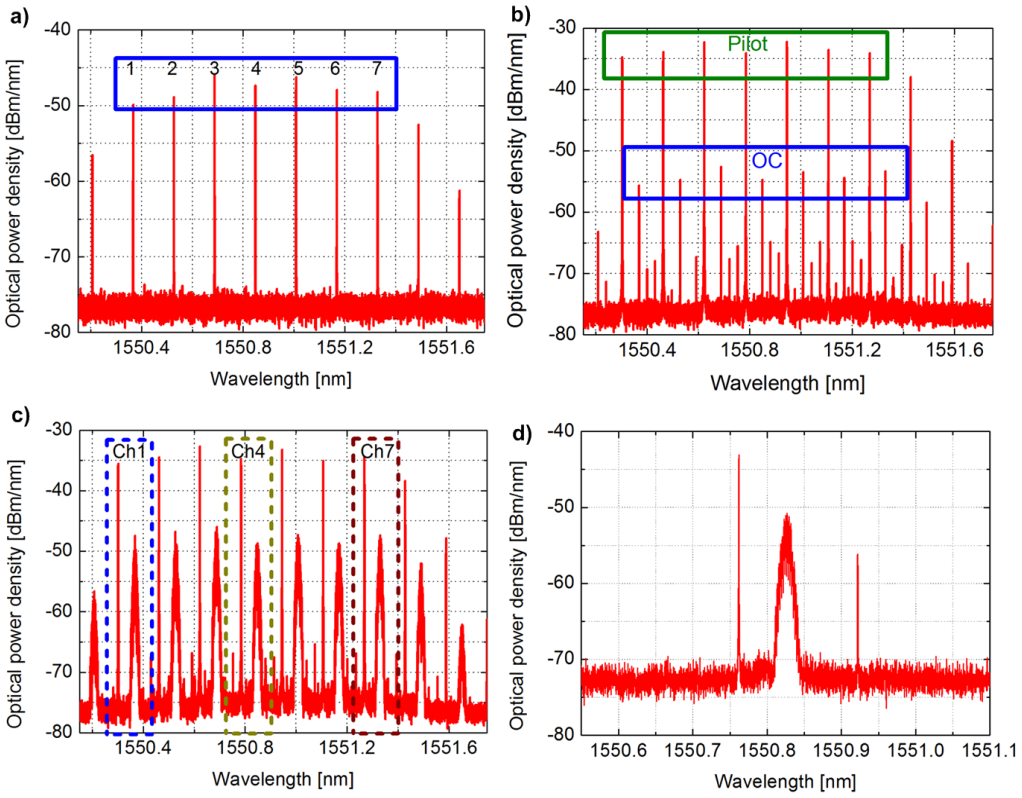

Figure 5.7: High resolution (20 MHz) optical spectra of: (a) data carriers/comb tones, (b) single side band SCM pilot tones added on the shorter wavelength side of each of the carriers, (c) modulated data channels with corresponding pilots, (d) one filtered channel at RN with pilot (left tone) and data.

5.3.2 Results and discussion

The performance of the DWDM-PON system (downlink) is verified by carrying out BER

measurements for two different scenarios: back-to-back (B2B) and 25 km SSMF transmission. The resulting BER (average of I & Q) versus received power recorded for three selected optical data channels (for clarity of demonstration) is shown in Fig. 5.8. The blue circles, red squares, and green triangles denote the performance of the left (Ch1), centre (Ch4), and right (Ch7) channels, respectively, in a B2B scenario. As can be seen in the figure, error-free operation for Ch1, Ch4 and Ch7 is achieved at -33, -33 and -34 dBm (at BER of 1e-9) respectively. The 1 dB penalty in the case of Ch1 and Ch4 can be mainly attributed to: the power asymmetry and slightly worse noise extinction ratio of the optical comb source (Ch1 case), and the crosstalk from neighbouring channels (Ch4 case). For the sake of clarity, the performance of only the middle channel when transmitted over 25 km of SSMF is shown in Fig. 5.8 and is denoted by the black line (crosses). The fibre transmission of the central channel results in a further 2 dB penalty (relative to the B2B performance of the central channel at 1e-9) yielding error-free operation at -31 dBm of received power. The outer channels (Ch1 and Ch7) both portrayed receiver sensitivities (at a BER of 1e-9) of -32 dBm (not shown in the figure). As such, the experimental results demonstrated here show the potential of the proposed SCM pilot tone scheme in terms of efficient OLT comb tone usage (7 tones for 7 users) compared to the optical pilot tone scheme (6 comb tones for 3 users). A trade-off of the SCM pilot scheme, however, is the reduced transmission distance of the downlink system. This is partly caused by the non-ideal electrical coupling (leakages and possible reflections due to the use of non-ideal coupling stages) at the transmitter side that res-

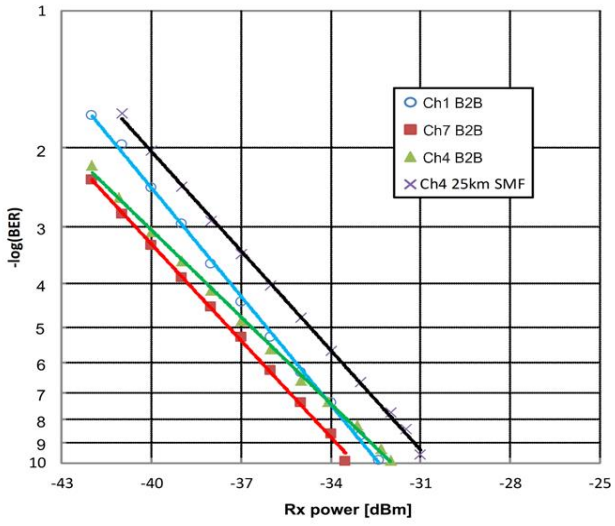

Figure 5.8: BER performance of the SCM pilot tone scheme with three selected channels in B2B configuration, and central channel for transmission through 25 km of SSMF.

-ults in a degraded signal-to-noise-ratio (SNR) of the data channels. Further improvements on the SCM pilot scheme are potentially possible with enhanced performance of the RF electronics at the OLT.

5.4 Carrier Pilot Tone Scheme

In this section, we describe a “carrier pilot tone” scheme, which entails subcarrier multiplexing a 1.25 GBaud QPSK data signal onto a RF tone and utilises the comb line carrier as the pilot. To enhance the spectral efficiency, single side-band (SSB) modulation is imposed for the SCM-QPSK signal. The carrier pilot scheme makes use of every optical comb tones for data channels as that in the SCM pilot case. The optical comb source employed at the OLT is a wavelength tunable comb based on an externally injected gain switched Fabry-Pérot (FP) laser [11]. Such an agile WDM transmitter would offer benefits to future reconfigurable access network designs, and also offers OLT component sparing and inventory savings. In order to illustrate the linewidth tolerance of the system we utilise a master laser with large amount of phase noise (60 MHz linewidth) to inject into the gain switched FP comb source. Experimental work is demonstrated with 100 km unrepeated downlink transmission.

5.4.1 Experimental configuration

The experimental setup of the proposed LR-UDWDM PON (downlink) with a tunable comb source at the OLT and carrier pilot tone aided direct detection at the ONU is illustrated in Fig. 5.9, with only the OLT part shown while the rest of the setup can be referred to Fig. 5.3. The wavelength tunable optical comb source at the OLT is based on a gain switched externally injected FP laser, achieved by driving the laser diode with a large amplified sinusoidal signal (24 dBm at 12.5 GHz) in conjunction with a dc bias current of 55 mA, while the laser is temperature controlled at 25°C. A commercially available modulated grating Y-branch tunable laser [12] that exhibits a 3-dB linewidth of about 60 MHz is used as the master laser. It is important to note that the external injection enables single mode operation of the FP laser and supports the wavelength tunability of the comb over the C-band [11] (note that in this experiment only one operating FP mode is discussed for clarity). Moreover, the external injection improves key comb parameters such as the spectral flatness, the background noise extinction and also transfers its linewidth to the slave comb lines [11]. The tunable gain

switched comb source, as illustrated in Fig. 5.10(a), yields 7 clearly resolved phase correlated optical tones within a 3-dB spectral envelope with each of the tones offset by an integer multiple of the drive frequency (12.5 GHz). The 3-dB optical linewidth of individual comb tones is measured to be ~60 MHz using the DSH method [10]. We will further discuss this large linewidth value later in the section. The comb signal is then optically amplified with an EDFA and passed through a tunable OBPF. This results in 5 chosen comb lines within a 3-dB spectral window and unwanted outer sidebands being suppressed to about 25 dB, as illustrated in Fig. 5.10(b). This signal is subsequently passed into a dual drive Mach-Zehnder modulator (DD-MZM) for SCM-QPSK data generation.

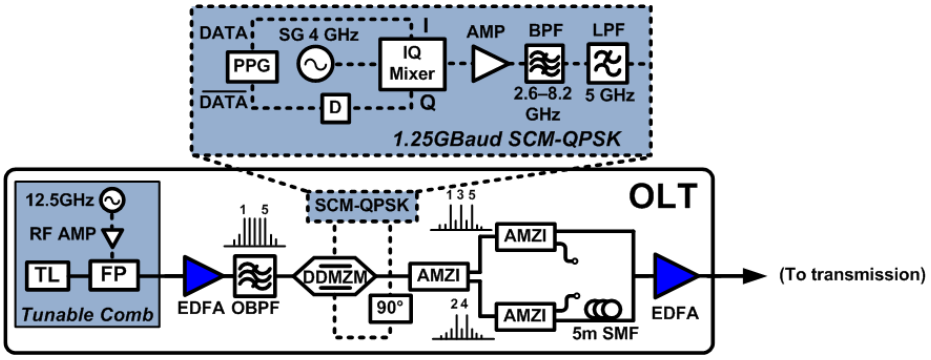

Figure 5.9: OLT configuration of the 100 km LR UDWDM PON downlink system. Inset shows the realisation of SCM-QPSK signal generation with low-cost analogue electronics.

The realisation of the electrical SCM-QPSK signal, with analogue electronics, is schematically illustrated as an inset of Fig. 5.9 (zoomed in shaded box). A PRBS of length 2^{15}-1 at a bit rate of 1.25 Gb/s is derived from a PPG. The data and inverse data streams are de-correlated by 12 bits and bit-aligned with the aid of different electrical cable lengths and a RF delay line (D). These two de-correlated data signals are then used to drive the in-phase (I) and quadrature (Q) inputs of an electrical IQ mixer to achieve a 1.25 GBaud electrical QPSK signal. A sine wave at 4 GHz derived from a signal generator (SG) is supplied to the LO input of the IQ mixer resulting in the QPSK signal being up-converted to a frequency of 4 GHz. The 1.25 Gbaud QPSK signal centred around 4 GHz is first band-pass and low-pass filtered to suppress the residual low and high frequency side-lobes (due to the lack of an appropriate BPF for the desire frequency band: 2.75-5.25 GHz), and then passed into a 90° electrical hybrid. The two outputs (offset by 90° in phase) of the electrical hybrid correspond to an identical copy, and a Hilbert transformed [13] version of the original SCM-QPSK signal respectively.

They are then applied to the two driving arms of the DD-MZM. By biasing the DD-MZM at quadrature point, the output of the modulator yields SSB generation of the modulating SCM-QPSK signal [14]. As such, the resulting 5-channel optical SSB-SCM-QPSK data and comb lines (carrier pilots) are passed through a 2-stage dis-interleaver based on the asymmetric Mach-Zehnder interferometers (AMZIs), with a free spectral range (FSR) of 25 GHz, to separate into odd and even channels with an extinction ratio of 40 dB. The 2 even channels are subsequently passed through a 5 m de-correlation fibre patch cord, and then passively re-combined with the 3 odd channels. The multiplexed signal consisting of five 1.25 GBaud QPSK channels and 5 pilot tones, as shown in Fig. 5.10(c), is amplified and then transmitted first directly (back-to-back) and subsequently through 100 km of SSMF to the RN.

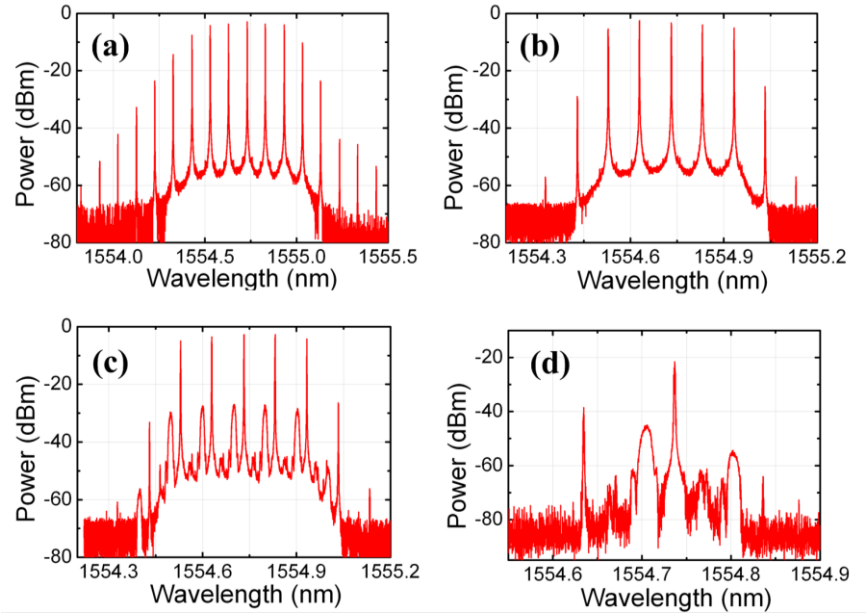

Figure 5.10: Optical spectra (100 MHz resolution) of: (a) injected gain switched FP comb source, (b) filtered comb lines at OLT, (c) OLT modulated output with 5-channel SSB-SCM-QPSK data and corresponding carrier pilot tones, (d) filtered output of RN with a pair of data channel and pilot.

The output from the RN with a wavelength and bandwidth tunable optical filter tuned to pick out the five different data + pilot pairs (one pair at a time) is illustrated in Fig. 5.10(d). Again this filter would be replaced by an AWG in a practical system. The residual tone and data on the short and long wavelength sides of the desired data + pilot pair are the leakage from neighbouring channels due to imperfect filtering. In this experiment, the filtered channel is detected within the ONU by using a receiver that consists of an avalanche photodiode (APD) and an integrated trans-impedance amplifier (TIA), as opposed to the optical pre-amplified

receiver used in the previous two pilot tone schemes. The APD receiver has a 3-dB bandwidth of 10 GHz. Electrical spectra shown in Fig. 5.11(a)-(c) illustrate the output of the APD, the IQ down-converted output (showing residual LO and its harmonic), and the LPF (933 MHz) output, respectively.

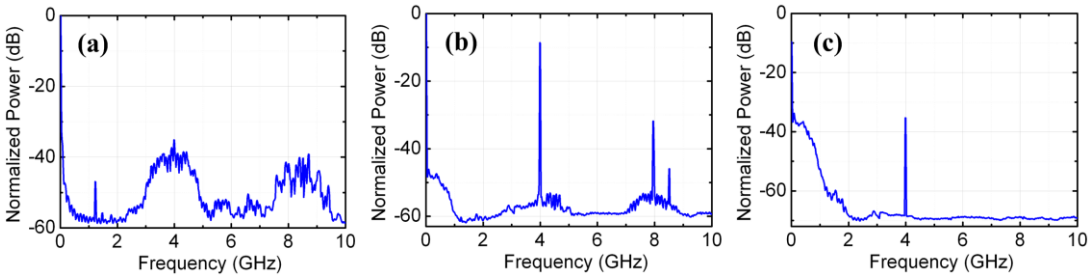

Figure 5.11: Electrical spectra acquired at ONU: (a) APD output, (b) IQ mixer output, (c) LPF output.

As mentioned earlier in the section, the 3-dB optical linewidth of the individual comb tones at the OLT is measured to be ~60 MHz using DSH method (electrical beat spectrum for one filtered comb line shown in Fig. 5.12(a)). The large linewidth with distorted lineshape, shown in Fig. 5.12(a), is mainly due to the additional low frequency phase noise (e.g. $1/f$ type frequency modulated (FM) noise [15]) transferred from the Y-branch injection master laser [12]. The large low frequency FM noise can be clearly seen from the FM-noise spectrum of the master Y-branch laser (as in Fig. 5.12(b)) measured with a modified DSH phase noise characterisation technique [15]. Such excess low frequency noise, in addition to the intrinsic white FM noise (linewidth deduced from the white FM noise part of Fig. 5.12(b): ~6 MHz), is expected to result in severely degraded BER performance for coherent optical communications, in particular for low symbol rate systems [15]. As such, the following experimental results regarding error free transmission of 1.25 GBaud optical QPSK clearly demonstrate the robust-

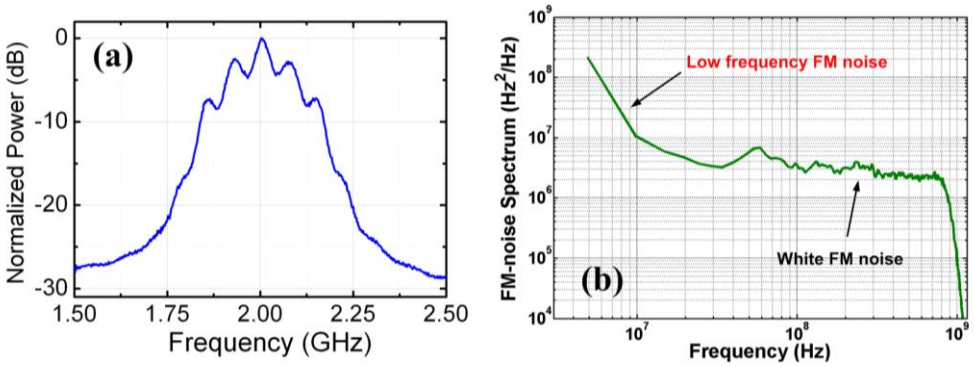

Figure 5.12: Optical phase noise characterisation at OLT: (a) DSH electrical beat spectrum of one filtered comb line, (b) measured FM-noise spectrum of the injection master Y-branch laser.

-ness of the proposed carrier pilot tone aided direct detection scheme against large transmitter laser phase noise.

5.4.2 Results and discussion

The performance of the LR UDWDM-PON downlink system is verified by carrying out BER measurements for two different scenarios: back-to-back (B2B) and 100 km SSMF transmission. The BER (average of I & Q) versus received power recorded for each of the transmitted 5 optical data channels is shown in Fig. 5.13. For the sake of clarity, the performance of only the worst (middle) channel in the B2B scenario is shown in Fig. 5.13 (denoted by the red squares). The fibre transmission of the middle channel (CH3) results in a 3 dB penalty (relative to the B2B performance of CH3 at 1e-9) yielding error free operation at -20 dBm of received power. All 5 channels (CH1-CH5) that are transmitted over 100 km of SSMF deliver very similar levels of performance with a receiver sensitivity (at BER of 1e-9) of -21 dBm for the best channel and -20 dBm for the worst. The 1 dB penalty in the case of the centre channels can be mainly attributed to the optical filtering at the RN (leakage of adjacent channels) and to the power asymmetry of the optical comb source. The received eye-diagrams of CH3 in the back-to-back and 100 km SSMF transmission scenarios are shown in Fig. 5.13 as insets. As such, the carrier pilot scheme presented in this section has offered an alternative pilot generation method to the SCM pilot tone scheme (note that the difference in receiver sensitivity is due to the use of an optical pre-amplifier in the SCM pilot case). The carrier pilot

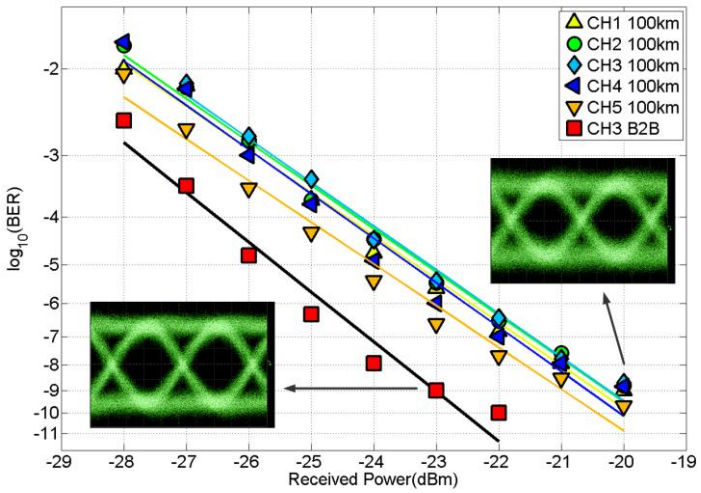

Figure 5.13: BER versus received optical power of 5 individual channels for the 100 km SSMF transmission scenario and for the worst channel (CH3) in a B2B scenario. Insets: eye-diagrams of CH3 (I data branch) in B2B and after 100 km SSMF.

scheme has the same efficient comb tone usage (5 tones for 5 users) as the SCM pilot scheme but it avoids the electrical leakages during RF pilot insertion process by reserving each comb line carrier as the corresponding pilot tone.

5.5 Summary

In this chapter we present a WDM-PON downlink scenario, using an injected gain switched comb source at the OLT and simple direct detection at the ONU. The OLT comb source has enabled dense WDM channel spacing with wavelength stability. The ONU receiver based on a novel pilot tone aided direct detection architecture supports the reception of advanced optical modulation format with high laser phase noise tolerance. Proof-of-concept experiments, entailing three different realisations of the pilot tone scheme, have demonstrated the feasibility of the proposed architecture with low symbol rate (1.25 and 2.5 GBaud) optical QPSK signals using large optical linewidth (5, 10, and 60 MHz) transmitter lasers. It is worth noting that the use of 1.25 GBaud QPSK for the carrier pilot tone scheme is due to the limited frequency range of our electrical IQ mixer for the SSB-SCM-QPSK data generation. With the restricted sub-carrier frequency (4 GHz), lower symbol rate has to be used to avoid the interference between data and pilot. The other two pilot schemes have pilot-data separation of 10 GHz and 8 GHz respectively therefore higher symbol rate could be employed.

The achieved experimental results presented in this chapter include: 1) a 3 × 5 Gb/s DWDM-PON downlink transmission over 50 km fibre, yielding worst channel receiver sensitivity (at 1e-9 BER) of -31 dBm; 2) a 7 × 5 Gb/s DWDM-PON downlink transmission over 25 km fibre with worst channel receiver sensitivity of -31 dBm; and 3) a 5 × 2.5 Gb/s LR UDWDM-PON downlink transmission over 100 km fibre, yielding worst case receiver sensitivity of -20 dBm. Note that the higher sensitivities in the first two cases are due to the use of an optical pre-amplifier at the receiver side. As such, the proposed pilot tone technique has enabled complex optical modulation signal to be delivered with simplified receiver design. Compared to the coherent optical access scheme being discussed in Chapter 4, the pilot tone aided direct detection technique compromises on receiver sensitivity; but in return offers simplicity and low cost through bypassing the optical coherent receiver architecture (which involves various high performance optoelectronic devices and power consuming digital or

analogue phase lock loop). It should be noted that, the practical limitation on the data rate of pilot tone schemes is typically determined by the achievable frequency separation between the comb lines (i.e. FSR of the comb source). Assuming a possible comb generation with ~40 GHz FSR (such as the resonance enhanced comb source in Section 3.2), 10 GBaud or higher symbol rate is in theory possible but the actual performance needs experimental justification. It is also worth noting that, the technique could be easily upgraded to accommodate higher order modulation formats and thus achieve higher data rate per channel without the need for dispersion compensation, and/or higher spectral efficiency for future dense and ultra-dense WDM-PON systems.

Reference

[1] T. Shao, M. Beltran, R. Zhou, P. M. Anandarajah, R. Llorente, and L. P. Barry, "60 GHz radio over fibre system based on gain-switched laser," J. Lightwave Technol., to be published (2014).

[2] R. Hui, B. Zhu, R. Huang, C. T. Allen, K. R. Demarest, and D. Richards, "Subcarrier multiplexing for high-speed optical transmission," J. Lightwave Technol. **20**, 417 (2002).

[3] L. G. Kazovsky, G. Kalogerakis, and W. T. Shaw, "Homodyne phase-shift-keying systems: past challenges and future opportunities," J. Lightwave Technol. **24**, 4876 (2006).

[4] S. Latkowski, S. K. Ibrahim, K. Shi, R. Zhou, A. D. Ellis, R. Maher, L. P. Barry, and P. M. Anandarajah, "Gain switched multi-carrier transmitter and pilot tone based receiver for long reach access networks," in *Proc. OFC 2012, OM2I.3.*

[5] P. M. Anandarajah, R. Zhou, V. Vujicic, M. D. G. Pascual, E. Martin, and L. P. Barry, "Long reach UDWDM PON with SCM-QPSK modulation and direct detection," in *Proc. OFC 2014, W2A.42.*

[6] P. M. Anandarajah, R. Maher, Y. Q. Xu, S. Latkowski, J. O'Carroll, S. G. Murdoch, R. Phelan, J. O'Gorman, and L. P. Barry, "Generation of coherent multicarrier signals by gain switching of discrete mode lasers," IEEE Photon. J. **3**, 112 (2011).

[7] P. M. Anandarajah, K. Shi, J. O' Carroll, A. Kaszubowska, R. Phelan, L. P. Barry, A. D. Ellis, P. Perry, D. Reid, B. Kelly, and J. O'Gorman, "Phase shift keyed systems based on a gain switched laser transmitter," Opt. Express **17**, 12668 (2009).

[8] R. Maher, K. Shi, L. P. Barry, J. O'Carroll, B. Kelly, R. Phelan, J. O'Gorman, and P. M. Anandarajah, "Implementation of a cost-effective optical comb source in a WDM-PON with 10.7Gb/s data to each ONU and 50km reach," Opt. Express **18**, 15672 (2010).

[9] T. Pfau, S. Hoffmann, and R. Noe, "Hardware-efficient coherent digital receiver concept with feedforward carrier recovery for M-QAM constellations," J. Lightwave Technol. **27**, 989 (2009).

[10] T. Okoshi, K. Kikuchi, and A. Nakayama, “Novel method for high resolution measurement of laser output spectrum,” Electron. Lett. **16**, 630 (1980).

[11] R. Zhou, S. Latkowski, J. O’Carroll, R. Phelan, L. Barry, and P. Anandarajah, “40nm wavelength tunable gain-switched optical comb source,” Opt. Express **19**, B415 (2011).

[12] R. T. Watts, K. Shi, Y. Yu, and L. P. Barry, “Detailed experimental phase noise characterization of Y-branch laser for use in coherent communication systems,” in *Proc. OFC 2013, JW2A.32.*

[13] S. Haykin, *Communication Systems* (John Wiley, 1994), Chap. 2.

[14] R. Hui and M. O’Sullivan, *Fibre Optic Measurement Techniques* (Academic Press, 2009), Chap.1.

[15] T. N. Huynh, L. Nguyen, and L. P. Barry, “Phase noise characterization of SGDBR lasers using phase modulation detection method with delayed self-heterodyne measurements,” J. Lightwave Technol. **31**, 1300 (2013).

Chapter 6

Conclusion and Future Work

Within the framework of this thesis, extensive studies have been presented on a novel type of optical frequency comb source as well as its usage in next generation access networks. The study of this proposed optical comb source is motivated by the anticipation of future access network evolution towards high performance wavelength division multiplexed passive optical networking (WDM-PON). The feasibility of employing such a comb source in an access network scenario is examined and verified through experimental studies. This chapter summarises the research outcomes achieved from these studies, and presents a few recommendations for future research.

6.1 Research Summary

The first and the second chapters of the thesis intend to deliver some background information based on which the proposed research has been carried out. In particular, Chapter 1 identifies the demand for high capacity WDM-PON based next generation optical access networks, as well as the benefits of employing optical comb source in a WDM-PON downlink scenario. In Chapter 2, the most commonly used comb generation techniques are inspected and compared with a direct modulation based gain switched comb source that has been recognised as a promising candidate for optical access applications due to its simplicity and potential low cost. As such, emphasis is placed on the gain switched optical comb source thereby becoming the main subject of investigation in the subsequent chapters. Salient results from the investigation can be concluded from three perspectives: the *generation, characterisation,* and *applications (in access networks)* of *gain switched optical frequency comb sources*.

Comb generation

In Chapter 3, optical injection is proposed to bring numerous benefits to a simple gain switched optical comb source. The combined injection and gain switching technologies have resulted in a novel type of injected gain switched comb source that contributes to the existing comb generation technologies. The enhanced properties that an injected gain switched comb source exhibits, compared to an un-injected case, include the increased comb line number, the reduced intensity and phase noise, the suppressed nonlinear distortion, and the wavelength tunability. Experimental work demonstrating these benefits has been presented through a few different comb generation scenarios:

- A *resonance enhanced comb source* is demonstrated based on an externally injected gain switched distributed feedback (DFB) laser, which has shown resonance frequency improved to over 2 times the inherent value of the free-running slave laser through strong optical injection. By simply changing the injection power and RF drive signal to the laser, various resonance frequencies can be obtained such that flexible tuning of the comb tone free spectral range (FSR) is achieved. Three FSR cases, at 25, 28, and 33 GHz, have been illustrated for the resonance enhanced comb generation. These cases correspond to comb line numbers (within a 3-dB spectral window) of 6, 5, and 4 lines respectively. The comb lines in all three FSR cases demonstrate identical (80 kHz) optical linewidth as the injection master laser.

- A *wavelength tunable comb* based on an externally injected gain switched Fabry-Pérot (FP) laser has been illustrated, which shows 40 nm wavelength tuning capability covering 1530 - 1570 nm. This is achieved with external optical injection into the slave laser at different FP longitudinal modes (thereby achieving single mode emission) and the subsequent gain switching at these modes. For all the 6 operating FP modes demonstrated within the wavelength tuning range, 5-8 coherent comb lines can be observed with the background noise extinction ratio exceeding 50 dB. Furthermore, bandwidth scaling of the comb source is demonstrated with an optical phase modulator, which yields doubling of the comb line numbers (14-16 lines) at each of the 3 selected exemplary operating modes/wavelengths. The optical linewidth of the comb lines are proven to be following that of the master laser through measurements of 14 chosen operating FP modes across the 40 nm wavelength range.

- *Compact comb generation* has been demonstrated with two different types of monolithically integrated lasers: an index patterned 2-section discrete mode (DM) laser and a passive feedback laser (PFL). The optical injection in these two devices is achieved by optimum injection/feedback from the master/phase section, respectively. A proof-of-concept 2-section DM laser has enabled comb generation at 5 GHz and 10 GHz FSR, with 9 comb lines and 3 comb lines in 3-dB spectral window for each case. A commercially available PFL device has enabled comb generation at 10 and 15 GHz FSRs yielding a 9 and 5-line (within a 3-dB spectral window) comb, respectively. Both devices have illustrated enhanced frequency response, improved comb shape and reduced nonlinearity. Further improvements are expected with progress in laser design and fabrication towards reduced parasitics.

Comb characterisation

Comb line characterisations have been carried out experimentally in Chapter 3 and Chapter 4 in terms of 3-dB optical spectral linewidth measurement, relative intensity noise (RIN) measurement, and detailed phase noise measurement involving frequency modulated (FM)-noise spectrum and phase-error variance (PEV) studies. These characterisations have provided basic insights into the noise properties of the injected gain switched optical comb source and offer important indications with respect to the system implementations of the comb source. Hence, the presented work can be considered as the second main novel contribution of this thesis.

- *Linewidth characterisations* of the resonance enhanced comb source and the wavelength tunable comb source in Chapter 3 are performed with a standard delayed self-heterodyne (DSH) linewidth measurement technique. The results have shown the dominance of injection master laser linewidth value over the injected gain switched comb lines. The narrow linewidth (<100 kHz for both comb sources) simultaneously transferred from a single master laser to all the generated comb tones highlights the potential of imposing multi-level optical modulation formats on each comb line. Another obvious advantage is the possible network savings associated with the replacement of multiple narrow linewidth lasers and their biasing/controlling circuits.

Hence, taking into account these advantages, the use of these comb sources in phase noise/linewidth sensitive coherent optical communication systems has been proposed.

- *RIN measurement* of the wavelength tunable comb source has been carried out in Chapter 3 with the help of a high-speed photodiode and an electrical spectrum analyser, at three of the operating wavelengths across a 40 nm tuning range. In all three cases, the averaged RIN (from dc to 10 GHz) of the individual comb lines is shown to be -120 dB/Hz or below, which is within 15 dB difference from that of the whole comb (around -135 dB/Hz). These results demonstrate the effective intensity noise reduction gained via the employment of external optical injection.

- *Detailed phase noise analysis* of an externally injected DFB comb source is given in Chapter 4 in the form of experimental and analytical evaluations on FM-noise spectrum and PEV of the individual comb lines. The experimental characterisation is carried out with a modified DSH method, and the analytical study is performed through adding additional linear and quadratic terms to the expression of FM-noise spectrum. The results have revealed that residual high frequency FM noise components exist in the comb lines due to certain injection conditions, which stay unnoticed in 3-dB spectral linewidth values but lead to unexpected oscillatory increase in the PEV. The influence of the residual phase noise has been inspected with digital coherent QPSK and 16 QAM systems, and a self-coherent optical DQPSK system. The results suggest the potential of the comb source in these systems whilst also highlighting the necessity of certain comb line flatness versus phase noise trade-off to avoid the relating receiver sensitivity penalties. These analyses are important guidelines to the employment and optimisation of injected gain switched comb sources in digital coherent/self-coherent optical access networks.

Access applications

The application of the gain switched comb source in optical access networks has been experimentally investigated in Chapter 4 and Chapter 5 with two types of WDM-PON downlink scenarios: a *coherent optical access network* with strict optical linewidth/phase noise requirements but offering an enhanced receiver sensitivity, and a *direct detection based access*

network with large laser phase noise tolerance but compromising on receiver sensitivity. These two types of systems, each exhibiting distinct features, could be deployed under different application scenarios depending on the specific requirement. For example, the coherent access solution could be applied to business users (e.g. commercial buildings) with high investments for high throughput content delivery; while the direct detection based access technique can be adopted to residential users requiring low cost and moderate data rate. The relating experimental demonstrations and discussions have formed the third major contribution of this thesis.

- In Chapter 4, a long reach (LR) WDM-PON downlink scenario using optical power splitter based "broadcast-and-select" optical distribution network (ODN) has been demonstrated with an externally injected DFB comb source deployed at the optical line terminal (OLT), and a digital coherent receiver employed at the optical network unit (ONU). The LR access system is an effective way for future metropolitan-access network consolidation which enhances networking efficiency through reduced site construction and management. With the help of a low phase noise optical comb source and advanced modulation formats (polarisation division multiplexed, quadrature phase shift keying and quadrature amplitude modulation: PDM-QPSK and PDM-16QAM), bandwidth intensive user data (10 Gb/s and 40 Gb/s per channel) can be delivered with reduced bandwidth occupancy thus enabling ultra-dense and dense (UD/D) WDM-PON systems with 10 GHz and 20 GHz channel spacing, respectively. The coherent optical receiver combined with advanced digital signal processing (DSP) and high forward error correction (FEC) limit at the ONU have enabled worst case receiver sensitivity of -44 dBm for the 7-channel PDM-QPSK system over 100 km fibre transmission, and -35.6 dBm worst case scenario for the 6-channel PDM-16QAM system over 80 km fibre transmission. The system loss budgets achieved in these two cases are 47 and 40 dB respectively.
- In Chapter 5, a novel "pilot tone" aided direct detection concept with arrayed waveguide grating (AWG) based "coloured" ODN has been proposed and demonstrated. By virtue of three types of (injected) gain switched optical comb sources at the OLT and a simple direct detection receiver architecture at the ONU,

D/UDWDM-PON downlink transmission over fibre length of 25, 50, and 100 km have been illustrated with 7 × 5 Gb/s, 3 × 5 Gb/s, and 5 × 2.5 Gb/s systems respectively, and worst channel receiver sensitivities achieved in these three cases are -31 dBm, -31 dBm (both with an optical pre-amplifier and a pin detector), and -20 dBm (using an APD: avalanche photo diode, without a pre-amplifier), all at a bit error rate (BER) of 1e-9. Salient features of the pilot tone aided direct detection scheme that have been demonstrated include: large laser phase noise tolerance, which enables low symbol rate optical QPSK format to be imposed with large transmitter laser linewidth of 10, 5, and 60 MHz, respectively; system simplification, by negating the need for a coherent receiver front-end, local oscillator laser, and optical frequency/phase tracking at the ONU. The trade-off of the pilot tone scheme compared to the coherent access case includes reduction in receiver sensitivity and lack of network agility.

In conclusion, this thesis has presented an optical frequency comb source for use in next generation access networks. Through extensive research outlined in Chapter 3-5, the generation of the proposed comb source has been demonstrated, the basic characteristics of the comb source have been investigated and proof-of-concept implementations of the comb source in access networks have been verified. With these contributions, the practical utilities of the comb source have been explored to a certain degree, but continued research remains possible. The following section probes into a few of these possibilities and discusses their prospective benefits.

6.2 Future Work

➢ Numerical investigation on the comb

Within the scope of this thesis, investigations on the generation and characteristics of the injected gain switched optical comb source have been carried out experimentally. One possible direction for further research is a detailed numerical study of the comb source, which has been lacking so far. Such a study could provide useful insights into the dynamic behaviour of the device. Through numerically simulating a free-running master laser, and a slave laser that is under gain switching and optical injection from the master, many physical characteristics of

the injected gain switched comb generation can be modelled and examined with great convenience. These characteristics include noise/jitter, frequency chirp, nonlinearities, etc., and the investigation process is easily controllable (through numerically manipulating the various interactions between master and slave lasers like injection power and wavelength detuning). Such a numerical study is expected to offer a comprehensive understanding of the injected gain switched comb source, and provide important perspectives regarding the estimation of system performance when utilising this type of comb source for data modulation and transmission.

➢ Coherent expansion of the comb

As discussed in Chapter 3, Section 3.3, the viability of an injected gain switched optical comb source in practical systems is expected to be greatly improved if the comb line number can be increased with system demand. This can be achieved with several comb expansion techniques, and an optical phase modulator is employed in Section 3.3 for the expansion of a wavelength tunable comb source that is based on an externally injected gain switched Fabry-Pérot (FP) laser. The potential issues with respect to the use of electro-optic modulators, however, include their large insertion losses and difficulties in photonics integration. Hence these issues might prove challenging for further scaling and utilisation of the expanded comb source.

Another possible approach for the coherent expansion of a wavelength tunable comb source, as proposed here, is by the use of cascading multiple injected gain switched FP lasers. The conceptual diagram illustrating the operating principle is shown in Fig. 6.1. In the figure, all the FP lasers (FP 1-N) are being gain switched by amplified sinusoidal signals from a signal generator. A wavelength tunable master laser injects into FP 1 and results in a tunable comb generation as that elaborated in Chapter 3. The output of FP 1 is then injecting into one of the longitudinal modes of a second FP 2 thus yielding the excitation of additional comb tones. The wavelength detuning between the seeding comb (FP 1 output) and the longitudinal mode of FP 2 can be eliminated through temperature tuning of the two lasers. Such a process can be repeated throughout the N stages of cascaded FPs, hence providing a simple, low loss and scalable technique for the comb expansion. Moreover, this method lends itself to photonic integration thereby potentially enhancing its compactness, cost efficiency and ease of manufacture.

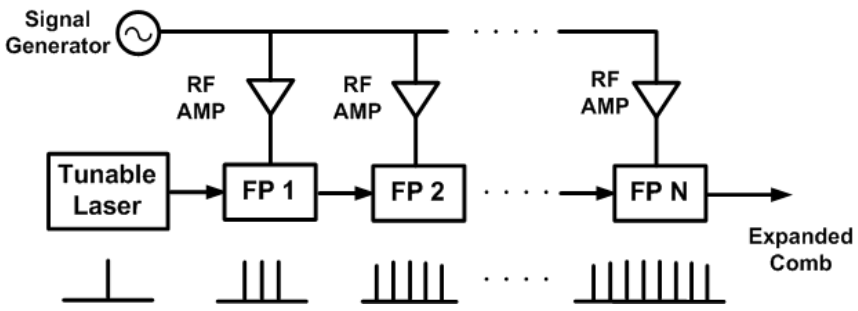

Figure 6.1: Schematic illustration of cascaded FP lasers for coherent expansion of the tunable comb.

➢ Reduced channel spacing in coherent access networks

As mentioned in Chapter 4, Section 4.3.2, the channel spacing of the downlink LR coherent D/UDWDM-PON systems could be reduced without influencing the receiver sensitivity at the FEC limit. The proof-of-concept verification has been shown with a reduced channel spacing of 15 GHz for the 6-channel, 6 GBaud PDM-16QAM signal in a back-to-back scenario. The logical next step is then to examine the transmission performance of the DWDM signal at the reduced spacing, and investigate the impact of inter-channel interference and nonlinear four-wave mixing (FWM) on the LR PON system. The investigation can be continued with further reduced channel spacing of 12.5 GHz and the introduction of aggressive filtering techniques such as digital Nyquist pulse shaping (root raised cosine filter with a zero roll-off factor).

➢ Improvement of the pilot tone scheme

In Chapter 5, the potentials of the pilot tone aided direct detection scheme for phase noise insensitive reception of low baud rate, advanced optical modulation formats has been demonstrated using QPSK signal. The utility of the scheme is expected to be further improved with the employment of higher order modulation formats such as high level QAM signals. This will result in enhanced spectral efficiency but as a trade-off, the increased signal-to-noise-ratio (SNR) requirement of the high order QAM formats might degrade the BER performance, resulting in a reduced system reach. A possible solution is to utilise the conventional LR PON concept and employ mid-span amplifiers (see Chapter 1, Section 1.3.2).

List of Publications

➢ Refereed Journal Papers

1. **Rui Zhou**, Sylwester Latkowski, John O'Carroll, Richard Phelan, Liam P. Barry, and Prince Anandarajah, "40nm wavelength tunable gain-switched optical comb source," Optics Express, vol. 19, no. 26, pp. B415-B420, December 2011.

2. **Rui Zhou**, Tam N. Huynh, Vidak Vujicic, Prince M. Anandarajah, and Liam P. Barry, "Phase noise analysis of injected gain switched comb source for coherent communications," Optics Express, vol. 22, no. 7, pp. 8120-8125, April 2014.

3. **Rui Zhou**, Prince M. Anandarajah, Robert Maher, Milen Paskov, Domaniç Lavery, Benn C. Thomsen, Seb J. Savory, and Liam P. Barry, "80-km coherent DWDM-PON on 20-GHz grid with injected gain switched comb source," IEEE Photonics Technology Letters, vol. 26, no. 4, pp. 364-367, February 2014.

4. Prince M. Anandarajah, **Rui Zhou**, Robert Maher, Domaniç Lavery, Milen Paskov, Benn Thomsen, Seb Savory, and Liam P. Barry, "Gain-switched multicarrier transmitter in a long-reach UDWDM PON with a digital coherent receiver," Optics Letters, vol. 38, no. 22, pp. 4797-4800, November 2013.

5. Vidak Vujicic, **Rui Zhou**, Prince M. Anandarajah, John O'Carroll, and Liam P. Barry, "Performance of a semi-Nyquist NRZ-DQPSK system employing a flexible gain-switched multicarrier transmitter," Journal of Optical Communications and Networking, vol. 6, no. 3, pp. 282-290, March 2014.

6. Tong Shao, Marta Beltrán, **Rui Zhou**, Prince M. Anandarajah, Roberto Llorente, and Liam P. Barry, "60 GHz Radio over fibre system based on gain-switched laser," Journal of Lightwave Technology, vol. 32, no. 20, pp. 3695-3703 (2014).

7. Aravind P. Anthur, Regan T. Watts, **Rui Zhou**, Prince Anandarajah, Deepa Venkitesh, and Liam P. Barry, "Penalty-free wavelength conversion with variable channel separation using gain-switched comb source," Optics Communications, vol. 324, pp. 69-72, 2014.

8. P. M. Anandarajah, S. Latkowski, C. Browning, **R. Zhou**, J. O'Carroll, R. Phelan, B. Kelly, J. O'Gorman, and L. P. Barry, "Integrated two-section discrete mode laser," IEEE Photonics Journal, vol. 4, no. 6, pp. 2085-2094 (2012).

➢ Reviewed Conference Papers

1. **Rui Zhou**, Sylwester Latkowski, John O'Carroll, Richard Phelan, Liam P. Barry, and Prince Anandarajah, "40nm wavelength tunable gain-switched optical comb source," in *37th European Conference and Exposition on Optical Communications (ECOC),* paper Tu.5.LeSaleve.3 (2011).

2. **Rui Zhou**, Vidak Vujicic, Tam N. Huynh, Prince M. Anandarajah, and Liam P. Barry, "Effective phase noise suppression in externally injected gain switched comb source for coherent optical communications," in *39th European Conference and Exposition on Optical Communications (ECOC),* paper P.2.5 (2013).

3. **Rui Zhou**, Prince M. Anandarajah, M. Deseada Gutierrez Pascual, John O'Carroll, Richard Phelan, Brian Kelly, and Liam P. Barry, "Monolithically integrated 2-section lasers for injection locked gain switched comb generation," in *Optical Fibre Communication Conference (OFC),* paper Th3A.3 (2014).

4. Prince M. Anandarajah, **Rui Zhou**, Robert Maher, M. Deseada Gutierrez Pascual, Frank Smyth, Vidak Vujicic, and Liam P. Barry, "Flexible optical comb source for super channel systems," in *Optical Fibre Communication Conference (OFC),* paper OTh3I.8 (2013).

5. Prince M. Anandarajah, **Rui Zhou**, Vidak Vujicic, M. Deseada Gutierrez Pascual, Eamonn Martin, and Liam P. Barry, "Long reach UDWDM PON with SCM-QPSK modulation and direct detection," in *Optical Fibre Communication Conference (OFC),* paper W2A.42 (2014).

6. Sean P. O Duill, **Rui Zhou**, Prince M. Anandarajah, and Liam P. Barry, "Numerical investigation into the dynamics of externally injected, gain-switched lasers for optical comb generation," in *40th European Conference and Exposition on Optical Communications (ECOC),* accepted for publication (2014).

7. Tam Huynh, **Rui Zhou**, Sylwester Latkowski, Frank Smyth, Liam Barry, and Prince

Anandarajah, “Multi-carrier transmitter for future access networks,” in *14th International Conference on Transparent Optical Networks (ICTON),* paper We.D3.2 (2012).

8. Prince M. Anandarajah, **Rui Zhou**, Robert Maher, M. Deseada Gutierrez Pascual, Frank Smyth, Vidak Vujicic, and Liam Barry, “Injection locked lasers for flexible optical comb sources,” in *Proceedings 15th International Conference on Transparent Optical Networks (ICTON),* paper Mo.C2.1 (2013).

9. M. Deseada Gutierrez Pascual, Prince M. Anandarajah, **Rui Zhou**, Frank Smyth, Sylwester Latkowski, and Liam P. Barry, “Cascaded Fabry-Pérot lasers for coherent expansion of wavelength tunable gain switched comb,” in *40th European Conference and Exposition on Optical Communications (ECOC),* accepted for publication (2014).

10. J. O’Carroll, P. M. Anandarajah, **R. Zhou**, R. Phelan, B. Kelly, J. O’Gorman, and L. P. Barry, “Transmission over 50 km using a directly modulated integrated two-section discrete mode laser at 1550 nm,” in *Proceedings Conference on Lasers and Electro-Optics Europe and International Quantum Electronics Conference (CLEO EUROPE/IQEC),* paper CB_7 (2013).

11. Sylwester Latkowski, Selwan K. Ibrahim, Kai Shi, **Rui Zhou**, Andrew D. Ellis, Robert Maher, Liam P. Barry, and Prince M. Anandarajah, “Gain switched multi-carrier transmitter and pilot tone based receiver for long reach access networks,” in *Proceedings Optical Fibre Communication Conference (OFC),* paper OM2I.3 (2012).

12. V. Vujicic, P. M. Anandarajah, C. Browning, **R. Zhou**, S. O’Duill, and Liam P. Barry, “Optical multicarrier based IM/DD DWDM-SSB-OFDM access networks with SOAs for power budget extension,” in *40th European Conference and Exposition on Optical Communications (ECOC),* accepted for publication (2014).

13. V. Vujicic, J. Pfeifle, R. T. Watts, P. C. Schindler, C. Weimann, **R. Zhou**, W. Freude, C. Koos, and L. P. Barry, “Flexible terabits/s Nyquist-WDM superchannels with net SE > 7bits/Hz using a gain-switched comb source,” in *Proceedings Conference on Lasers and Electro-Optics (CLEO),* paper SW1J.3 (2014).